Characterization of the Anterior Insular Cortex's Functional Connectivity in the Macaque Monkey

Dissertation

zur Erlangung des Grades eines
Doktors der Naturwissenschaften

der Mathematisch-Naturwissenschaftlichen Fakultät
und
der Medizinischen Fakultät
der Eberhard-Karls-Universität Tübingen

vorgelegt
von

Jennifer Smuda
aus Mainz, Deutschland

Juni – 2019

Tag der mündlichen Prüfung: ...11.09.2019.....

Dekan der Math.-Nat. Fakultät: Prof. Dr. W. Rosenstiel

Dekan der Medizinischen Fakultät: Prof. Dr. I. B. Autenrieth

1. Berichterstatter:	Dr. Henry Evrard
2. Berichterstatter:	Prof. Dr. Andreas Nieder
Prüfungskommission:	Prof. Dr. Laura Busse
	Prof. Dr. Nikos Logothetis

Erklärung / Declaration:

Ich erkläre, dass ich die zur Promotion eingereichte Arbeit mit dem Titel:

„Characterization of the Anterior Insular Cortex's Functional Connectivity in the Macaque Monkey"

selbständig verfasst, nur die angegebenen Quellen und Hilfsmittel benutzt und wörtlichoder inhaltlich übernommene Stellen als solche gekennzeichnet habe. Ich versichere an Eides statt, dass diese Angaben wahr sind und dass ich nichts verschwiegen habe. Mir ist bekannt, dass die falsche Abgabe einer Versicherung an Eides statt mit Freiheitsstrafe bis zu drei Jahren oder mit Geldstrafe bestraft wird.

I hereby declare that I have produced the work entitled:

***„Characterization of the Anterior Insular Cortex's Functional Connectivity in the Macaque Monkey"**,*

submitted for the award of a doctorate, on my own (without external help), have used only the sources and aids indicated and have marked passages included from other works, whether verbatim or in content, as such. I swear upon oath that these statements are true and that I have not concealed anything. I am aware that making a false declaration under oath is punishable by a term of imprisonment of up to three years or by a fine.

Tübingen, den 27.06.2019 .....

Datum / Date Unterschrift /Signature

To my parents, Andrea and Manfred

"There is grandeur in this view of life, with its several powers, having been originally breathed into a few forms or into one; and that, whilst this planet has gone cycling on according to the fixed law of gravity, from so simple a beginning endless forms most beautiful and most wonderful have been, and are being, evolved."

Charles Darwin

CONTENTS

1

ABSTRACT

The insular cortex, the fifth cortical lobe, hidden deep within the Sylvian fissure in the primate brain, is active during many different tasks ranging from the detection of primary interoceptive events to the integration of hedonic, motivational, and social signals. With its position as a rich club hub within the salience network and its vast ranging network of connections with cortical and subcortical brain structures, the most anterior agranular part of the insula is ideally positioned to evaluate salient events and allocate resources to accordingly optimize homeostasis.

Whilst functional imaging has implicated the activity of the anterior insula in many different interoceptive, emotional, and cognitive functions, local electrical microstimulation (EMS) has revealed its influence in autonomic regulation. Such influence has been proposed to be asymmetrical, with parasympathetic and sympathetic processes being predominantly represented in the left and right anterior insula, respectively. In monkeys, one architectonic area within the ventral anterior insular cortex (VEN area) hosts two specialized neuronal morphotypes, the fork neuron and the von Economo neuron (VEN). The VEN, with its interconnections with both, prefrontal cortex and brainstem autonomic centres, has been attributed a unique role in the maintenance of homeostasis and autonomic responses as well as neurobiological mechanisms contributing to subjective awareness.

To further our understanding of the insula's role, especially of the VEN area, in autonomic processes and to uncover if any observed asymmetry in autonomic regulation would also be mirrored by an asymmetric whole-brain activity regulation, we conducted EMS in the left and right VEN areas in three

anaesthetized macaque monkeys during high-resolution functional magnetic resonance imaging (fMRI). In addition, to examine basic whole-brain activity changes, we investigated the role of the left and right VEN area in the salience network and in the dynamic control of the default mode network and the central executive network.

Using a general linear model analysis, we found the VEN area to be functionally connected to monosynaptic and polysynaptic cortical and subcortical brain regions. However, the alternate stimulation of the left and right VEN area did not reveal any asymmetry in global brain activity response patterns. Employing a seed-based correlation analysis, we found that EMS reduced the insula's functional correlations with mainly contralateral cortical areas, while correlations to ipsilateral and midline structures remained constant. Further, we showed that EMS led to a shutdown of the insula's functional correlation with the contralateral salience and default mode networks. However, most remarkably, right-sided – but not left-sided - EMS shut down the central executive network bilaterally and conspicuously increased the ipsilateral salience network.

The present results strengthen the insula's role as a major hub in the salience network, and its ability to not only switch global brain activity between networks but also to regulate these networks. While this regulation appears to be asymmetric and might influence emotional, cognitive, and behavioural processes, global brain activity, evoked by EMS, did not display asymmetries. It did, however, indicate functional connections to monosynaptic and polysynaptic cortical and subcortical brain areas, underlining the insula's ability to integrate polymodal stimuli in an interoceptive self-referential domain. This could contribute to the detection and evaluation of salient events, regulation of autonomic processes, and perhaps engendering self-awareness in humans.

To further investigate the role of the VEN area in the regulation of network activities, the present experiment should now be replicated in alert monkeys involved in passive or active behavioural paradigms. With the introduction of

salient physiological and/or environmental challenges, which are most likely to engage the insula, the crucial role of the VEN area in brain and body regulation could be revealed.

2

THE INSULAR CORTEX

The insular cortex, often referred to as the insula, is a distinct portion of the cerebral cortex hidden deep within the Sylvian fissure in primate brains. In each hemisphere of the brain, the Sylvian fissure separates the temporal lobe from the frontal and parietal lobes. By virtue of being hidden deep within the Sylvian fissure, the insula remained poorly understood until the early 1990s.

The first documented historical sketch of this hidden lobe was published by Andreas Vesalius in the 1543 edition of *De corporis humani fabrica libri septem* (see *quinta septimi libra figura* in Vesalius, 1543). About one hundred years later, in 1641, the Danish anatomist Casper Bartholin referred to the original sketch of Vesalius and added another view of a dissected brain, exposing the insula (see figure 9 in Bartholin, 1641). However, besides providing a pictoral depiction, neither of them actually described this brain area, and it was even left out of Bartholin's seminal work *Institutiones Anatomicae Das ist: Künstliche Zerlegung Menschlichen Leibes*, which was published seven years later and included meticulous details about the anatomy of the human body and brain (Bartholin, 1648). Another sketch of an exposed insula was published in 1783 by the Scottish anatomist Alexander Monro, who illustrated this portion of the brain in a picture of a ventrally resected brain (Monro, 1783). Notwithstanding, it took a further three years for the first recorded written mention of the insula to be published. In his book *Traité d'anatomie et de physiologie* (1786), Felix Vicq-d'Azyrs described it as 'the cortical area between the Sylvian fissure and the corpus striatum' (Vicq-d'Azur, 1786). A more detailed description was published ten years later by the pioneering physician Johann Christian Reil in his book *Exercitationum anatomicarum fasciculus primus de structura nervorum* (Reil, 1796). In 1859, in the

first edition of Grays Anatomy, Henry Gray renamed the region *Island of Reil*, in honour of Reil's exemplary work (Gray and Carter, 1859; Fusar-Poli et al., 2009). Several studies, detailing the architecture of the insula as well as its connections with other brain areas, have been published in the century since Reil's initial description (Brodmann, 1909; Economo and Koskinas, 1925; Rose, 1928; Brockhaus, 1940; Roberts and Akert, 1963; Sanides, 1968; Jones and Burton, 1976; Mesulam and Mufson, 1982b, 1982a; Mufson and Mesulam, 1982). However, it wasn't until the widespread use of the functional magnetic resonance imaging technique (fMRI) in the early 2000s (see subchapter *Functional Magnetic Resonance Imaging*), which revealed the insula's association with many different interoceptive, affective, and cognitive processes (see subchapter *Connectivity and Functions of the Insular Cortex*), that the interest of scientists in the insular cortex was greatly peaked.

A PubMed search performed in early 2019, with *insular cortex* or *insula* as a keyword in the title, yielded a total of 32 publications between 1900 and 1980, whereas yielded 50 times as many publications years since, highlighting the increased attention this brain area has attracted in the last decades.

The Development and Morphology of the Insular Cortex

The development of the human insular cortex starts about six weeks into gestation (Kalani et al., 2009) and is, therefore, one of the first cortical structures to show differentiation (Wai et al., 2008). It presents itself on the surface of the cerebral hemispheres until the faster and more extensive development of the surrounding cortical areas, like the frontal, parietal, and temporal lobe, shift it to the inside of the then newly formed Sylvian fissure (the completion of the Sylvian fissure only occurs after birth (Streeter, 1912)). In species lacking severe

cortical development, the insula remains on the cerebral surface permanently (Rose, 1928).

Once fully developed, the human insular cortex consists of an anteroventral agranular sector, an intermediate dysgranular sector, and a posterodorsal granular sector (Mesulam and Mufson, 1985). The anterior sector contains three short gyri as well as an accessory and a transverse gyrus, which all meet anteriorly at the insular apex. The posterior sector comprises two long gyri (anterior and posterior), which are divided by the postcentral sulcus (Ture et al., 1999). The development of the gyri begins around the 22nd week of gestation (Cunningham, 1891). Interestingly, the composition of the insula varies significantly between individuals and even between the two hemispheres, during development and in the adult brain (Cunningham, 1892).

The main arterial supply for the insula stems from the middle cerebral artery (Uddin et al., 2017), whereas the venous system is a combination of superficial and deep venous connections (Mesulam and Mufson, 1982a).

In monkeys, the appearance of the insula, with an approximate surface area of 160mm^2, differs from humans in the sense that it is rather smooth (lissencephalic) and thus lacks pronounced sulci and gyri (Mesulam and Mufson, 1982a, 1985). Despite its smooth surface, like in humans, the macaque insula can be subdivided into different cytoarchitectonic sectors: an agranular sector with three agranular, cellular strata and a layer of myelinated fibres; a dysgranular region with beginnings of a granular layer IV; and a granular region with a layer IV as well as an incipient sub lamination of layer III (Mesulam and Mufson, 1982a). These sectors can be further subdivided into distinct smaller architectonic areas with sharply defined borders and consistent topological arrangements (Evrard et al., 2014). The agranular sector in the anterior portion of the insula contains seven areas, the posterior-lateral (Iapl), the posterior-medial (Iapm), the intermediate

(Iai), the lateral (Ial), and the medial (Iam) agranular insula, as well as the anterior area of the ventral fundus of the insula (Ivfa) and the posterior agranular insula (Iap). The dysgranular region comprises four areas, namely the dorsal area (Idd), the mound dysgranular insula (Idm), the ventral area (Idv), and the posterior area of the ventral fundus of the insula (Ivfp). Finally, the granular region comprises the posterior area (Idfp) and the anterior area (Idfa) of the dorsal fundus, as well as the dorsal (Igd) and ventral (Igv) areas of the granular insula (Evrard et al., 2014). Notably, the lateral agranular insula, located in the ventral anterior insular cortex (vAIC), contains two extraordinary neuron types: the von Economo neurons and the fork neurons (Horn and Evrard, in preparation).

The von Economo neuron (VEN), a specialized projection neuron in layer Vb, was already noted in the late 19th and early 20th century by several anatomists (for a review see Butti et al. (2013)), including Wladimir A. Betz (Betz, 1881), Carl Hammarberg (Hammarberg, 1895), and Santiago Felipe Ramón y Cajal (Ramon y Cajal, 1904). The first complete description was, however, published by Constantin von Economo in 1918, who initially assumed it to be a pathological formation of the brain (Economo and Deuticke, 1918). Subsequently, after noticing these neurons frequently in the cingulate and insular cortex, he concluded them not to be an abnormality but a new, specialized cell type and described them in his seminal publication *Eine neue Art Spezialzellen des Lobus Cinguli und Lobus Insulae* in 1926 (Economo, 1926). Remarkable for these neurons are the thick apical, and basal dendrites, as well as the elongated, spindle, shaped perikaryon (Economo, 1926; Seeley et al., 2012). Furthermore, the dendrites are very symmetrical and display narrow dendritic arborisation (Watson et al., 2006; Allman et al., 2010b). In humans, VENs start developing in the 36th week of gestation but are only sparsely present during the time of birth. Within the next

eight month their quantity increases, with more neurons emerging in the right than the left hemisphere (Allman et al., 2010a), before it starts declining and reaching a steady level at four years of age. Besides humans and monkeys (Evrard et al., 2012), these neurons have been found in many other species with advanced social skills like great apes (Nimchinsky et al., 1999), cetaceans (Butti et al., 2009), elephants (Hakeem et al., 2009), bowheads (Raghanti et al., 2015), and others (Butti and Hof, 2010). Though their specific function remains a mystery until today, they have been found to be selectively depleted in the behavioural variant of frontotemporal dementia (bvFTD) (Seeley et al., 2006), Alzheimer's disease, and schizophrenia (Brune et al., 2010), and are also suggested to be involved in intuition and social emotions (Allman et al., 2010b), awareness (Craig, 2009), autonomic regulation (Butti et al., 2013), interoception (Santos et al., 2011), and interoceptive predictive coding (Seth et al., 2011). For a detailed account, please refer to the review of Franco Cauda (Cauda et al., 2013).

Connectivity of the Insular Cortex

The insular cortex is a brain region that is involved in a multitude of processes, from temperature detection to emotional awareness (Nieuwenhuys, 2012). Its manifold functions are owed to an extensive network of connections throughout the brain, involving cortical and subcortical structures alike (Evrard, 2019). Extensive tract tracing studies in the past decades have painted a detailed picture of these connections, though new connections are still discovered and our understanding of the complexity remains to be completed. Using the unearthed connections, attempts have been made to understand the eminent complex functions of the insula and to explain its involvement in crucial homeostatic and emotional processes.

The American neuroanatomist and neuroscientist A.D. Craig was the first to suggest computational and integrational processes that advance from the granular-to-dysgranular-to-agranular portions of the insula. In his model, he proposed that primary interoceptive feelings advance from the posterior insula to the mid-insula, where they are being integrated with homeostatic motor functions, arriving from the hypothalamus and the amygdala, as well as sensory environmental conditions, arriving from the entorhinal cortex and the temporal poles. Upon further advancement of this integrated information to the anterior insular cortex (AIC), hedonic conditions, arriving from the nucleus accumbens and the orbitofrontal cortex, as well as motivational, socials, and cognitive conditions, arriving from the anterior cingulate cortex (ACC), the ventromedial prefrontal cortex, and the dorsolateral prefrontal cortex, are being integrated, leading to subjective awareness of oneself in space and time (Craig, 2009a).

The innervation of the different insula parts has been extensively studied and it was found that the posterior part of the insula, namely Igd and Igv, receive inputs from the suprageniculate nucleus of the thalamus (Burton and Jones, 1976), which, in turn, is innervated by the spinal cord (Craig, 2004), the superior temporal sulcus (Yeterian and Pandya, 1989), as well as the frontal eye field (Huerta et al., 1986) and the superior colliculus (Burton and Jones, 1976; Evrard, 2019). The auditory belt and the parabelt have bidirectional connections with the posterior insula (Hackett et al., 1998). Projections from the posterior insula further innervate vestibular nuclei in the brainstem (Akbarian et al., 1994) as well as the primary vestibular cortex (Mesulam and Mufson, 1982b).

Another granular portion of the insula, the dorsal fundus, comprising the subareas Idfa and Idfp, receives input from the basal part of the ventromedial nucleus of the thalamus (VMb) and the posterior part of the ventromedial nucleus of the thalamus (VMpo), respectively (Craig, 2014) and acts as the primary interoceptive cortex. The inputs it receives (e.g. temperature, itch, pain,

or sensual touch) are being conducted from the organs via "unmyelinated C or thinly myelinated Aδ primary afferent fibres" to the lamina I of the spinal cord, or from the cranial nerves (vagal and glossopharyngeal) to the nucleus tractus solitarii, before they reach the thalamus (VMb and VMpo, respectively). These inputs are organized somatotopically with the presentation of the foot, arm, and face in the posterior part (Idfp) and the taste and viscera in the more anterior part (Idfa) (Evrard, 2019). This primary interoceptive information is forwarded to the dorsal mid insula, comprising the dysgranular subarea Idd, where it is integrated with more information, arriving from the dorsolateral area of the striatum (Chikama et al., 1997), the posterior cingulate cortex (Morecraft et al., 2004), the supplementary motor area (Luppino et al., 1993), the ventral premotor cortex (Gerbella et al., 2011), as well as some other higher order cortical areas. At this stage, in the Idd, a representation of self-related processes, independent of the surrounding, is created in the form of body ownership and feeling of agency (Evrard, 2019). Ventral to the Idd lie the Idm, Idv, and the Ivfp, likewise dysgranular areas, thought to be responsible for interpersonal and social-emotional behaviour, social approach behaviour (Caruana et al., 2011), and vocalization (Remedios et al., 2009). Furthermore, the mid-insula has been implicated in the judgment of learning (Hu et al., 2017) and food motivation behaviour (Avery et al., 2017). Input arrives from the amygdala (Amaral and Price, 1984), the anterior cingulate cortex (Mesulam and Mufson, 1982b), the pre-supplementary motor area (Luppino et al., 1993), and other high-order cortical areas. Additionally, connections to the lateral hypothalamus and the periaqueductal grey have been shown (Evrard, 2019).

Finally, distinct areas in the anterior, agranular portion of the insula receive inputs from the primary olfactory cortex (Iam, Iai, Ial, Iapm, and Iapl) (Carmichael et al., 1994), the basal nucleus of the amygdala (Iam, Iapm, Ial) (Carmichael and Price, 1995a), the ventroposterior medial nucleus of the

thalamus (Iapm and Ial) (Carmichael and Price, 1995b), as well as the other parts of the insula. Computing the final integration steps, the AIC re-represents interoceptive and exteroceptive information, emotions, cognition, as well as information pre-processed in different parts of the insula which leads to the highest state of integration and with this to sentient awareness of oneself (Craig, 2009a; Evrard, 2019).

Functions of the Insular Cortex

These complex integration and computation processes of a multitude of different inputs and signals from cortical and subcortical areas might be the reason why the insula is active during so many different tasks (for summarizing reviews see Nieuwenhuys (2012) and Uddin et al. (2017)).

Especially the vAIC, housing the VEN in the Ial, is active during a wide array of functions connected to emotional awareness and subjective interoceptive feelings (Craig, 2002). Craig and his team showed in 2000, by applying graded cooling stimuli to subjects palms during positron emission tomography recordings, that whilst the initial, objective representation of the stimulus occurs in the dorsal margin of the middle/posterior insula, the subjective, perceived thermal intensity correlated with activity in the AIC (Craig et al., 2000). Another famous experiment in the context of subjectively perceiving bodily feelings in the AIC is the detection of one's heartbeat, as shown by Critchley and his team in 2004 (Critchley et al., 2004). Additionally, the AIC shows activation during sympathetic arousal, heart rate increase, and cardiorespiratory sensation (Hassanpour et al., 2018). However, the activation of the AIC is not limited to the perception of bodily feelings alone but also shows activation during emotions and cognitive tasks. Leibenluft et al. showed mothers pictures of their own child, compared to unfamiliar children, and noticed an increase in AIC activation

during reported expressions of feelings of maternal love (Leibenluft et al., 2004). Hennenlotter and his team reported that viewing or making a smile leads to similar activation of the AIC, amongst other regions (Hennenlotter et al., 2005). Also during empathy, e.g. has during the reaction of others to pain, the AIC is involved (Lamm et al., 2010), as well as during pleasant musical experiences (Koelsch et al., 2006). Connecting bodily feelings to social feelings was also shown to involve the AIC. Terasawa et al. (2012) found that the AIC mediates bodily sensibility and social anxiety while the subjects were answering questions about their bodily states during an fMRI recording (Terasawa et al., 2013). To locate the gustatory emotion of disgust, Jabbi and his team had subjects experience disgust themselves, view other people experience disgust, or imagine disgust, and found the AIC to be active (Jabbi et al., 2008).

Another connection between interoception, exteroception, emotions, and cognition and the AIC's involvement was given by Salomon and his team in 2016. They noticed that visual attention changed, depending on the timing of stimulus presentation synchronous or asynchronous to the heartbeat (Salomon et al., 2016). Furthermore, the insula was reported to be active during a visual self-recognition task (Devue et al., 2007).

Using an anti-saccade task, known to produce conscious and unconscious errors, Klein et al. showed the left and right AIC to be active during the occurrence of conscious errors. The authors attributed this increased activity to an "enhanced awareness of the autonomic reaction to the error, or to the higher autonomic response itself" (Klein et al., 2007). Ploran et al. gradually revealed pictures and showed a positive blood-oxygen-level-dependant signal change in the AIC, as well as in the frontal operculum, the frontal cortex, and the thalamus, during the moment of recognition (Ploran et al., 2007). Furthermore, the feeling of knowing, whilst recalling words, also led to the activation of the AIC, among others (Kikyo et al., 2002). The AIC also showed activation during different discrimination

tasks like a time perception task (Livesey et al., 2007), where subjects had to discriminate durations under different conditions, or a visual discrimination task, where the subjects had to decide which of two lines was longer (Deary et al., 2004). Moreover, Nelson and his team suggested that the AIC plays a crucial role in task-level control as well as focal attention by analysing resting-state functional connectivity fMRI data (Dosenbach et al., 2006; Dosenbach et al., 2007; Nelson et al., 2010).

The insula has also been implicated in several diseases like autism (Uddin and Menon, 2009), schizophrenia (Wylie and Tregellas, 2010), bipolar disorder (Yin et al., 2018), depression (Kandilarova et al., 2018), addiction (Droutman et al., 2015), obsessive-compulsive disorder (Stein et al., 2006), anxiety (Kawaguchi et al., 2016; Mendez-Ruette et al., 2019) (Goodkind et al., 2015; Gogolla, 2017), and the above mentioned bvFTD. In bvFTD, the social-emotional functions of the patients are impaired (Lough et al., 2006; Rankin et al., 2006), seemingly related to an early aggregation of the TAR DNA-binding protein 43 (Nana et al., 2019), a hallmark protein for motor neuron diseases (Neumann et al., 2006) and a subsequent, selective decay of VENs in the early stages of the disease (Kim et al., 2012).

In coma-causing brain stem lesions, Fischer and his collaborators found in 2016 that a lesion in the rostral dorsolateral pontine tegmentum, a brain region densely connected to the ventral vAIC as well as the pregenual anterior cingulate cortex (pACC) in healthy subjects, was correlated with coma. Furthermore, in coma patients, the connections between the vAIC and the pACC was disrupted.

Irene Tracey and her collaborators slowly induced anaesthesia in healthy volunteers during fMRI scans, whilst presenting different stimuli, and noticed that stimulus-evoked activity in the dorsal anterior insular cortex (dAIC) was decreasing during the onset of loss of behavioural responsiveness. During anaesthesia, and therefore during the loss of consciousness, the dAIC was

additionally found to have less functional connections to other parts of the brain. It was further suggested that the dAIC acts as a "potential cortical gate responsible for loss of behavioural responsiveness" (Warnaby et al., 2016).
Many of these findings once more indicate the vital role the insula plays in consciousness and awareness, as already suggested by A.D. Craig (Craig, 2002, 2009a).

Electrical Microstimulation of the Insular Cortex

To further establish and expand the knowledge about the insula's function and to uncover its intricate details, yet another method, besides tract tracing (Mesulam and Mufson, 1982b) and functional imaging (Caria et al., 2007), has been employed in the past decades: electrical microstimulation of neuronal elements. With the earliest studies conducted in 1870 by Gustav Fritsch and Eduard Hitzig (Fritsch and Hitzig, 1870) in the brains of dogs (for details see the chapter *Electrical Microstimulation*), electrical microstimulation soon became an established method to investigate the functions of a brain area. In the 1940s, Melissa Hines and Geoffrey M. Boynton conducted one of the first notable stimulation studies in foetal monkeys (66-days) and found that the artificial evocation of action potentials in the areas, that would later form the insula cortex and the frontal operculum, led to the contraction of contralateral muscles, whereas stimulation of other brain areas produced no such effect. In older monkeys (85-days), more elaborate muscle movements were observable (Hines and Boynton, 1940). A few years later, Kaada et al. stimulated neuronal elements in the insular cortex of adult anaesthetized macaque monkeys with square wave pulses. They found inhibition of the respiratory movements after stimulation with 40 – 100 Hz, followed by a return to the regular breathing pattern. Additionally, during these high-frequency stimulations, an increase in blood

pressure was observed. However, with a lower stimulation frequency (10 — 20 Hz), the blood pressure was decreasing. With this, the team showed the insula's involvement in breathing regulation (Kaada et al., 1949). Subsequently, Wilder Penfield and his colleague Herbert Jasper stimulated neuronal elements in the posterior insular cortex of awake humans, whilst most of their fellow researchers were working with monkey models and found auditory sensations to be elicited (Penfield and Jasper, 1954; Penfield and Perot, 1963). Two years later, in October 1956, José Guillermo Frontera published an extensive study detailing stimulations in the insular cortex of monkeys, finding them to elicit different kind of movements and muscle contractions (Frontera, 1956).

After the 1950s the stimulations in the insular cortex of different species declined but in the 1990s this approach was resumed by Oppenheimer and his team, which stimulated cells in the insular cortex of humans and found that they were able to induce bradycardia after left side stimulation and tachycardia after right side stimulation (Oppenheimer et al., 1992). This asymmetry, however, could not be replicated in either the present study nor in a study published by Chouchou and his team in early 2019. The latter authors electrically stimulated the insulae of 47 patients and were not able to confirm a lateralized effect. However, they did find that the stimulation of the posterior insula predominantly led to tachycardia, whereas stimulation of the anterior median insula led to bradycardia (Chouchou et al., 2019).

Ostrowsky and her colleagues stimulated neuronal elements in the anterior and posterior insular cortex of 43 human patients and were able to elicit noxious sensations in 32 % with stimulations in the right upper posterior part and innocuous sensations in the bilateral posterior part of the insular cortex in 37% of patients. Noxious and innocuous areas overlapped and showed a tendency for somatotopic organization (Ostrowsky et al., 2002). With this, the team corroborated previous studies indicating the involvement of the insular cortex in

pain (e.g. Casey et al. (1994)). In 2008, Afif et al. stimulated the upper portion of the middle short gyrus of the insula in awake patients and were able to elicit painful responses suggesting once more the insula's involvement in pain processing (Afif et al., 2008). Two years later, the same team stimulated neuronal elements in the middle gyrus of the insula of 25 patients and uncovered that they were able to elicit a lowering of voice intensity and speech arrest (Afif et al., 2010). Similar results were obtained by Mazzola and her team in 2017, who also found speech impairments after relaying stimulating pulses to the insulae of 222 patients. Furthermore, they found more than 82 % of stimulations to evoke clinically relevant responses such as somatosensory, auditory, vestibular, gustatory, and olfactory sensations (Mazzola et al., 2017). In other studies, the same team found that these responses can be allocated to different parts of the insula, with the anterior parts showing visceral reactions and the posterior parts being involved in somatosensory functions as well as pain perception (Mazzola et al., 2019) and vestibular responses (Mazzola et al., 2014). Pain perception was also investigated by the same team in 2012, in a study revisiting Wilder Penfield's results from the 1950s. While they found only 1.4 % of stimulations in the posterior insular cortex and the neighbouring parietal operculum to elicit pain, they did not find other cortical sides to elicit pain during stimulation, not even brain areas that are active in the perception of pain like, for example, the somatosensory areas. They, therefore, concluded that only the stimulation of the posterior insula or the parietal operculum activates the pain network (Mazzola et al., 2012) (for more information on networks see subchapter *The Insular Cortex as a Network Hub*). The involvement of the insula in another network was shown by Koubeissi and his team in 2014. When they stimulated the left claustrum and the left AIC of an epileptic patient, they were able to disrupt behavioural signs of consciousness. They, therefore, concluded these structures to be part of a network that subserves consciousness (Koubeissi et al., 2014).

Caruana and his team found that stimulations in the insula of an awake monkey can elicit emotional behaviours like disgust and affiliative states and with this tied the insula to social and communicative behaviours (Caruana et al., 2011). The involvement of the insula in recognition of disgust was shown by Papagno and her team five years later when they delivered stimulations to the left insula of patients and found them to perform worse in recognising disgust in other people's faces. However, resection of the left insula still allowed the patients to recognize disgust, indicating the insula working in a network (Papagno et al., 2016).

The studies mentioned above provide a small window into the various functions of the insula and the different ways to study them but, taken together with the results described in *Connectivity and Functions of the Insular Cortex*, paint already an exhaustive picture of the multifariousness and complexity of this brain area.

The Insular Cortex as a Network Hub

Humans have been fascinated by the mysteries of the brain for almost three thousand years, with reports dating back as early as the 6th century B.C.E. (Crivellato and Ribatti, 2007). To facilitate the studies on this complex organ, the brain was segregated into smaller units sharing similar characteristics like cytoarchitecture (Brodmann, 1909) or receptor types (Zilles and Palomero-Gallagher, 2017). A myriad of brain regions and parcellations were thusly discovered and summarized in atlases (von Bonin and Bailey, 1947; Allen Institute for Brain Science, 2004; Saleem and Logothetis, 2006; Economo and Koskinas, 2008; Mai et al., 2015) to aid the study of particular brain regions.

Early lesion studies by the French anatomist Paul Broca (Broca, 1861) and later by German neurologist Carl Wernicke (Wernicke, 1874), as well as early electrical microstimulation studies (Fritsch and Hitzig, 1870; Ferrier, 1875), initially

suggested that a cognitive or motor function is localized in a specific brain region. This view, however, was cast aside quickly, because the amount of tasks the brain can attend to vastly exceeds the number of regions which constitute it. Additionally, studies reported that single neuronal events can influence the brain globally (Logothetis et al., 2012) and that neuronal correlates of a given task can be found in several brain regions simultaneously. Furthermore, the advancement of techniques like functional magnetic resonance imaging (Ogawa et al., 1990a; Logothetis, 2002) and positron emission tomography (Raichle, 1983), allowing the investigation of the whole brain, revealed that brain regions react in concert to a given task and by this form *functional networks*.

The first functional network that was discovered fortuitously was the default mode network (DMN), a fixed set of brain regions displaying higher metabolic activity during resting state than during task engagement (Greicius et al., 2003). The seminal meta-analysis by Gordon L. Shulman and colleagues in 1997 (Shulman et al., 1997) and later by Bernard Mazoyer (Mazoyer et al., 2001) and Marcus Raichle (Raichle et al., 2001) brought this phenomenon to broader attention in the neuroscientific community. The regions comprising this network, which is thought to mediate introspection and self-referential processes (Wen et al., 2013), are portions of the posterior parietal cortex, the posterior cingulate cortex, and the ventromedial prefrontal cortex (Buckner et al., 2008). Whilst they are displaying lower metabolic activity during a task, another set of brain regions, including the intraparietal sulcus, the frontal eye field, some regions of the precentral sulcus, as well as the middle temporal area, are more active during the engagement in a task and are therefore summarized in the central executive network (CEN) (Fox et al., 2005). In the last few years researchers have grouped several other brain regions together, which exhibit functional connectivity, and conflated them into networks like the frontoparietal network, which includes the intraparietal sulcus, the inferior parietal lobe, the dorsal premotor cortex, and the

frontal eye field (Ptak, 2012) and was suggested to control attention (Scolari et al., 2015); or the cingulo-opercular network, which includes the medial frontal cortex, the AIC, and the frontal operculum (Vaden et al., 2013) and is thought to be relevant for tonic alertness (Sadaghiani and D'Esposito, 2015).

Another network, first described in 2007 by William Seeley and Michael Greicius (Seeley et al., 2007) is the salience network (SN). It has been shown that this complex of brain regions performs a bottom-up detection of salient stimuli and assesses their relevance to facilitate access to resources for the management of autonomic reactivity and the adjustment of top-down signals (Eckert et al., 2009; Menon and Uddin, 2010; Chen et al., 2016). It comprises the AIC, the ACC, as well as the subcortical structures amygdala, ventral striatum, substantia nigra, and ventral tegmental area (Seeley et al., 2007). The SN appears to be the most flexible network in terms of temporally and spatially varying connectivity with other networks while continually maintaining a high degree of network centrality over time (Chen et al., 2016).

The human SN was found to be divisible into a ventral and dorsal network, with the ventral part rooted in the vAIC and the dorsal part rooted in the dAIC (Touroutoglou et al., 2012). Whilst the ventral SN regulates homeostatic processes, as well as interoceptive and affective experiences, the dorsal part is involved in attention (Corbetta et al., 2008). A similar division could also be found in macaque monkeys, though the dorsal SN seems to be present to a lesser extent. Similar to humans, the macaque vAIC displays correlations to areas like the anterior and mid-cingulate cortices, the orbitofrontal cortex, the amygdala, and the putamen. Furthermore, correlations were found with the frontoinsula, as well as to the temporal and dorsolateral striate cortex, the frontal cortex, and the mid and posterior insula. The dorsal SN, as in humans, correlates with other regions of the insula, with parts of the frontal and cingulate cortex, and the right

intraparietal sulcus of the parietal cortex. These correlations are however weaker than in humans. Whilst they still allow a clear separation from the ventral network, it suggests at the same time that the macaque dorsal SN is less evolved than in humans, though some additional correlations have been found to e.g. the bilateral subgenual anterior and the posterior cingulate cortex, the pallidum, the basal forebrain, the caudate, the thalamus, the hippocampus, and the cerebellum, as well as very high correlations to the putamen and the temporal and occipital cortex (Touroutoglou et al., 2016).

Julia Sliwa and Winrich Freiwald at Rockefeller University were able to distinguish another network in the macaque brain, the social interaction network. By analysing whole brain fMRI scans, which were acquired during the presentation of static or moving stimuli, they were able to uncover a network that seemingly supports social interaction analysis. Anchored in the medial and ventrolateral prefrontal cortex, the network includes the ACC as well as parts of the inferior parietal lobule and the orbitofrontal cortex (Sliwa and Freiwald, 2017).

Several other networks were discovered in the macaque monkey like the lateral grasping network, which was hypothesized to be crucial for the integration of perceptual, cognitive, limbic, and hand-related sensorimotor processes and which is consisting of the inferior parietal, the ventral premotor, and the ventrolateral prefrontal cortex (Borra, 2014); a network to process scenes, consisting of extra striate areas and a scene-selective medial place patch in the parahippocampal gyrus (Kornblith); or different networks in the prefrontal cortex like the orbital prefrontal network, consisting of the olfactory and taste cortices, the inferior temporal gyrus, the insula cortex, and the frontoparietal operculum, thought to play a role in the integration of multimodal sensory information and the assessment of stimuli ; the medial prefrontal network, consisting of the hypothalamus, the brainstem, the anterior and posterior

cingulate cortex, the rostral and dorsal superior temporal gyrus, the amygdala, the hippocampus, and the entorhinal cortex, thought to modulate visceral functions; the ventrolateral prefrontal network, rooted from the ventral to the principal sulcus, thought to be involved in object working memory and memory retrieval; the dorsal prefrontal network, rooted from the dorsal to the principal sulcus and the frontal pole, though to be involved in self-centred functions; or the caudolateral prefrontal network, rooted from the rostral to the arcuate sulcus and the caudal principal sulcus, thought to be involved in eye movements, attention, shape selectivity, and working memory for spatial position (Saleem et al., 2014).

The AIC, with its manifold connections to cortical and subcortical areas (Mesulam and Mufson, 1982b, 1982a; Mufson and Mesulam, 1982) and its ability to integrate interoceptive and exteroceptive signals with cognitive and emotional inputs (Nguyen et al., 2016) from all modalities (Bamiou et al., 2003; Nieuwenhuys, 2012), has been described as a major, causal control hub of the SN (Menon and Uddin, 2010; Chen et al., 2015; Cai et al., 2016). As this, it has been suggested to regulate the DMN (Bonnelle et al., 2012; Chen et al., 2013) by top-down regulation (Wen et al., 2013). Disruptions in this regulation (e.g. damage to white matter tracts within the SN) can lead to malfunctioning of the DMN (Jilka et al., 2014) or diseases like the attention-deficit/hyperactivity disorder (Cai et al., 2015) and major depressive disorder (Hamilton et al., 2016). Hyperconnectivity within the SN has been shown to be connected to autism (Uddin et al., 2013).

However, the tasks of the AIC in a network context seem to extend beyond the regulation of the DMN. In 2008, Sridharan and his team performed Granger causality analysis in two separate human fMRI datasets (resting state and visual attention task) and reported the AIC to be driving the switching between the DMN and the CEN (Sridharan et al., 2008). Furthermore, the AIC was suggested

to play an essential role in perception by heightening the alertness to stimuli or tasks, which are important to an individual's homeostasis (Sterzer and Kleinschmidt, 2010). Additionally, the AIC was reported to be involved in inhibition tasks (Swick et al., 2011) as well as in the detection of and the orientation to salient events (Cai et al., 2014) to guide goal-directed behaviour (Dosenbach et al., 2007).

In an attempt to explain how the AIC fulfils such a versatile role within the SN, it was suggested that the insula is a rich club hub (van den Heuvel and Sporns, 2013). Rich club hubs are nodes, which display a high degree of connectivity inside and outside of their network (Michel, 2017), e.g. the precuneus, the superior frontal and superior parietal cortex, as well as the subcortical hippocampus, the putamen, and the thalamus, and which share strong connections with other high degree nodes (van den Heuvel and Sporns, 2011). Through such an organization, the brain manages efficient signal transmission over short pathways saving time, materials, and energy (Laughlin and Sejnowski, 2003) and sustains only short transmission delays, minimizing interferences and enabling fast synchronisation (Gomez-Gardenes et al., 2010) and thusly boosting the robustness of the system (van den Heuvel and Sporns, 2013).

The unravelling of the functional principles of the brain by analysing functional networks has become more practical in recent years with the significant advancements in collecting and storing big data, augmented computer power, and new perspectives and outlooks on research (Bassett and Sporns, 2017; Bzdok and Yeo, 2017). Under these premises, more details about the inner workings of the human mind shall be unveiled in the near future.

3

ELECTRICAL MICROSTIMULATION

During electrical microstimulation in the brain, a small, confined population of neuronal elements is stimulated by an electrical current from a nearby microelectrode. This method has been used extensively to study connectivity (Field et al., 2008; Matsui et al., 2011; Pérez-Cervera et al., 2018), to probe cortical functions (Romo et al., 1998; Graziano et al., 2002; Moore et al., 2003), to investigate diseases of the brain (Munari et al., 1993; Valentin et al., 2002; MacKinnon et al., 2005), to study perception (Salzman et al., 1990; Cohen and Newsome, 2004; Murphey and Maunsell, 2007), and to restore neurological functions (Grill and Kirsch, 2000; Bierer and Middlebrooks, 2004; Bradley et al., 2005).

About eighty years after the discovery of *animal electricity* by Italian physician Luigi Galvani in the 18th century (Kazamel and Warren, 2017), the physicians Gustav Fritsch and Eduard Hitzig were among the first scientists to successfully use electrical microstimulation in the brain to elicit muscular movements on the contralateral side in the awake but restrained dog in 1870 (Fritsch and Hitzig, 1870). Shortly thereafter, the primate motor cortex was probed, and its organization studied. David Ferrier did his electrical microstimulation experiments in monkeys (Ferrier, 1875), whereas Charles Sherrington and Albert Grünbaum conducted their experiments in great apes (Grünbaum and Sherrington, 1902). Around the same time, the first studies in the human brain were performed by neurosurgeons Fedor Krause (Krause, 1909) and Harvey Cushing (Cushing, 1909), showing that electrical microstimulation can cause sensory responses. Wilder Penfield, a former student of Krause, and Edwin Boldrey built upon that discovery and obtained, by employing the same method,

the first extensive map of the body's somatic, motor, and sensory representation in the cerebral cortex of men in 1937 (Penfield and Boldrey, 1937). Several other studies followed (Penfield, 1947; Penfield and Perot, 1963; Asanuma and Sakata, 1967; Brindley and Lewin, 1968) but it wasn't until 1975 that James Byrne Ranck explained, in his ground-breaking publication, the fundamental basis of electrical microstimulation of the mammalian central nervous system (Ranck, 1975).

Functional Mechanisms of Electrical Microstimulation

The neuronal resting state membrane potential results from uneven ion distributions between the inside and the outside of the cell. The concentration of potassium ions within the cell is approximately 30 times higher than in the extracellular space (140 mM and 3.5 – 5 mM, respectively), whereas the sodium concentration in the extracellular space is significantly higher than in the cytosol (145 mM and 10 – 15 mM, respectively). Since the plasma membrane acts as a diffusion barrier that is only selectively permeable for potassium ions, the Na^+/K^+-ATPase is continuously active, transporting two potassium ions in and three sodium ions out. This leads to a negative charge of the intracellular space (-95 mV) compared to the extracellular space (+60 mV) and generates a resting state membrane potential of around -70 mV (Pape et al., 2005). All the above values have been canonically averaged over literature and vary depending on the cell type. (The resting membrane potential for a specific cell, which is beyond the scope of the present section, can be calculated using the Goldman-Hodgkin-Katz equation (Goldman, 1943; Hodgkin and Katz, 1949)).

When an action potential arrives beyond the post-synaptic plate, voltage-dependent sodium channels open and sodium enters the cell, leading to a depolarization of the cell membrane up to +30 mV (overshoot). 1 – 2 ms after opening, these channels start to spontaneously close by dislocating the

intracellular protein domain between the third and fourth transmembrane segment into the pore of the channel. When the sodium channels begin to be deactivated, delayed rectifying potassium channels open and potassium flows out of the cell into the extracellular space, hyperpolarizing the cell membrane to a potential that is lower than the resting state membrane potential (-95 mV, undershoot). After the closing of the potassium channels, the membrane potential is restored to its baseline (-70 mV) by the sodium-potassium pump. Due to the non-excitability of the voltage-dependent sodium channels and a membrane potential that is too hyperpolarized to activate the delayed rectifying channels, this part of the neuron is unable to produce or propagate an action potential for several milliseconds. This period is called refractory time and allows the action potential to only propagate forward (orthodromic propagation) (Pape et al., 2005).

During electrical microstimulation, the extracellularly injected current changes the voltage on the outside of the cell, leading to a change in the membrane potential (Ranck, 1981), which, in turn, leads to an opening of the sodium and potassium channels of the membrane, generating an action potential. Interestingly, this action potential is not limited to an orthodromic propagation, like naturally generated potentials, but can travel antidromically, since initially, no channels are in the refractory period.

Electrical microstimulations can be conducted with different kinds of electrodes, namely bipolar and monopolar electrodes. A bipolar electrode, in this context, comprises two same sized electrodes with the same impedance, arranged slightly apart but both within the brain matter. A monopolar electrode can be either a cathode or an anode.

Both electrode types have advantages and disadvantages, and the selection of an appropriate electrode depends on the experimenter's needs. If the experiment

has a simultaneous recording component, besides the microstimulation, bipolar electrodes offer a higher signal-to-noise-ratio as well as smaller stimulation artefacts than monopolar electrodes (Gabriel, 2011). If only electrical microstimulation is conducted either electrode will stimulate approximately the same area with low currents. With higher currents, the monopolar electrode has a greater effective current spread (Valenstein and Beer, 1961; Stark et al., 1962).
The monopolar stimulation electrode can be either an anode or a cathode, with the ground electrode being outside of the brain. If the stimulating monopolar electrode is an anode, electrons will be taken up from the extracellular space, rendering it more negative and leading to a hyperpolarization of the cell membrane. In contrast, the use of a cathode as the monopolar stimulation source leads to the addition of negative charge to the extracellular space, which, in turn, leads to a depolarization of the membrane. However, every outward current that locally depolarizes a cell membrane comes with an opposite, same sized inward current at a nearby location. Since this rectifying inward current is spread over a large area, the resulting hyperpolarization will be smaller than the depolarization, and the action potential can propagate. If the stimulus is too strong, and the resulting hyperpolarization is as prominent or more prominent than the depolarization, the action potential will be blocked (anodal surround blocking) (Ranck, 1975).

Which Elements are excited during Electrical Microstimulation in the Mammalian Central Nervous System?

This question was posed by American neuroscientist James Byrne Ranck in his seminal 1975 paper (Ranck, 1975) and remains, until today, not fully answered, though much progress has been made in the last four decades. (Histed et al., 2009; Borchers et al., 2011; Ohayon et al., 2013) (See chapter *Advantages and Limitations of Electrical Microstimulation*).

It is now known, that myelinated axons, mainly the axon initial segments and the nodes of Ranvier, the neuronal elements with the highest density of sodium channels (Catterall, 1981; Freeman et al., 2016), need the least amount of current to be excited, with large fibres needing less current than small fibres (Nowak and Bullier, 1998b; Rattay, 1999; Borchers et al., 2011).

However, the direct excitation of neuronal elements is highly dependent on several different parameters:

The current, and with it the voltage, spreads in a spherical fashion from the electrode tip. According to the Maxwell equations (given the spherical symmetry, the conservation of charge, the resistivity characteristics of homogeneity, the isotropy, and the consistency, as well as an assumed magnetization constant of 0), the voltage decreases over distance, limiting the radius of the sphere that leads to successful stimulation. The size of the radius of the sphere depends on (i) the size of the electrode tip, (ii) the resistivity of the tissue, (iii) the orientation of the electrode, (iv) the waveform of the stimulus as well as (v) the currents duration and the strength.

(i) The electrodes tip size has a substantial influence on the near field current-density and therefore needs to be selected with care. Generally, small tipped electrodes with low currents minimize tissue damage and can recruit high-threshold neurons (Tehovnik, 1996).

(ii) The resistivity of brain regions influences the current spread and varies from area to area, depending on the tissue composition. As a general note, it was found that grey matter has a lower resistivity than white matter (Robinson, 1962).

(iii) The orientation of the fibres regarding the electrode is equally decisive to determine which neuronal elements are being stimulated. With an electrode orientation transversal to the fibre tract orientation, the

current needed to elicit an action potential, if one can be generated at all, is significantly higher compared to a longitudinal orientation (Rushton, 1927; Rudin and Eisenman, 1954). Therefore, fibres lying along the equipotential line will not be stimulated (Ranck, 1981).

(iv) The waveform of the stimulus can be monophasic or biphasic, with different phase parameters. Whilst monophasic stimuli are known to initiate action potentials efficiently; they lead to tissue damage due to the negative electrode charge during inter-pulse intervals, which slowly discharges through Faradaic reactions.

Biphasic pulses are less damaging to the tissue, but at the same time, are less efficient in generating action potentials and are more corrosive to the electrode. In a biphasic pulse, an action potential generating first phase is followed by a second phase, reversing the electrochemical processes generated by the stimulation and thus minimizing tissue damage. In a charged balanced biphasic pulse the reversal phase has the same size as the exciting phase, in a charged imbalanced biphasic pulse, the reversal phase is smaller to minimize the extent of electrode corrosion (Merrill et al., 2005).

(v) The effects of the current strength and duration are strongly intertwined. With a reduction of the strength but an increase of the duration, the same amount of excitation can be reached and vice versa. Furthermore, both parameters can be used to determine the chronaxies of neuronal elements. The *chronaxie* is the time that a current, with a double rheobase strength, needs to flow to be exciting. The *rheobase current* is the current strength that evokes action potentials 50 % of the times, with assumed infinite stimulus duration (Ranck, 1981; Tehovnik et al., 2006). A positive correlation can be found between the chronaxie values and the

refractory period (Shizgal et al., 1991), whereas a negative correlation can be found with the conduction velocity of axons (West and Wolstencroft, 1983; Nowak and Bullier, 1998a). Chronaxie values can be used to determine the needed current strength for the stimulation of a particular neuronal element. If the chronaxie values are not known through prior experimentation, they can be ascertained empirically (Geddes and Bourland, 1985), otherwise they can be obtained from the literature. Chronaxie values for large, myelinated axons and small, non-myelinated axons in cats (West and Wolstencroft, 1983), cell bodies and axons in rats (Nowak and Bullier, 1998b) and cats (Asanuma et al., 1976; Shizgal et al., 1991), for A- and C-fibres in peripheral nerves in cats (Li and Bak, 1976), for pyramidal tract neurons in monkeys (Tehovnik et al., 2006), and for humans retina cells (Rushton and Brindley, 1978) have been described in literature.

Besides the direct activation described above, neurons can also be activated indirectly (Tehovnik et al., 2006; Histed et al., 2013). By polysynaptic signal propagation (Asanuma and Rosén, 1973; McIlwain, 1982; Logothetis et al., 2010; Matsui et al., 2011; Vincent et al., 2017) activation can be elicited in brain regions, which are not directly connected with the stimulation site (Vincent et al., 2007; Honey et al., 2009). This indirect activation can greatly exceed the direct activation (London et al., 2010) and can be measured for example electrophysiologically (Tehovnik et al., 2006) or with fMRI recordings (Tolias et al., 2005).

Advantages and Limitations of Electrical Microstimulation

For the past 200 years, electrical microstimulation of neuronal elements in the brain has been a powerful tool used to further our understanding of the brain; its behaviour, its functions, and its connectivity.

What makes it such a tremendously reliable method, is the opportunity to precisely perturb a confined population of cells (Ranck, 1981; Tolias et al., 2005) with very small currents (Ranck, 1975; Tolias et al., 2005) deep within the brain matter (Vincent et al., 2007) to elicit a mimesis of natural activity (Sultan et al., 2007; Histed et al., 2013). Furthermore, it can easily be combined with other methods, like fMRI (Tolias et al., 2005; Matsui et al., 2011) or optogenetics (Ohayon et al., 2013), to uncover, for instance, functional connectivity (Logothetis et al., 2010).

However, unto this day, the significant drawbacks, besides its invasiveness (Ranck, 1975), are the nescience of which neuronal elements are being stimulated, the possibility of stimulating fibres of passage (Ohayon et al., 2013), and the inability to only stimulate specific subpopulations (Ranck, 1975; Ohayon et al., 2013). Nonetheless, it has been and will stay a widely used method to uncover the secrets of the brain.

4

MAGNETIC RESONANCE IMAGING

Magnetic resonance imaging (MRI) is arguably the most prevalent, non-invasive imaging method used in research and medicine today. With a remarkable history of development, comprising many different contributors, it managed to emerge as one of the most useful diagnostic tools that is available to the modern day scientists and physicians.

With the discovery of the X-rays on the 8th of November in 1895 by Wilhelm Conrad Röntgen (Dunn, 2001), who was awarded the first Nobel Prize in Physics in 1901 “in recognition of the extraordinary services he has rendered by the discovery of the remarkable rays subsequently named after him” (Nobel Foundation, 1901), the field of diagnostic radiology was born. Almost 50 years later, on the 16th of June 1949, a publication about ultrasound waves for diagnostic purposes by George Döring Ludwig furthered the field (Ludwig and Struthers, 1949). However, by far, the most significant advancement in the field was the invention of the MR method.

Using the principle of the rotating magnetic field, discovered by Nikola Tesla in 1882 (Swezey, 1958; Roguin, 2004), the American physicist Isidor Isaac Rabi measured the single states of the rotation of atoms and molecules and was able to determine their mechanical and magnetic moments and with this laid the groundwork for the modern MR methods. He was awarded the Nobel Prize in Physics in 1944 "for his resonance method for recording the magnetic properties of atomic nuclei" (Nobel Foundation, 1944). Subsequently, the physicists Felix Bloch (Bloch, 1946) and Edward Mills Purcell (Purcell et al., 1945) modified the method to be used on liquids and solids and received the Nobel Prize in Physics in 1952 “for their development of new methods for nuclear magnetic precision

measurements and discoveries in connection therewith". Shortly thereafter, the physician Raymond Damadian proposed to use this method to distinguish cancerous from healthy tissue (Damadian, 1971). He developed a full body scanner and was able to produce the first ever MR scan of a thorax on the 3rd of July in 1977. However, his method was slow and was soon replaced by a different approach.

The chemist Paul Christian Lauterbur used the MR method to create one-dimensional images of water vials, which he reconstructed to obtain two-dimensional images and realized that this method could be used for biomedical applications (Lauterbur, 1973). Around the same time, the British physicist Sir Peter Mansfield reduced the scanning time from hours to minutes, evolving the method to a rapid imaging technique (Mansfield and Grannell, 1973; Garroway et al., 1974). Both Lauterbur and Mansfield were awarded the Nobel Prize in Medicine in 2003 "for their discoveries concerning magnetic resonance imaging" (Nobel Foundation, 2003).

Since the first scan in 1977, the number of publications with *MRI* in the title has skyrocketed. A search in the web of sciences citation index in early 2019 revealed that 737124 publications have been listed between 1977 and 2019, reflecting the popularity of the method.

The Physics behind Magnetic Resonance Imaging

The MR technique has been refined and improved over the years, however, the basic principles for its functioning remained the same. The following paragraphs will explain the physics founding the method with the information obtained from the books *Nuclear Magnetic Resonance-Basic Principles (Rahman, 1986)* and *How does MRI work? An Introduction to the Physics and Function of Magnetic*

Resonance Imaging (Weishaupt et al., 2014) and the publication *What we can do and what we cannot do with fMRI* (Logothetis, 2008).

The total angular momentum of an atomic nucleus can be represented as the nuclear spin. Electrons, protons, and neutrons have half-integer spins and are called fermions (Bannwarth et al., 2011), in contrast to bosons, which have full integer spins (Pelte, 2005). All spins constitute a magnetic moment, with the protons and neutrons magnetic moment being smaller than the electrons.

When an atom possess an even number of nucleons (protons and neutrons), all spins will pair up with an antiparallel spin, and the resulting net spin will be 0. However, if the number of nucleons is odd, the net spin will be an integral multiple of ½. This is the case for hydrogen (^{1}H) and carbon (^{13}C), the elements of most interest to the MR measurements, since they are most abundant in living tissue (Cooper, 2000).

At rest, the spins of subatomic particles are randomly oriented, but when an external, uniform magnetic field, B_0, is applied, the spins are quantized and will adopt one of (2*spin number +1) orientations. In the case of ^{1}H and ^{13}C, which both have a spin quantum number of ½, there will be two possible orientations (spin up and spin down).

The energetically more favourable orientation is the spin-up state, where the spins are aligned with B_0. A slight excess of spins in this orientation (which follows the Boltzmann distribution (Widom, 2002) and increases with field strength) leads to a longitudinal net magnetization. A change from longitudinal magnetization to transversal magnetization, as well as a synchronization of phases between different nuclei, can be achieved by emitting an electromagnetic radiation field B1 or radio frequency (RF) pulse, perpendicular to B0, with precisely the nuclear precession frequency. The nuclear precession frequency, also called Larmor precession, is the frequency with which the spins precess

about an external magnetic field. After the RF pulse, the spins between nuclei will dephase again, and the net magnetization will return to the longitudinal state. These processes can be described in two different ways: the longitudinal relaxation, T_1 (spin-lattice relaxation), and the transverse relaxation, T_2 (spin-spin relaxation) (Bloch, 1946).

The spin-lattice relaxation, T1: The nucleus is not only influenced by B_0 but also by a fluctuating field generated by the surrounding lattice (the regular arrangement of molecules in a solid). When the lattice field aligns with the Larmor frequency, the spin can change from the down state to the upstate. The excess rotational or translational energy will be exchanged from the nucleus to the lattice generating the T_1 signal. Since this process is more efficient in gases and liquids than in solids, due to their loose lattices, the resulting T_1 time is shorter, leading to a dark contrast in the resulting image.

The spin-spin relaxation, T2: During the spin-spin relaxation, the energy transfer occurs between the spins rather than between the nucleus and the lattice. Each spin acts as a small magnet and has a static component as well as a rotating component, which moves with the Larmor frequency perpendicular to B_0. This static component influences neighbouring spins, independent of B_0. If it opposes the main magnetic field, the influenced neighbouring spins will precess slower and vice versa. The interactions only occur during great proximity and end once the spins move apart, resulting in the recovery of their original frequency. These molecular interactions lead to the pure T_2 effect. However, unavoidable inhomogeneities in B_0 lead to the inhomogeneous T_2 effect, also called T_2^*. Gases and liquids appear with a lighter contrast than solids in T_2 and T_2^* weighted images.

It is important to note that T_1 and T_2 occur simultaneously and independently of each other with T_2 always being smaller or equal to T_1 and T_2^* being smaller than

T_2. Both parameters occur in the order of seconds, leading to a low temporal resolution.

Functional Magnetic Resonance Imaging

The possible applications of the MR method massively exceed the pure anatomical depiction and nowadays is commonly used by scientists and physicians worldwide to investigate the functions of the brain.

The brain, though making up only 2 % of the body weight, is receiving about 12 – 15 % of the cardiac output and consumes circa 20 % of the body's oxygen (Cipolla, 2010). This remarkably high metabolic need can be utilized to decipher the functional working principles of the brain. 50 – 60 % of the brain's energy is used to maintain electrophysiological processes, namely, the maintenance of ion gradients and the transport of neurotransmitters (Ames, 2000). To adequately deliver the needed resources, sufficient blood flow is required. The correlation between blood flow and energy demand has been proposed already at the end of the nineteenth century, when Italian physiologist Angelo Mosso discovered an increase in localized brain pulsation when subjects, with skull bone lesions above the frontal lobe, engaged in cognitive tasks, such as mathematical problems (Mosso, 1881). About one decade later, the British pathologists Charles Roy and Charles Sherrington found experimental proof of this correlation by investigating the expansion and contraction of the brain in dogs, cats, and rabbits as a consequence of nerve stimulation, reduction of blood flow and breathing, drugs, or muscle movements and concluded that "the brain possesses an intrinsic mechanism by which its vascular supply can be varied locally in correspondence with local variations of functional activity" (Roy and Sherrington, 1890). Despite these convincing arguments British physiologist Sir Leonard Hill claimed, after a thorough investigation in 1896, that there was no connection between blood flow

and neural activity (Hill, 1896). Subsequently, research in this field abated until University of Pennsylvania scientists Seymour S. Kety & Carl F. Schmidt developed a method in 1945 to, for the first time, measure cerebral blood flow quantitatively. They introduced the nitrous oxide technique, which allowed, with the determination of arterial and cerebral venous blood concentrations of nitrous oxide and the application of the Fick principle (Fick, 1870), to calculate the cerebral blood flow (Kety and Schmidt, 1948). However, these measurements were only possible for the whole brain, not for specific brain areas. To accurately determine the "rates of energy metabolism in specific discrete regions of the brain in normal and altered states of functional activity" (Sokoloff, 1977) the desoxyglucose autoradiography method was developed by the American neuroscientist Louis Sokoloff and his team in 1977, where 2-deoxy-D-[14C]glucose was used as a tracer in alert laboratory animals (Sokoloff et al., 1977). The first measurements in humans were performed around the same time using radiotracers (Ter-Pogossian et al., 1969; Ter-Pogossian et al., 1970; Raichle et al., 1976), which are still used in modern day positron emission tomography (PET) (Raichle, 1983).

Besides PET, the fMRI method also uses the principle of activity-coupled blood flow to indicate brain function. Initially, the externally introduced rare earth material, contrast agent gadolinium was used in dogs (Belliveau et al., 1990) and one year later in humans (Belliveau et al., 1991), to depict brain activity. However, the need for an external-contrast-agent-free method arose, which was met by the blood-oxygen-level-dependant (BOLD) contrast mechanism, first described by Japanese biophysicist Seiji Ogawa (Ogawa et al., 1990a; Ogawa et al., 1990b) in rats. It utilizes the naturally occurring contrast agent deoxyhaemoglobin, which is paramagnetic and therefore leads to signal dropout where it occurs.

The magnetic properties of haemoglobin were already noticed by British physicist Michael Faraday in the nineteenth century (Faraday et al., 1932) and were further studied by the chemists Linus Pauling and Charles Coryell, who discovered a severe difference between the magnetic behaviour of oxygenated and deoxygenated haemoglobin. Whereas oxyhaemoglobin contains no unpaired electrons, deoxyhaemoglobin contains four electrons and therefore acts paramagnetic (Pauling and Coryell, 1936). This feature was exploited by American biochemist Keith Thulborn (Thulborn et al., 1982) in 1982, nine years before Ogawa did his ground-breaking studies, and he used this difference to demonstrate "the feasibility of measuring the state of oxygenation of blood in vivo with MRI" (Raichle, 2009).

The potential of the BOLD contrast to indicate brain activity in a particular brain area was swiftly appreciated and applied to humans (Bandettini et al., 1992; Frahm et al., 1992; Kwong et al., 1992; Menon et al., 1992; Ogawa et al., 1992). Furthermore, it was combined with other methods like electrophysiology (Logothetis et al., 2001; Logothetis et al., 2012), microstimulation (Logothetis et al., 2010; Matsui et al., 2011), electro-encephalography (Menon et al., 1997; Bonmassar et al., 1999; Krakow et al., 2000), or magnetoencephalography (Dale and Halgren, 2001). The combinational methods of electrophysiology and microstimulation will be further discussed in the section *Combining fMRI with Electrophysiology or Microstimulation*.

The need for sufficient metabolic resources during neuronal activity leads to an increase in blood flow and glucose consumption. Interestingly, oxygen consumption increases only moderately (Fox and Raichle, 1986; Fox et al., 1988), leading to a decrease in deoxyhaemoglobin. Naturally, one would therefore expect a negative BOLD signal, since, as stated previously, the deoxyhaemoglobin leads to a signal dropout in the confined spaces of the blood

vessels (Ogawa et al., 1990a; Ogawa et al., 1990b). However, the increased blood flow is flushing out deoxyhaemoglobin and replacing it with oxyhaemoglobin, leading to a positive BOLD signal (Akgoren et al., 1994; Chaigneau et al., 2003). The positive BOLD signal therefore represents neuronal activity. However, it was unknown for the first 21 years after the discovery of the BOLD contrast, which part of the neuronal activity is being represented. In 2001 the Greek neuroscientist Nikos Logothetis published a seminal paper uncovering the mechanisms underlying the BOLD signal (Logothetis et al., 2001). He and his team conducted experiments in the visual system of anesthetized macaque monkeys and discovered that the BOLD signal is more closely linked to "the input and intracortical processing of a given area rather than its spiking output". The BOLD signal alterations, after a visual stimulus, were closer to the simultaneously measured local field potentials (LFP) than to the multiunit activity (MUA). They suggested that the spatial summation of several millimetres occurring in the LFP but not in the MUA (only several hundred micrometres) could be one of the factors contributing to this correlation.

Though significant advances have been made in recent years in understanding the mechanisms behind the BOLD signal, it still needs to be kept in mind that it represents the mass activity of neurons. One voxel of 55µl contains 5.5 million neurons (Logothetis, 2008), highlighting the need for carefully interpreting results and of combining fMRI with other methods.

Combining fMRI with Electrical Microstimulation or Electrophysiology

The combination of two, in themselves highly evolved and complicated methods is not an easy endeavour and comes with its unique set of problems.

fMRI and electrical microstimulation: The combination of fMRI and electrical microstimulation has been successfully established by several groups

over the years (e.g. Logothetis et al. (2010); Matsui et al. (2012); Moeller et al. (2017)). However, two major problems arise with the nexus of these two sophisticated techniques.

Firstly, commercially available equipment, like a stimulation source, cannot be placed in the MR environment. Placing the stimulation source outside, however, leads to an increased cable length. Since the cable connecting the stimulation source and the electrode always needs to be charged, more current will be lost in a longer cable. To avoid this loss of current and a subsequent resulting weaker stimulation than anticipated, the recharging of the cable can be measured indirectly with a sensor and the missing current can be additionally injected so that the electrode can deliver the set intensity. Furthermore, the current source can be built to custom not to contain any magnetic parts and can therefore be introduced into the MR environment and be placed as close to the electrode as possible, significantly decreasing cable length. The second major problem that arises with the combination of fMRI and electrical microstimulation are interferences, which can enter through the current source and can propagate to the electrode, disturbing the MRI acquisition. To bypass this, a high-frequency filter can be introduced into the current source.

The combination of fMRI and electrical microstimulation is an excellent tool to perturb local, small populations of neuronal elements and to monitor the effects on the whole brain. It has been often used in the past 20 years to unveil functional connectivity patterns and to advance our understanding of the brain.

One of the first studies was conducted by Tolias et al. in 2005, where they delivered electrical microstimulations to the visual system of anaesthetized macaque monkeys and found that the current spread further than calculations had predicted. From this, they concluded that injected current could spread via horizontal connections (Tolias et al., 2005). Also stimulating in the visual system

of awake and anaesthetized macaque monkeys, Logothetis and his team uncovered in 2010 that the stimulation of neocortical afferents leads to a disruption of cortico-cortical signal propagation and silencing of said neocortical outputs (Logothetis et al., 2010). Matsui and his team confirmed in 2011 and 2012 that electrical microstimulation does not only effect monosynaptic targets but can also propagate polysynaptically when they stimulated in the somatosensory areas in anaesthetized macaque monkeys (Matsui et al., 2011; Matsui et al., 2012). Similar findings were obtained by Sultan et al. in 2007 for the visual system in awake macaque monkeys (Sultan et al., 2007). In 2013 Premereur and her colleagues showed task-dependent modulation of occipital areas by delivering electrical microstimulations to the frontal eye field of awake monkeys performing a visually guided saccade task or two different kinds of passive fixation tasks (Premereur et al., 2013). In 2016 the same team stimulated face and body patches in monkeys and found a higher BOLD signal in face and body processing systems, respectively and therefore suggested that these two systems are largely separated in the monkey (Premereur et al., 2016). Arsenault et al. found in 2014 that electrical microstimulation in the VTA in monkeys leads to an overall activation in the dopaminergic reward system and with this suggested that the VTA might regulate "stimulus-specific reinforcement and motivation as well as in modulating activity throughout the reward system" (Arsenault et al., 2014). Moeller and his team used the combination of fMRI and electrical microstimulation in 2017 and found that the electrical microstimulation of face patches in the awake macaque monkeys lead to a distortion of face perception, whereas non-face object could still be perceived correctly (Moeller et al., 2017). In 2018 Caprara and her team conducted electrical microstimulations in the posterior part of the anterior intraparietal area during fMRI recordings and

found that ultra-fast shape processing information flow occurs between the parietal and frontal cortex (Caprara et al., 2018).
The combination of electrical microstimulation in the insular cortex and fMRI in the anaesthetized macaque monkey was the main topic of this thesis and will be described in details in the attached paper by Smuda et al. 2019.

fMRI and electrophysiology: Combining fMRI with electrophysiology is an extremely appealing approach since both methods can complement each other and minimize, to some extent, each other's weaknesses. Whilst fMRI has a rather poor temporal resolution and can, as previously discussed, only reflect mass activity (Logothetis, 2008), electrophysiology can fill these shortcomings by being able to capture fast neuronal events from small populations. Electrophysiology's limitation of being only able to capture activity on a small scale will be complemented by the global recording scale of the fMRI. Therefore, with the combination of a mesoscopic (electrophysiology) and a macroscopic (fMRI) method, greater multidimensional preciseness is achieved, which significantly aids the unravelling of the mysteries of the brain.

However, this approach remains a challenge until this day and has, to my knowledge, so far only been achieved by one lab worldwide. In 2001, the above-mentioned renowned neuroscientist Nikos Logothetis published the first paper detailing results from such combination experiments (Logothetis et al., 2001) and followed up with a fine-grained account of the method in the pioneering publication *Simultaneous recording of neuronal signals and functional NMR imaging* (Oeltermann et al., 2007) in 2007. In the experimental series, which was conducted for the present thesis, fMRI was not only combined with electrical microstimulation but also with electrophysiology. However, the data has not been analysed yet. Therefore no results are presented in the current work. In the

following section, the problems and solutions of this combination method will be presented nonetheless to show the extensiveness of work that went into designing and conducting these additional experiments.

In their pioneering experiments, as well as in the experiments underlying the present thesis, commercially available recording equipment could not be used in the MRI environment due to the magnetic properties of many components, e.g. the microelectrodes. Custom made glass-coated platinum-iridium electrodes, with an exposed tip, were used as a substitute.

Specially made, non-magnetic micro drives were used to position the electrodes inside the custom made polyether ether ketone (PEEK) chambers, filled with a mixture of 0.9% sodium chloride and 0.6% agar-agar in deuterium water. The filling of the chambers facilitated a secure connection between the animal and the ground contact, which was inserted into the chamber and consisted of a high capacity silver electrode paddle. Another ground wire was inserted into the animals' mouth, which was isolated from the amplifier.

The microelectrode holder was designed in a particular way to minimize induced voltages.

Commercially available electrophysiological recording setups allow the user to record the voltage inside the subjects' brain and to forward it to the preamplifier. For that, the preamplifier should be positioned near the electrode, to have the shortest possible cable length in order to avoid signal loss and interferences. However, the alterations of the strong magnetic field during MRI recordings would cripple the preamplifier, if it were positioned within the MRI environment, requiring it to be moved outside of the setup leading, in turn, to longer cable length. To avoid degradation of the amplitude of the neuronal signal through high capacitance, interference, or other kinds of signal loss, the electrode used in the above-mentioned experiments did not record the voltage, but the

current in the brain, which is insensitive to the length of the cables. The current was converted into voltage only at the amplifier stage where no interference would occur.

All the cables connected to the animal were passed through a feed-through mechanism, preventing radiofrequency pulses from entering the magnet and distorting the recorded images. Additionally, special precautions were taken to avoid passive interferences and loops forming "inside" and "outside" the cables by using rotational symmetry cables.

Other interferences were originating in the equipment to maintain the animals' health and anaesthesia, namely the infusion line and the electrocardiogram (ECG). Whilst the infusion line could be grounded with the addition of a silver wire, the ECG needed a newly designed preamplifier that would overcome the main problems of ground-loop formation, test pulse generation, and the occurrence of capacitively coupled interference currents.

Interferences effecting the electrode but originating further away, so-called far-interferences, were compensated using a far-interference compensation.

A sensor close to the electrode measured these emerging interferences and forwarded them to the far-interference compensation component, which, in turn, send an equally big but opposite signal to the mouth electrode. If more than one recording electrode was in use, the signals were sent to the grounding wire in the respective chamber, neutralizing the interference.

Hitherto, the combination of fMRI and electrophysiology was not only used to further the understanding of the BOLD signal, as it was done in the seminal publication of Nikos Logothetis in 2001 (Logothetis et al., 2001), but it was also employed to develop a novel technique called Neural-Event-Triggered (NET) fMRI (Logothetis et al., 2012). In this approach, electrophysiologically recorded ripple events, detected in the hippocampus, were used to align the average time

courses of the BOLD signal. Thus, the authors were able to show "that during off-line memory consolidation, synergistic thalamocortical activity may be orchestrating a privileged interaction state between hippocampus and cortex by silencing the output of subcortical centres involved in sensory processing or potentially mediating procedural learning" in awake and anesthetised animals.
This ground-breaking study was the beginning of a new and exciting chapter, which enables the analysis of multi-structure activity in the brain (Logothetis, 2015). It grandly furthers the field of brain research and will be continued by the data, which was collected in the present experiment series. The analysis of this data will follow subsequently to this work and will provide new insights into the effects of insula activity on the whole brain.

5

PROJECT SUMMARY

Research Aims

The insular cortex, a cortical lobe located bilaterally in the depth of the Sylvian fissure in primates, is an important integration hub within the brain. It consists of three distinct sectors: an anteroventral agranular sector, an intermediate dysgranular sector, and a posterodorsal granular sector. Each sector can be further parcellated into smaller, sharply delimited architectonic areas (Evrard et al., 2014). In the last decades, tract tracing and other methods have uncovered a widespread net of connections between the insula and other cortical and subcortical brain areas, especially limbic structures (Mesulam and Mufson, 1982b, 1982a; Mufson and Mesulam, 1982), whilst functional imaging has implicated the insula to be active during many different tasks (Craig, 2009b). Its widespread connections enable the insula to receive a broad spectrum of information, including interoceptive and exteroceptive afferents as well as integrate these afferents with hedonic, motivational, social, and cognitive activities. The integration processes occur within the insula in a posterior-to-mid-to-anterior gradient, hypothetically leading in humans to an ultimate homeostatically contextualized representation of the neurobiological self, which provides the basis for engendering subjective awareness of feelings in the anterior insular cortex (Craig, 2002; Evrard, 2019). Notably, one particular region of the human anterior insular cortex, the frontoinsula, hosts a specialized neuronal morphotype, the von Economo neuron (VEN), which has been shown to decline selectively in the early stages of neuropsychiatric disorders characterized indeed by a reduction in self-conscious feelings (Kim et al., 2011). A smaller homolog VEN population occurs also in the anterior insular cortex in

the macaque monkey, where it is precisely confined to one architectonic area, the lateral agranular area of the insula (Ial or 'VEN area') (Evrard et al., 2012; Horn and Evrard, in preparation). The VEN is a long-range layer Vb projection neuron with an atypical morphology: it has a large spindle-shaped perikaryon with a unique, thick apical and equally thick basal dendrite (Economo, 1926; Seeley et al., 2012). Although the function of the VEN is not fully understood yet, it has been implicated in the modulation of autonomic regulation (Butti et al., 2013) and the representation of internal bodily states (Allman et al., 2010b; Santos et al., 2011).

At the functional network level, the human anterior insular cortex has been identified as a "rich club hub" within the salience network (SN), a network dedicated to the detection of salient events and the subsequent management of autonomic reactivity (Eckert et al., 2009; Menon and Uddin, 2010; Chen et al., 2016). A similar SN also occurs in the macaque monkey and involves, in particular, the ventral anterior insular cortex, where the VEN area is localized (Touroutoglou et al., 2016). The major involvement of the insula in the SN allows not only the evaluation of information's relevance (Michel, 2017) but also the regulation of the activity of other key networks, including the default mode network (DMN) and the central execution network (CEN) (Goulden et al., 2014; Chen et al., 2016).

Electrical microstimulations of this rich club hub in human patients and monkeys have shown asymmetric autonomic responses, depending on the stimulated hemisphere (Oppenheimer et al., 1992; Caruana et al., 2011).

To investigate if, besides the autonomic functions, also the global brain activity appears to asymmetrically regulated upon microstimulation, the left and right VEN areas of three anaesthetized macaque monkeys were separately electrically microstimulated with 100 Hz, biphasic, charged-balanced pulses during

functional magnetic resonance imaging data acquisition. The obtained data was analysed using a general linear model. Thereafter, to investigate the anterior insula's function on a network level, how it acts within the SN, and how it influences other networks, a seed-based correlation analysis was performed on the stimulation dataset as well as on a dataset collected during resting state functional imaging recordings.

Analysis Pathway

To analyse the collected data, different analysis methods were employed, which are described in detail in the appended manuscript. However, the manuscript does not mention the numerous analysis pathways, which were attempted on a trial and error basis in order to mature the final and most optimal analytical approach used for the manuscript. Several toolboxes and methods were studied, tested, and discarded after they proofed inadequate for the given project. This exploration provided the author with a unique background on the relevant data analysis and confidence in the selection of the final tools.

The analytical toolboxes tested in the present project included SPM (Statistical Parametric Mapping (Ashburner, 2012)), Brain voyager (Goebel, 2012), Free surfer (Fischl, 2012), lipsia (Lohmann et al., 2001) and an in-house toolbox. Given the data structure of the stimulation dataset and the resting state dataset, the latter consisting of recorded resting state imaging data combined with electrophysiological recordings (Oeltermann et al., 2007) to eventually conduct a neural-event-triggered fMRI (NETfMRI) analysis (Logothetis et al., 2012; Logothetis, 2015), the in-house toolbox was chosen. The in-house toolbox has been specially developed for the analysis of NETfMRI data but was also optimized for the use of microstimulation datasets (Logothetis et al., 2010). A continuous pipeline was developed and adapted by the author for the current

project, which guaranteed maximal continuity between the analyses of these two different datasets.

After deciding on the toolbox, a reduction of the dimensionality of the data was attempted, to facilitate the data visualization, to reduce abundant features and noise, and to accelerate computational processes. However, classical methods like principal component analysis (PCA), independent component analysis (ICA), or non-negative matrix factorization (NNMF) did not prove successful in the present work.

PCA is a popular analysing technique to reduce dimensionality with minimal information loss by creating variables which are as close to the original dataset as possible but are not defined a priori (Jolliffe and Cadima, 2016). ICA, as an extension of PCA, can minimize the statistical dependence between its components (with PCA the statistical independence occurs only until the second order (Comon, 1994)). The main difference to other methods is that it is statistically independent and non-Gaussian (Tharwat, 2018). NNMF reduces the dimensionality by dividing the dataset into several matrices, none of which have negative elements. Subsequently, meaningful features can be extracted and further analyzed (Gillis, 2014).

However, the dimensionality could not be reduced in the present dataset. It was therefore used for further analysis without any kind of dimensionality reducing preprocessing.

To analyse the networks, the recently developed task-related edge density technique was tested. The strength of this approach is its independence of a hemodynamic response model and dimensionality reduction, making it assumption-free. It is capable of identifying "edges in a brain network that differentially respond in unison to a task onset and that occur in dense packs with similar characteristics" (Lohmann et al., 2016). By this, dynamic networks

can be detected, which might be missed with conventional methods. However, interpreting the obtained results in a biologically meaningful way is, so far, difficult, since not enough datasets have been processed to understand underlying patterns. Therefore, for the network analysis in the present work, a seed-based correlation analysis was chosen. This method, as well as the other methods eventually employed for analysing the current dataset, are detailed in the attached manuscript.

Results and Conclusion

In the present study, the left and right VEN area of anaesthetized macaque monkeys was electrically microstimulated during separate functional magnetic imaging data acquisition, to investigate subsequent whole brain responses and network activity.

The general linear model analysis of this data revealed that EMS in the left and right VEN area leads to similar, ipsilateral activation patterns of monosynaptically and polysynaptically connected cortical and subcortical areas. Besides brain areas near the stimulation side, limbic regions, midline subcortical areas, and distant cortical areas showed positive blood-oxygen-level-dependent changes in response to the EMS. Notably, the distant cortical areas included mainly visual areas and to a lesser extent auditory, vestibular, and somatosensory areas. Despite our original hypothesis, no distinct asymmetric differences in the overall brain-wide activation patterns were observed when comparing the effects of left and right-sided stimulations.

The seed-based correlation analysis (SBCA) revealed that EMS in the left and right VEN area tends to reduce the activity correlations of the ventral anterior insular cortex with other brain areas compared to the resting state. However, mainly contralateral cortical correlations were reduced, whereas ipsilateral,

especially limbic, correlations were rather strengthened, leading to an ipsilateralized correlation pattern with only a few contralateral midline regions still strongly correlated.

At the network level, the SBCA further revealed that EMS in the left and right VEN area shuts down the contralateral SN, as well as the contralateral DMN. Right-sided stimulation led to a complete, bilateral shutdown of the CEN and an upregulation of the ipsilateral SN. Left-sided stimulation, however, did not show such an effect. Despite the absence of asymmetrical brain action at the whole brain level (see above), these later results identified an asymmetric regulation of functional networks by the anterior insular cortex.

Taken together, these results support the idea of the insula's role as a rich club hub within the SN and indicate its ability to not only switch between networks but to up- and down- regulate the DMN and the CEN to react adequately to salient stimuli. This network regulation appears to be asymmetric, with a more prominent effect from the right insula that could influence behaviour, emotions, and cognition. The data further suggests that the regulation of the networks might be mediated, at least in part, by the VEN area. Within this area, due to their long and fast transmitting axons, the VEN could provide rapid information exchange and, with this, real-time updating of generative models and network regulation. Further, the uncovered functional connections of the VEN area with monosynaptically and polysynaptically connected cortical and subcortical brain areas, reflect the multitude of inputs arriving in the insula from different sensory modalities. These polymodal signals could then be ultimately integrated with bodily states in the anterior insular cortex and provide a self-reference, simultaneously encompassing the detection and evaluation of salient events, the regulation of interoceptive predictions and autonomic processes, and the engendering of the subjective awareness of feelings in humans.

Outlook and Future Perspectives

The objective of the present project was the investigation of the global brain activity in response to electrical microstimulations in the left and right VEN area. On that account, stimulation-electrodes were inserted into the VEN areas of three anaesthetized macaque monkeys and stimulations were delivered alternately, whilst functional magnetic resonance images data were recorded. The subsequently discovered results shed light on the behaviour of the anaesthetized macaque monkey's brain, in response to EMS from a global brain activity perspective as well as a network perspective. But what would be the brain's response if it were not under opioid anaesthesia? To answer this intriguing question, similar stimulation experiments would have to be conducted in awake animals. Though previous literature has shown that the used opioid anaesthesia has no measurable effect on the visual system and its responses to visual stimuli (Logothetis et al., 2010), it is unknown how the activity of the insula is influenced. As an integration hub for interoceptive and exteroceptive signals, multi-modal stimuli, as well as cognitive, emotional, and motivational information (Nguyen et al., 2016; Evrard, 2019), the insula is suggested to play an essential role in self-awareness (Craig, 2009a). How the neurobiological mechanisms underlying the primal homolog of this unique human functionality are influenced by the anaesthesia and how this, in turn, influences the brain's networks would be an interesting question for future studies. These suggested studies could verify and substantiate the present results, extend them, and, additionally, provide a framework for future studies of the insula in anaesthetized subjects.

Another valuable derivative of conducting EMS in awake monkeys would be the possibility to monitor physiological parameters for changes after the stimulation. Though multiple bodily functions were monitored during the present study like

the heart rate, the breathing rate, the temperature, the CO_2 and oxygen levels, and skin blood flow, most of these parameters were regulated manually to obtain a good and deep anaesthesia and, therefore, they did not provide any information on potential changes elicited by the EMS. Prior studies have shown effects on the heart rate after EMS in the left and right insular cortex and indicated an asymmetrical response. Since in awake animals, there is no need to adapt the physiological parameters manually, changes can be recorded and appropriately analysed. In addition, the alert macaque monkey could be subject to passive or active emotional processing tasks likely to engage the anterior insular cortex, which would further enhance the chances to detect and perturb both brain activity and bodily physiology.

Another exciting research path that was opened up by the present study is the stimulation of other nodes in the salience network, e.g. the amygdala. Would the salience network react in similar ways if a node, which is not a rich club hub, would be stimulated? Would the CEN still be shut down by right-sided stimulation? Would the contralateral SN and DMN be shut down, whereas the ipsilateral right SN would be upregulated? These questions would be interesting to answer and with that to either strengthen or weaken the extraordinary role that has been accredited to the insular cortex.

The current project provides an exciting and novel window into the functions of the insular cortex, its influence on the global brain activity, and its involvement in functional networks. At the same time, it raises the afore-mentioned questions and opens the door to walk unprecedented paths of investigating the particular brain area that is the insular cortex.

6

BIBLIOGRAPHY

Afif, A., Hoffmann, D., Minotti, L., Benabid, A. L., and Kahane, P. (2008). *Middle short gyrus of the insula implicated in pain processing*. Pain 138 (3).

Afif, A., Minotti, L., Kahane, P., and Hoffmann, D. (2010). *Middle short gyrus of the insula implicated in speech production: intracerebral electric stimulation of patients with epilepsy*. Epilepsia 51 (2).

Akbarian, S., Grusser, O. J., and Guldin, W. O. (1994). *Corticofugal connections between the cerebral cortex and brainstem vestibular nuclei in the macaque monkey*. J Comp Neurol 339 (3).

Akgoren, N., Fabricius, M., and Lauritzen, M. (1994). *Importance of nitric oxide for local increases of blood flow in rat cerebellar cortex during electrical stimulation*. Proc Natl Acad Sci U S A 91 (13).

Allen Institute for Brain Science. 2004. Allen Mouse Brain Atlas.

Allman, J. M., Tetreault, N. A., Hakeem, A. Y., Manaye, K. F., Semendeferi, K., Erwin, J. M., Park, S., Goubert, V., and Hof, P. R. (2010a). *The von Economo neurons in frontoinsular and anterior cingulate cortex in great apes and humans*. Brain Struct Funct 214 (5-6).

Allman, J. M., Tetreault, N. A., Hakeem, A. Y., Manaye, K. F., Semendeferi, K., Erwin, J. M., Park, S., Goubert, V., and Hof, P. R. (2010b). *The von Economo neurons in the frontoinsular and anterior cingulate cortex*. Ann N Y Acad Sci 1225.

Amaral, D. G., and Price, J. L. (1984). *Amygdalo-cortical projections in the monkey (Macaca fascicularis)*. J Comp Neurol 230 (4).

Ames, A., 3rd. (2000). *CNS energy metabolism as related to function*. Brain Res Brain Res Rev 34 (1-2).

Arsenault, J. T., Rima, S., Stemmann, H., and Vanduffel, W. (2014). *Role of the primate ventral tegmental area in reinforcement and motivation*. Curr Biol 24 (12).

Asanuma, H., Arnold, A., and Zarzecki, P. (1976). *Further study on the excitation of pyramidal tract cells by intracortical microstimulation*. Exp Brain Res 26 (5).

Asanuma, H., and Rosén, I. (1973). *Spread of mono- and polysynaptic connections within cat's motor cortex*. Experimental Brain Research 16 (5).

Asanuma, H., and Sakata, H. (1967). *Functional Organization of a Cortical Efferent System Examined with Focal Depth Stimulation in Cats*. Journal of Neurophysiology 30 (1).

Ashburner, J. (2012). *SPM: a history*. Neuroimage 62 (2).

Avery, J. A., Powell, J. N., Breslin, F. J., Lepping, R. J., Martin, L. E., Patrician, T. M., Donnelly, J. E., Savage, C. R., and Simmons, W. K. (2017). *Obesity is associated with altered mid-insula functional connectivity to limbic regions underlying appetitive responses to foods*. J Psychopharmacol 31 (11).

Bamiou, D. E., Musiek, F. E., and Luxon, L. M. (2003). *The insula (Island of Reil) and its role in auditory processing. Literature review*. Brain Res Brain Res Rev 42 (2).

Bandettini, P. A., Wong, E. C., Hinks, R. S., Tikofsky, R. S., and Hyde, J. S. (1992). *Time course EPI of human brain function during task activation*. Magn Reson Med 25 (2).

Bannwarth, H., Kremer, B. P., and Schulz, A. (2011). *Basiswissen Physik, Chemie und Biochemie*. Vol. 2. Berlin: Springer.

Bartholin, C. (1641). *Institutiones Anatomicae, novis recentiorum opinionibus et observationibus figurisque auctae*

Bartholin, C. (1648). *Institutiones Anatomicae Das ist: Künstliche Zerlegung Menschlichen Leibes* Copenhagen: Moltken

Bassett, D. S., and Sporns, O. (2017). *Network neuroscience*. Nat Neurosci 20 (3).

Belliveau, J. W., Kennedy, D. N., Jr., McKinstry, R. C., Buchbinder, B. R., Weisskoff, R. M., Cohen, M. S., Vevea, J. M., Brady, T. J., and Rosen, B. R. (1991). *Functional mapping of the human visual cortex by magnetic resonance imaging*. Science 254 (5032).

Belliveau, J. W., Rosen, B. R., Kantor, H. L., Rzedzian, R. R., Kennedy, D. N., McKinstry, R. C., Vevea, J. M., Cohen, M. S., Pykett, I. L., and Brady, T. J. (1990). *Functional cerebral imaging by susceptibility-contrast NMR*. Magn Reson Med 14 (3).

Betz, W. (1881). *Ueber die feinere Structur der Gehirnrinde des Menschen* Centralblatt für die Medicinischen Wissenschaften 19.

Bierer, J. A., and Middlebrooks, J. C. (2004). *Cortical responses to cochlear implant stimulation: channel interactions*. J Assoc Res Otolaryngol 5 (1).

Bloch, F. (1946). *Nuclear Induction*. Physical Review 70 (7-8).

Bonmassar, G., Anami, K., Ives, J., and Belliveau, J. W. (1999). *Visual evoked potential (VEP) measured by simultaneous 64-channel EEG and 3T fMRI*. Neuroreport 10 (9).

Bonnelle, V., Ham, T. E., Leech, R., Kinnunen, K. M., Mehta, M. A., Greenwood, R. J., and Sharp, D. J. (2012). *Salience network integrity predicts default mode network function after traumatic brain injury*. Proc Natl Acad Sci U S A 109 (12).

Borchers, S., Himmelbach, M., Logothetis, N., and Karnath, H. O. (2011). *Direct electrical stimulation of human cortex - the gold standard for mapping brain functions?* Nat Rev Neurosci 13 (1).

Bradley, D. C., Troyk, P. R., Berg, J. A., Bak, M., Cogan, S., Erickson, R., Kufta, C., Mascaro, M., McCreery, D., Schmidt, E. M., Towle, V. L., and Xu, H. (2005). *Visuotopic Mapping Through a Multichannel Stimulating Implant in Primate V1*. Journal of Neurophysiology 93 (3).

Brindley, G. S., and Lewin, W. S. (1968). *The sensations produced by electrical stimulation of the visual cortex*. J Physiol 196 (2).

Broca, P. P. (1861). *Remarques sur le siège de la faculté du langage articulé, suivies d'une observation d'aphémie (perte de la parole)*. Bulletin de la Société Anatomique (6).

Brockhaus, H. (1940). *Die Cyto- und Myeloarchitektonik des Cortex claustralis und des Claustrum beim Menschen*. Journal fuer Psychologie und Neurologie 40.

Brodmann, K. (1909). *Vergleichende Lokalisationslehre der Grosshirnrinde in ihren Prinzipien dargestellt auf Grund des Zellenbaues*. Barth.

Brune, M., Schobel, A., Karau, R., Benali, A., Faustmann, P. M., Juckel, G., and Petrasch-Parwez, E. (2010). *Von Economo neuron density in the anterior cingulate cortex is reduced in early onset schizophrenia*. Acta Neuropathol 119 (6).

Buckner, R. L., Andrews-Hanna, J. R., and Schacter, D. L. (2008). *The brain's default network: anatomy, function, and relevance to disease*. Ann N Y Acad Sci 1124.

Burton, H., and Jones, E. G. (1976). *The posterior thalamic region and its cortical projection in New World and Old World monkeys*. J Comp Neurol 168 (2).

Butti, C., and Hof, P. R. (2010). *The insular cortex: a comparative perspective*. Brain Struct Funct 214 (5-6).

Butti, C., Santos, M., Uppal, N., and Hof, P. R. (2013). *Von Economo neurons: clinical and evolutionary perspectives*. Cortex 49 (1).

Butti, C., Sherwood, C. C., Hakeem, A. Y., Allman, J. M., and Hof, P. R. (2009). *Total number and volume of Von Economo neurons in the cerebral cortex of cetaceans*. J Comp Neurol 515 (2).

Bzdok, D., and Yeo, B. T. T. (2017). *Inference in the age of big data: Future perspectives on neuroscience*. Neuroimage 155.

Cai, W., Chen, T., Ryali, S., Kochalka, J., Li, C. S., and Menon, V. (2016). *Causal Interactions Within a Frontal-Cingulate-Parietal Network During Cognitive Control: Convergent Evidence from a Multisite-Multitask Investigation*. Cereb Cortex 26 (5).

Cai, W., Chen, T., Szegletes, L., Supekar, K., and Menon, V. (2015). *Aberrant Cross-Brain Network Interaction in Children With Attention-Deficit/Hyperactivity Disorder and Its Relation to Attention Deficits: A Multisite and Cross-Site Replication Study*. Biol Psychiatry.

Cai, W., Ryali, S., Chen, T., Li, C. S., and Menon, V. (2014). *Dissociable roles of right inferior frontal cortex and anterior insula in inhibitory control: evidence from intrinsic and task-related functional parcellation, connectivity, and response profile analyses across multiple datasets*. J Neurosci 34 (44).

Caprara, I., Premereur, E., Romero, M. C., Faria, P., and Janssen, P. (2018). *Shape responses in a macaque frontal area connected to posterior parietal cortex*. Neuroimage 179.

Caria, A., Veit, R., Sitaram, R., Lotze, M., Weiskopf, N., Grodd, W., and Birbaumer, N. (2007). *Regulation of anterior insular cortex activity using real-time fMRI*. Neuroimage 35 (3).

Carmichael, S. T., Clugnet, M. C., and Price, J. L. (1994). *Central olfactory connections in the macaque monkey*. J Comp Neurol 346 (3).

Carmichael, S. T., and Price, J. L. (1995a). *Limbic connections of the orbital and medial prefrontal cortex in macaque monkeys*. J Comp Neurol 363 (4).

Carmichael, S. T., and Price, J. L. (1995b). *Sensory and premotor connections of the orbital and medial prefrontal cortex of macaque monkeys*. J Comp Neurol 363 (4).

Caruana, F., Jezzini, A., Sbriscia-Fioretti, B., Rizzolatti, G., and Gallese, V. (2011). *Emotional and social behaviors elicited by electrical stimulation of the insula in the macaque monkey*. Curr Biol 21 (3).

Casey, K. L., Minoshima, S., Berger, K. L., Koeppe, R. A., Morrow, T. J., and Frey, K. A. (1994). *Positron emission tomographic analysis of cerebral structures activated specifically by repetitive noxious heat stimuli*. J Neurophysiol 71 (2).

Catterall, W. A. (1981). *Localization of sodium channels in cultured neural cells*. J Neurosci 1 (7).

Cauda, F., Torta, D. M., Sacco, K., D'Agata, F., Geda, E., Duca, S., Geminiani, G., and Vercelli, A. (2013). *Functional anatomy of cortical areas characterized by Von Economo neurons*. Brain Struct Funct 218 (1).

Chaigneau, E., Oheim, M., Audinat, E., and Charpak, S. (2003). *Two-photon imaging of capillary blood flow in olfactory bulb glomeruli*. Proc Natl Acad Sci U S A 100 (22).

Chen, A. C., Oathes, D. J., Chang, C., Bradley, T., Zhou, Z. W., Williams, L. M., Glover, G. H., Deisseroth, K., and Etkin, A. (2013). *Causal interactions between fronto-parietal central executive and default-mode networks in humans*. Proc Natl Acad Sci U S A 110 (49).

Chen, T., Cai, W., Ryali, S., Supekar, K., and Menon, V. (2016). *Distinct Global Brain Dynamics and Spatiotemporal Organization of the Salience Network*. PLoS Biol 14 (6).

Chen, T., Michels, L., Supekar, K., Kochalka, J., Ryali, S., and Menon, V. (2015). *Role of the anterior insular cortex in integrative causal signaling during multisensory auditory-visual attention*. Eur J Neurosci 41 (2).

Chikama, M., McFarland, N. R., Amaral, D. G., and Haber, S. N. (1997). *Insular cortical projections to functional regions of the striatum correlate with cortical cytoarchitectonic organization in the primate*. J Neurosci 17 (24).

Chouchou, F., Mauguiere, F., Vallayer, O., Catenoix, H., Isnard, J., Montavont, A., Jung, J., Pichot, V., Rheims, S., and Mazzola, L. (2019). *How the insula speaks to the heart: Cardiac responses to insular stimulation in humans*. Hum Brain Mapp.

Cipolla, M. J. (2010). *The Cerebral Circulation - Integrated Systems Physiology: From Molecule to Function*: Morgan & Claypool Life Sciences.

Cohen, M. R., and Newsome, W. T. (2004). *What electrical microstimulation has revealed about the neural basis of cognition*. Curr Opin Neurobiol 14 (2).

Comon, P. (1994). *Independent component analysis, A new concept?* Signal Processing 36 (3).

Cooper, G. M. (2000). *The Cell: A Molecular Approach*. 2nd edition ed: Sinauer Associates Inc.

Corbetta, M., Patel, G., and Shulman, G. L. (2008). *The reorienting system of the human brain: from environment to theory of mind*. Neuron 58 (3).

Craig, A. D. (2002). *How do you feel? Interoception: the sense of the physiological condition of the body*. Nat Rev Neurosci 3 (8).

Craig, A. D. (2004). *Distribution of trigeminothalamic and spinothalamic lamina I terminations in the macaque monkey*. J Comp Neurol 477 (2).

Craig, A. D. (2009a). *Emotional moments across time: a possible neural basis for time perception in the anterior insula*. Philos Trans R Soc Lond B Biol Sci 364 (1525).

Craig, A. D. (2009b). *How do you feel-now*. Nature Neuroscience 10.
Craig, A. D. (2014). *Topographically organized projection to posterior insular cortex from the posterior portion of the ventral medial nucleus in the long-tailed macaque monkey*. J Comp Neurol 522 (1).
Craig, A. D., Chen, K., Bandy, D., and Reiman, E. M. (2000). *Thermosensory activation of insular cortex*. Nat Neurosci 3 (2).
Critchley, H. D., Wiens, S., Rotshtein, P., Ohman, A., and Dolan, R. J. (2004). *Neural systems supporting interoceptive awareness*. Nat Neurosci 7 (2).
Crivellato, E., and Ribatti, D. (2007). *Soul, mind, brain: Greek philosophy and the birth of neuroscience*. Brain Res Bull 71 (4).
Cunningham, D. J. (1891). *Development of the Gyri and Sulci on the Surface of the Island of Reil of the Human Brain*. J Anat Physiol 25 (Pt 3).
Cunningham, D. J. (1892). *Contribution to the Surface Anatomy of the Cerebral Hemispheres.* . Vol. 7. Dublin: Royal Irish Academy.
Cushing, H. (1909). *A note upon the faradic stimulation of the postcentral gyrus in conscious patients*. Brain 32 (1).
Dale, A. M., and Halgren, E. (2001). *Spatiotemporal mapping of brain activity by integration of multiple imaging modalities*. Curr Opin Neurobiol 11 (2).
Damadian, R. (1971). *Tumor Detection by Nuclear Magnetic Resonance*. Science 171 (3976).
Deary, I. J., Simonotto, E., Meyer, M., Marshall, A., Marshall, I., Goddard, N., and Wardlaw, J. M. (2004). *The functional anatomy of inspection time: an event-related fMRI study*. Neuroimage 22 (4).
Devue, C., Collette, F., Balteau, E., Degueldre, C., Luxen, A., Maquet, P., and Bredart, S. (2007). *Here I am: the cortical correlates of visual self-recognition*. Brain Res 1143.
Dosenbach, N. U., Fair, D. A., Miezin, F. M., Cohen, A. L., Wenger, K. K., Dosenbach, R. A., Fox, M. D., Snyder, A. Z., Vincent, J. L., Raichle, M. E., Schlaggar, B. L., and Petersen, S. E. (2007). *Distinct brain networks for adaptive and stable task control in humans*. Proc Natl Acad Sci U S A 104 (26).
Dosenbach, N. U., Visscher, K. M., Palmer, E. D., Miezin, F. M., Wenger, K. K., Kang, H. C., Burgund, E. D., Grimes, A. L., Schlaggar, B. L., and Petersen, S. E. (2006). *A core system for the implementation of task sets*. Neuron 50 (5).
Droutman, V., Read, S. J., and Bechara, A. (2015). *Revisiting the role of the insula in addiction*. Trends Cogn Sci 19 (7).
Dunn, P. (2001). *Wilhelm Conrad Röentgen (1845-1923), the discovery of x rays and perinatal diagnosis*. Vol. 84.
Eckert, M. A., Menon, V., Walczak, A., Ahlstrom, J., Denslow, S., Horwitz, A., and Dubno, J. R. (2009). *At the heart of the ventral attention system: the right anterior insula*. Hum Brain Mapp 30 (8).
Economo, C. v. (1926). *Eine neue Art Spezialzellen des Lobus Cinguli und Lobus Insulae*. Zeitschrift für die gesamte Neurologie und Psychiatrie 100 (1).
Economo, C. v., and Deuticke, F. (1918). *Die Encephalitis lethargica*. Jahrbücher für Psychiatrie und Neurologie 31.
Economo, C. v., and Koskinas, G. N. (1925). *Die Cytoarchitektonik der Hirnrinde des erwachsenen Menschen*. Berlin: Springer.
Economo, C. v., and Koskinas, G. N. (2008). *Atlas of Cytoarchitectonics of the Adult Human Cerebral Cortex*. 1 ed: Karger.
Evrard, H. C. (2019). *The organization of the primate insular cortex*. Frontiers in Neuroanatomy.
Evrard, H. C., Forro, T., and Logothetis, N. K. (2012). *Von Economo neurons in the anterior insula of the macaque monkey*. Neuron 74 (3).
Evrard, H. C., Logothetis, N. K., and Craig, A. D. (2014). *Modular architectonic organization of the insula in the macaque monkey*. J Comp Neurol 522 (1).
Faraday, M., Martin, T., and Royal Institution of Great, B. (1932). *Faraday's diary : being the various philosophical notes of experimental investigation*.

Ferrier, D. (1875). *Experiments on the brain of monkeys.—No. I*. Proceedings of the Royal Society of London 23 (156-163).
Fick, A. (1870). *Ueber die Messung dea Blutquantums in den Herzventrikela*. Verhandlungen der Physikalisch-medizinische Gesellschaft zu Würzburg.
Field, C. B., Johnston, K., Gati, J. S., Menon, R. S., and Everling, S. (2008). *Connectivity of the primate superior colliculus mapped by concurrent microstimulation and event-related FMRI*. PLoS One 3 (12).
Fischl, B. (2012). *FreeSurfer*. Neuroimage 62 (2).
Fox, M. D., Snyder, A. Z., Vincent, J. L., Corbetta, M., Van Essen, D. C., and Raichle, M. E. (2005). *The human brain is intrinsically organized into dynamic, anticorrelated functional networks*. Proc Natl Acad Sci U S A 102 (27).
Fox, P. T., and Raichle, M. E. (1986). *Focal physiological uncoupling of cerebral blood flow and oxidative metabolism during somatosensory stimulation in human subjects*. Proc Natl Acad Sci U S A 83 (4).
Fox, P. T., Raichle, M. E., Mintun, M. A., and Dence, C. (1988). *Nonoxidative glucose consumption during focal physiologic neural activity*. Science 241 (4864).
Frahm, J., Bruhn, H., Merboldt, K. D., and Hanicke, W. (1992). *Dynamic MR imaging of human brain oxygenation during rest and photic stimulation*. J Magn Reson Imaging 2 (5).
Freeman, S. A., Desmazieres, A., Fricker, D., Lubetzki, C., and Sol-Foulon, N. (2016). *Mechanisms of sodium channel clustering and its influence on axonal impulse conduction*. Cell Mol Life Sci 73 (4).
Fritsch, G., and Hitzig, E. (1870). *Uber die elektrische Erregbarkeit des Grosshirns*. Arch Anat Physiol Wissen (37).
Frontera, J. G. (1956). *Some results obtained by electrical stimulation of the cortex of the island of Reil in the brain of the monkey (Macaca mulatta)*. J Comp Neurol 105 (3).
Fusar-Poli, P., Howes, O., and Borgwardt, S. (2009). *Johann Cristian Reil on the 200th anniversary of the first description of the insula (1809)*. J Neurol Neurosurg Psychiatry 80 (12).
Gabriel, D. A. (2011). *Effects of monopolar and bipolar electrode configurations on surface EMG spike analysis*. Med Eng Phys 33 (9).
Garroway, A. N., Grannell, P. K., and Mansfield, P. (1974). *Image formation in NMR by a selective irradiative process*. Journal of Physics C: Solid State Physics 7 (24).
Geddes, L. A., and Bourland, J. D. (1985). *The strength-duration curve*. IEEE Trans Biomed Eng 32 (6).
Gerbella, M., Belmalih, A., Borra, E., Rozzi, S., and Luppino, G. (2011). *Cortical connections of the anterior (F5a) subdivision of the macaque ventral premotor area F5*. Brain Struct Funct 216 (1).
Gillis, N. (2014). *The Why and How of Nonnegative Matrix Factorization*. arXiv:1401.5226.
Goebel, R. (2012). *BrainVoyager--past, present, future*. Neuroimage 62 (2).
Gogolla, N. (2017). *The insular cortex*. Curr Biol 27 (12).
Goldman, D. E. (1943). *Potential, Impedance, and Rectification in Membranes*. J Gen Physiol 27 (1).
Gomez-Gardenes, J., Zamora-Lopez, G., Moreno, Y., and Arenas, A. (2010). *From modular to centralized organization of synchronization in functional areas of the cat cerebral cortex*. PLoS One 5 (8).
Goodkind, M., Eickhoff, S. B., Oathes, D. J., Jiang, Y., Chang, A., Jones-Hagata, L. B., Ortega, B. N., Zaiko, Y. V., Roach, E. L., Korgaonkar, M. S., Grieve, S. M., Galatzer-Levy, I., Fox, P. T., and Etkin, A. (2015). *Identification of a common neurobiological substrate for mental illness*. JAMA Psychiatry 72 (4).
Goulden, N., Khusnulina, A., Davis, N. J., Bracewell, R. M., Bokde, A. L., McNulty, J. P., and Mullins, P. G. (2014). *The salience network is responsible for switching between the default mode network and the central executive network: replication from DCM*. Neuroimage 99.
Gray, H., and Carter, H. V. (1859). *Gray's Anatomy: Descriptive and Surgical*. 1 ed. Philadelphia, PA, USA Blanchard and Lea.
Graziano, M. S., Taylor, C. S., and Moore, T. (2002). *Complex movements evoked by microstimulation of precentral cortex*. Neuron 34 (5).

Greicius, M. D., Krasnow, B., Reiss, A. L., and Menon, V. (2003). *Functional connectivity in the resting brain: a network analysis of the default mode hypothesis*. Proc Natl Acad Sci U S A 100 (1).

Grill, W. M., and Kirsch, R. F. (2000). *Neuroprosthetic Applications of Electrical Stimulation*. Assistive Technology 12 (1).

Grünbaum, A. S. F., and Sherrington, C. S. (1902). *Observations on the physiology of the cerebral cortex of some of the higher apes. (Preliminary communication.)*. Proceedings of the Royal Society of London 69 (451-458).

Hackett, T. A., Stepniewska, I., and Kaas, J. H. (1998). *Thalamocortical connections of the parabelt auditory cortex in macaque monkeys*. J Comp Neurol 400 (2).

Hakeem, A. Y., Sherwood, C. C., Bonar, C. J., Butti, C., Hof, P. R., and Allman, J. M. (2009). *Von Economo neurons in the elephant brain*. Anat Rec (Hoboken) 292 (2).

Hamilton, J. P., Glover, G. H., Bagarinao, E., Chang, C., Mackey, S., Sacchet, M. D., and Gotlib, I. H. (2016). *Effects of salience-network-node neurofeedback training on affective biases in major depressive disorder*. Psychiatry Res Neuroimaging 249.

Hammarberg, C. (1895). *Studien über Klinik und Pathologie der Idiotie, nebst untersuchungen über die normale Anatomie der Hirnrinde*: Berling.

Hassanpour, M. S., Simmons, W. K., Feinstein, J. S., Luo, Q., Lapidus, R. C., Bodurka, J., Paulus, M. P., and Khalsa, S. S. (2018). *The Insular Cortex Dynamically Maps Changes in Cardiorespiratory Interoception*. Neuropsychopharmacology 43 (2).

Hennenlotter, A., Schroeder, U., Erhard, P., Castrop, F., Haslinger, B., Stoecker, D., Lange, K. W., and Ceballos-Baumann, A. O. (2005). *A common neural basis for receptive and expressive communication of pleasant facial affect*. Neuroimage 26 (2).

Hill, L. (1896). *The physiology and pathology of the cerebral circulation an experimental research*.

Hines, M., and Boynton, E. P. (1940). *The maturation of 'excitability'in the precentral gyrus ofthe young monkey*. Contributions to Embryonology 178.

Histed, M. H., Bonin, V., and Reid, R. C. (2009). *Direct activation of sparse, distributed populations of cortical neurons by electrical microstimulation*. Neuron 63 (4).

Histed, M. H., Ni, A. M., and Maunsell, J. H. (2013). *Insights into cortical mechanisms of behavior from microstimulation experiments*. Prog Neurobiol 103.

Hodgkin, A. L., and Katz, B. (1949). *The effect of sodium ions on the electrical activity of giant axon of the squid*. J Physiol 108 (1).

Honey, C. J., Sporns, O., Cammoun, L., Gigandet, X., Thiran, J. P., Meuli, R., and Hagmann, P. (2009). *Predicting human resting-state functional connectivity from structural connectivity*. Proc Natl Acad Sci U S A 106 (6).

Horn, F. M., and Evrard, H. C. (in preparation). *Novel elemental localization in the primate cerebral cortex*.

Hu, X., Liu, Z., Chen, W., Zheng, J., Su, N., Wang, W., Lin, C., and Luo, L. (2017). *Individual Differences in the Accuracy of Judgments of Learning Are Related to the Gray Matter Volume and Functional Connectivity of the Left Mid-Insula*. Front Hum Neurosci 11.

Huerta, M. F., Krubitzer, L. A., and Kaas, J. H. (1986). *Frontal eye field as defined by intracortical microstimulation in squirrel monkeys, owl monkeys, and macaque monkeys: I. Subcortical connections*. J Comp Neurol 253 (4).

Jabbi, M., Bastiaansen, J., and Keysers, C. (2008). *A common anterior insula representation of disgust observation, experience and imagination shows divergent functional connectivity pathways*. PLoS One 3 (8).

Jilka, S. R., Scott, G., Ham, T., Pickering, A., Bonnelle, V., Braga, R. M., Leech, R., and Sharp, D. J. (2014). *Damage to the Salience Network and interactions with the Default Mode Network*. J Neurosci 34 (33).

Jolliffe, I. T., and Cadima, J. (2016). *Principal component analysis: a review and recent developments*. Philos Trans A Math Phys Eng Sci 374 (2065).

Jones, E. G., and Burton, H. (1976). *Areal differences in the laminar distribution of thalamic afferents in cortical fields of the insular, parietal and temporal regions of primates*. J Comp Neurol 168 (2).

Kaada, B. R., Pribram, K. H., and Epstein, J. A. (1949). *Respiratory and vascular responses in monkeys from temporal pole, insula, orbital surface and cingulate gyrus; a preliminary report*. J Neurophysiol 12 (5).

Kalani, M. Y., Kalani, M. A., Gwinn, R., Keogh, B., and Tse, V. C. (2009). *Embryological development of the human insula and its implications for the spread and resection of insular gliomas*. Neurosurg Focus 27 (2).

Kandilarova, S., Stoyanov, D., Kostianev, S., and Specht, K. (2018). *Altered Resting State Effective Connectivity of Anterior Insula in Depression*. Front Psychiatry 9.

Kawaguchi, A., Nemoto, K., Nakaaki, S., Kawaguchi, T., Kan, H., Arai, N., Shiraishi, N., Hashimoto, N., and Akechi, T. (2016). *Insular Volume Reduction in Patients with Social Anxiety Disorder*. Front Psychiatry 7.

Kazamel, M., and Warren, P. P. (2017). *History of electromyography and nerve conduction studies: A tribute to the founding fathers*. J Clin Neurosci 43.

Kety, S. S., and Schmidt, C. F. (1948). *The Nitrous Oxide Method for the Quantitative Determination of Cerebral Blood Flow in Man: Theory, Procedure and Normal Values*. J Clin Invest 27 (4).

Kikyo, H., Ohki, K., and Miyashita, Y. (2002). *Neural correlates for feeling-of-knowing: an fMRI parametric analysis*. Neuron 36 (1).

Klein, T. A., Endrass, T., Kathmann, N., Neumann, J., von Cramon, D. Y., and Ullsperger, M. (2007). *Neural correlates of error awareness*. Neuroimage 34 (4).

Koelsch, S., Fritz, T., DY, V. C., Muller, K., and Friederici, A. D. (2006). *Investigating emotion with music: an fMRI study*. Hum Brain Mapp 27 (3).

Koubeissi, M. Z., Bartolomei, F., Beltagy, A., and Picard, F. (2014). *Electrical stimulation of a small brain area reversibly disrupts consciousness*. Epilepsy Behav 37.

Krakow, K., Allen, P. J., Symms, M. R., Lemieux, L., Josephs, O., and Fish, D. R. (2000). *EEG recording during fMRI experiments: image quality*. Hum Brain Mapp 10 (1).

Krause, F. (1909). *Die operative Behandlung der Epilepsie*. Med Klin Berlin 5.

Kwong, K. K., Belliveau, J. W., Chesler, D. A., Goldberg, I. E., Weisskoff, R. M., Poncelet, B. P., Kennedy, D. N., Hoppel, B. E., Cohen, M. S., Turner, R., and et al. (1992). *Dynamic magnetic resonance imaging of human brain activity during primary sensory stimulation*. Proc Natl Acad Sci U S A 89 (12).

Lamm, C., Meltzoff, A. N., and Decety, J. (2010). *How do we empathize with someone who is not like us? A functional magnetic resonance imaging study*. J Cogn Neurosci 22 (2).

Laughlin, S. B., and Sejnowski, T. J. (2003). *Communication in neuronal networks*. Science 301 (5641).

Lauterbur, P. C. (1973). *Image Formation by Induced Local Interactions: Examples Employing Nuclear Magnetic Resonance*. Nature 242 (5394).

Leibenluft, E., Gobbini, M. I., Harrison, T., and Haxby, J. V. (2004). *Mothers' neural activation in response to pictures of their children and other children*. Biol Psychiatry 56 (4).

Li, C. L., and Bak, A. (1976). *Excitability characteristics of the A- and C-fibers in a peripheral nerve*. Exp Neurol 50 (1).

Livesey, A. C., Wall, M. B., and Smith, A. T. (2007). *Time perception: manipulation of task difficulty dissociates clock functions from other cognitive demands*. Neuropsychologia 45 (2).

Logothetis, N. K. (2002). *The neural basis of the blood-oxygen-level-dependent functional magnetic resonance imaging signal*. Philos Trans R Soc Lond B Biol Sci 357 (1424).

Logothetis, N. K. (2008). *What we can do and what we cannot do with fMRI*. Nature 453 (7197).

Logothetis, N. K. (2015). *Neural-Event-Triggered fMRI of large-scale neural networks*. Curr Opin Neurobiol 31.

Logothetis, N. K., Augath, M., Murayama, Y., Rauch, A., Sultan, F., Goense, J., Oeltermann, A., and Merkle, H. (2010). *The effects of electrical microstimulation on cortical signal propagation*. Nat Neurosci 13 (10).

Logothetis, N. K., Eschenko, O., Murayama, Y., Augath, M., Steudel, T., Evrard, H. C., Besserve, M., and Oeltermann, A. (2012). *Hippocampal-cortical interaction during periods of subcortical silence*. Nature 491 (7425).

Logothetis, N. K., Pauls, J., Augath, M., Trinath, T., and Oeltermann, A. (2001). *Neurophysiological investigation of the basis of the fMRI signal*. Nature 412 (6843).

Lohmann, G., Muller, K., Bosch, V., Mentzel, H., Hessler, S., Chen, L., Zysset, S., and von Cramon, D. Y. (2001). *LIPSIA--a new software system for the evaluation of functional magnetic resonance images of the human brain*. Comput Med Imaging Graph 25 (6).

Lohmann, G., Stelzer, J., Zuber, V., Buschmann, T., Margulies, D., Bartels, A., and Scheffler, K. (2016). *Task-Related Edge Density (TED)-A New Method for Revealing Dynamic Network Formation in fMRI Data of the Human Brain*. PLoS One 11 (6).

London, M., Roth, A., Beeren, L., Hausser, M., and Latham, P. E. (2010). *Sensitivity to perturbations in vivo implies high noise and suggests rate coding in cortex*. Nature 466 (7302).

Lough, S., Kipps, C. M., Treise, C., Watson, P., Blair, J. R., and Hodges, J. R. (2006). *Social reasoning, emotion and empathy in frontotemporal dementia*. Neuropsychologia 44 (6).

Ludwig, G. D., and Struthers, F. W. (1949). *Considerations underlying the use of Ultrasound to detect Gallstones and Foregn Bodies in Tissue*. Naval Medical Research Institute Reports, Project #004 001 (Report No. 4).

Luppino, G., Matelli, M., Camarda, R., and Rizzolatti, G. (1993). *Corticocortical connections of area F3 (SMA-proper) and area F6 (pre-SMA) in the macaque monkey*. J Comp Neurol 338 (1).

MacKinnon, C. D., Webb, R. M., Silberstein, R., Tisch, S., Asselman, P., Limousin, P., and Rothwell, J. C. (2005). *Stimulation through electrodes implanted near the subthalamic nucleus activates projections to motor areas of cerebral cortex in patients with Parkinson's disease*. European Journal of Neuroscience 21 (5).

Mai, J., Majtanik, M., and Paxinos, G. (2015). *Atlas of the Human Brain*. 4th ed: Academic Press

Mansfield, P., and Grannell, P. K. (1973). *NMR 'diffraction' in solids?* Journal of Physics C: Solid State Physics 6 (22).

Matsui, T., Koyano, K. W., Tamura, K., Osada, T., Adachi, Y., Miyamoto, K., Chikazoe, J., Kamigaki, T., and Miyashita, Y. (2012). *FMRI activity in the macaque cerebellum evoked by intracortical microstimulation of the primary somatosensory cortex: evidence for polysynaptic propagation*. PLoS One 7 (10).

Matsui, T., Tamura, K., Koyano, K. W., Takeuchi, D., Adachi, Y., Osada, T., and Miyashita, Y. (2011). *Direct comparison of spontaneous functional connectivity and effective connectivity measured by intracortical microstimulation: an fMRI study in macaque monkeys*. Cereb Cortex 21 (10).

Mazoyer, B., Zago, L., Mellet, E., Bricogne, S., Etard, O., Houde, O., Crivello, F., Joliot, M., Petit, L., and Tzourio-Mazoyer, N. (2001). *Cortical networks for working memory and executive functions sustain the conscious resting state in man*. Brain Res Bull 54 (3).

Mazzola, L., Isnard, J., Peyron, R., and Mauguiere, F. (2012). *Stimulation of the human cortex and the experience of pain: Wilder Penfield's observations revisited*. Brain 135 (Pt 2).

Mazzola, L., Lopez, C., Faillenot, I., Chouchou, F., Mauguiere, F., and Isnard, J. (2014). *Vestibular responses to direct stimulation of the human insular cortex*. Ann Neurol 76 (4).

Mazzola, L., Mauguiere, F., and Isnard, J. (2017). *Electrical Stimulations of the Human Insula: Their Contribution to the Ictal Semiology of Insular Seizures*. J Clin Neurophysiol 34 (4).

Mazzola, L., Mauguiere, F., and Isnard, J. (2019). *Functional mapping of the human insula: Data from electrical stimulations*. Rev Neurol (Paris) 175 (3).

McIlwain, J. T. (1982). *Lateral spread of neural excitation during microstimulation in intermediate gray layer of cat's superior colliculus*. J Neurophysiol 47 (2).
Mendez-Ruette, M., Linsambarth, S., Moraga-Amaro, R., Quintana-Donoso, D., Mendez, L., Tamburini, G., Cornejo, F., Torres, R. F., and Stehberg, J. (2019). *The Role of the Rodent Insula in Anxiety*. Front Physiol 10.
Menon, R. S., Ogawa, S., Kim, S. G., Ellermann, J. M., Merkle, H., Tank, D. W., and Ugurbil, K. (1992). *Functional brain mapping using magnetic resonance imaging. Signal changes accompanying visual stimulation*. Invest Radiol 27 Suppl 2.
Menon, V., Ford, J. M., Lim, K. O., Glover, G. H., and Pfefferbaum, A. (1997). *Combined event-related fMRI and EEG evidence for temporal-parietal cortex activation during target detection*. Neuroreport 8 (14).
Menon, V., and Uddin, L. Q. (2010). *Saliency, switching, attention and control: a network model of insula function*. Brain Struct Funct 214 (5-6).
Merrill, D. R., Bikson, M., and Jefferys, J. G. (2005). *Electrical stimulation of excitable tissue: design of efficacious and safe protocols*. J Neurosci Methods 141 (2).
Mesulam, M. M., and Mufson, E. J. (1982a). *Insula of the old world monkey. I: Architectonics in the insulo-orbito-temporal component of the paralimbic brain*. J Comp Neurol 212 (1).
Mesulam, M. M., and Mufson, E. J. (1982b). *Insula of the old world monkey. III: Efferent cortical output and comments on function*. J Comp Neurol 212 (1).
Mesulam, M. M., and Mufson, E. J. (1985). *The Insula of Reil in Man and Monkey*. Springer.
Michel, M. (2017). *A role for the anterior insular cortex in the global neuronal workspace model of consciousness*. Conscious Cogn 49.
Moeller, S., Crapse, T., Chang, L., and Tsao, D. Y. (2017). *The effect of face patch microstimulation on perception of faces and objects*. Nat Neurosci 20 (5).
Monro, A. (1783). *Observations on the Structure and Functions of the Nervous System*. University of St. Andrews. Library.
Moore, T., Armstrong, K. M., and Fallah, M. (2003). *Visuomotor origins of covert spatial attention*. Neuron 40 (4).
Morecraft, R. J., Cipolloni, P. B., Stilwell-Morecraft, K. S., Gedney, M. T., and Pandya, D. N. (2004). *Cytoarchitecture and cortical connections of the posterior cingulate and adjacent somatosensory fields in the rhesus monkey*. J Comp Neurol 469 (1).
Mosso, A. (1881). *Ueber Den Kreislauf Des Blutes Im Menschlichen Gehirn*: von Veit & Company.
Mufson, E. J., and Mesulam, M. M. (1982). *Insula of the old world monkey. II: Afferent cortical input and comments on the claustrum*. J Comp Neurol 212 (1).
Munari, C., Kahane, P., Tassi, L., Francione, S., Hoffmann, D., Lo Russo, G., and Benabid, A. L. (1993). *Intracerebral low frequency electrical stimulation: a new tool for the definition of the "epileptogenic area"?* Acta Neurochir Suppl (Wien) 58.
Murphey, D. K., and Maunsell, J. H. (2007). *Behavioral detection of electrical microstimulation in different cortical visual areas*. Curr Biol 17 (10).
Nana, A. L., Sidhu, M., Gaus, S. E., Hwang, J. L., Li, L., Park, Y., Kim, E. J., Pasquini, L., Allen, I. E., Rankin, K. P., Toller, G., Kramer, J. H., Geschwind, D. H., Coppola, G., Huang, E. J., Grinberg, L. T., Miller, B. L., and Seeley, W. W. (2019). *Neurons selectively targeted in frontotemporal dementia reveal early stage TDP-43 pathobiology*. Acta Neuropathol 137 (1).
Nelson, S. M., Dosenbach, N. U., Cohen, A. L., Wheeler, M. E., Schlaggar, B. L., and Petersen, S. E. (2010). *Role of the anterior insula in task-level control and focal attention*. Brain Struct Funct 214 (5-6).
Neumann, M., Sampathu, D. M., Kwong, L. K., Truax, A. C., Micsenyi, M. C., Chou, T. T., Bruce, J., Schuck, T., Grossman, M., Clark, C. M., McCluskey, L. F., Miller, B. L., Masliah, E., Mackenzie, I. R., Feldman, H., Feiden, W., Kretzschmar, H. A., Trojanowski, J. Q., and Lee, V. M. (2006).

Ubiquitinated TDP-43 in frontotemporal lobar degeneration and amyotrophic lateral sclerosis. Science 314 (5796).
Nguyen, V. T., Breakspear, M., Hu, X., and Guo, C. C. (2016). *The integration of the internal and external milieu in the insula during dynamic emotional experiences*. Neuroimage 124 (Pt A).
Nieuwenhuys, R. (2012). *The insular cortex: a review*. Prog Brain Res 195.
Nimchinsky, E. A., Gilissen, E., Allman, J. M., Perl, D. P., Erwin, J. M., and Hof, P. R. (1999). *A neuronal morphologic type unique to humans and great apes*. Proc Natl Acad Sci U S A 96 (9).
Nobel Foundation, T. *The Nobel Prize in Physics* 1901.
Nobel Foundation, T. *The Nobel Prize in Physics* 1944.
Nobel Foundation, T. *The Nobel Prize in Medicine* 2003.
Nowak, L. G., and Bullier, J. (1998a). *Axons, but not cell bodies, are activated by electrical stimulation in cortical gray matter. I. Evidence from chronaxie measurements*. Exp Brain Res 118 (4).
Nowak, L. G., and Bullier, J. (1998b). *Axons, but not cell bodies, are activated by electrical stimulation in cortical gray matter. II. Evidence from selective inactivation of cell bodies and axon initial segments*. Exp Brain Res 118 (4).
Oeltermann, A., Augath, M. A., and Logothetis, N. K. (2007). *Simultaneous recording of neuronal signals and functional NMR imaging*. Magn Reson Imaging 25 (6).
Ogawa, S., Lee, T. M., Kay, A. R., and Tank, D. W. (1990a). *Brain magnetic resonance imaging with contrast dependent on blood oxygenation*. Proc Natl Acad Sci U S A 87 (24).
Ogawa, S., Lee, T. M., Nayak, A. S., and Glynn, P. (1990b). *Oxygenation-sensitive contrast in magnetic resonance image of rodent brain at high magnetic fields*. Magn Reson Med 14 (1).
Ogawa, S., Tank, D. W., Menon, R., Ellermann, J. M., Kim, S. G., Merkle, H., and Ugurbil, K. (1992). *Intrinsic signal changes accompanying sensory stimulation: functional brain mapping with magnetic resonance imaging*. Proc Natl Acad Sci U S A 89 (13).
Ohayon, S., Grimaldi, P., Schweers, N., and Tsao, D. Y. (2013). *Saccade modulation by optical and electrical stimulation in the macaque frontal eye field*. J Neurosci 33 (42).
Oppenheimer, S. M., Gelb, A., Girvin, J. P., and Hachinski, V. C. (1992). *Cardiovascular effects of human insular cortex stimulation*. Neurology 42 (9).
Ostrowsky, K., Magnin, M., Ryvlin, P., Isnard, J., Guenot, M., and Mauguiere, F. (2002). *Representation of pain and somatic sensation in the human insula: a study of responses to direct electrical cortical stimulation*. Cereb Cortex 12 (4).
Papagno, C., Pisoni, A., Mattavelli, G., Casarotti, A., Comi, A., Fumagalli, F., Vernice, M., Fava, E., Riva, M., and Bello, L. (2016). *Specific disgust processing in the left insula: New evidence from direct electrical stimulation*. Neuropsychologia 84.
Pape, H. C., Silbernagl, S., Klinke, R., Rothenburger, A., Kurtz, A., and Gay, R. (2005). *Physiologie*: Georg Thieme Verlag.
Pauling, L., and Coryell, C. D. (1936). *The Magnetic Properties and Structure of Hemoglobin, Oxyhemoglobin and Carbonmonoxyhemoglobin*. Proc Natl Acad Sci U S A 22 (4).
Pelte, D. (2005). *Physik fuer Biologen*. Vol. 1. Berlin: Springer.
Penfield, W. (1947). *Some observations on the cerebral cortex of man*. Proc R Soc Lond B Biol Sci 134 (876).
Penfield, W., and Boldrey, E. (1937). *Somatic motor and sensory representation in the cerebral cortex of man as studied by electrical stimulation*. Brain 60 (4).
Penfield, W., and Jasper, H. H. (1954). *Epilepsy and the functional anatomy of the human brain*: Little, Brown.
Penfield, W., and Perot, P. (1963). *The Brain's Record of Auditory and Visual Experience. A Final Summary and Discussion*. Brain 86.
Pérez-Cervera, L., Caramés, J. M., Fernández-Mollá, L. M., Moreno, A., Fernández, B., Pérez-Montoyo, E., Moratal, D., Canals, S., and Pacheco-Torres, J. 2018. Mapping Functional Connectivity in the Rodent Brain Using Electric-Stimulation fMRI. In *Preclinical MRI: Methods and*

Protocols, edited by M. L. García Martín and P. López Larrubia. New York, NY: Springer New York, 117-134.

Ploran, E. J., Nelson, S. M., Velanova, K., Donaldson, D. I., Petersen, S. E., and Wheeler, M. E. (2007). *Evidence accumulation and the moment of recognition: dissociating perceptual recognition processes using fMRI*. J Neurosci 27 (44).

Premereur, E., Janssen, P., and Vanduffel, W. (2013). *FEF-microstimulation causes task-dependent modulation of occipital fMRI activity*. Neuroimage 67.

Premereur, E., Taubert, J., Janssen, P., Vogels, R., and Vanduffel, W. (2016). *Effective Connectivity Reveals Largely Independent Parallel Networks of Face and Body Patches*. Curr Biol 26 (24).

Ptak, R. (2012). *The frontoparietal attention network of the human brain: action, saliency, and a priority map of the environment*. Neuroscientist 18 (5).

Purcell, M. E., Torrey, C. H., and Pound, V. R. (1945). *Resonance Absorption by Nuclear Magnetic Moments in a Solid*. 69 (37).

Raghanti, M. A., Spurlock, L. B., Treichler, F. R., Weigel, S. E., Stimmelmayr, R., Butti, C., Thewissen, J. G., and Hof, P. R. (2015). *An analysis of von Economo neurons in the cerebral cortex of cetaceans, artiodactyls, and perissodactyls*. Brain Struct Funct 220 (4).

Rahman, A. U. (1986). *Nuclear Magnetic Resonance-Basic Principles*. New York: Springer.

Raichle, M. E. (1983). *Positron emission tomography*. Annu Rev Neurosci 6.

Raichle, M. E. (2009). *A brief history of human brain mapping*. Trends Neurosci 32 (2).

Raichle, M. E., Grubb, R. L., Jr., Gado, M. H., Eichling, J. O., and Ter-Pogossian, M. M. (1976). *Correlation between regional cerebral blood flow and oxidative metabolism. In vivo studies in man*. Arch Neurol 33 (8).

Raichle, M. E., MacLeod, A. M., Snyder, A. Z., Powers, W. J., Gusnard, D. A., and Shulman, G. L. (2001). *A default mode of brain function*. Proc Natl Acad Sci U S A 98 (2).

Ramon y Cajal, S. (1904). *Textura del Sistema Nervioso del Hombre y de los Vertebrados, tomo II, primera parte.* . Imprenta y Libreria de Nicolas Moya.

Ranck, J. B., Jr. (1975). *Which elements are excited in electrical stimulation of mammalian central nervous system: a review*. Brain Res 98 (3).

Ranck, J. B., Jr. 1981. Extracellular Stimulation. In *Electrical Stimulation Research Techniques*, edited by M. M. Patterson and K. R. P.: Academic Press, 1-36.

Rankin, K. P., Gorno-Tempini, M. L., Allison, S. C., Stanley, C. M., Glenn, S., Weiner, M. W., and Miller, B. L. (2006). *Structural anatomy of empathy in neurodegenerative disease*. Brain 129 (Pt 11).

Rattay, F. (1999). *The basic mechanism for the electrical stimulation of the nervous system*. Neuroscience 89 (2).

Reil, J. C. (1796). *Exercitationum anatomicarum fasciculus primus de structura nervorum*: In officina Curtiana Venalis.

Remedios, R., Logothetis, N. K., and Kayser, C. (2009). *An auditory region in the primate insular cortex responding preferentially to vocal communication sounds*. J Neurosci 29 (4).

Roberts, T. S., and Akert, K. (1963). *Insular and opercular cortex and its thalamic projection in Macaca mulatta*. Schweiz Arch Neurol Neurochir Psychiatr 92.

Robinson, B. W. (1962). *Localization of intracerebral electrodes*. Exp Neurol 6.

Roguin, A. (2004). *Nikola Tesla: the man behind the magnetic field unit*. J Magn Reson Imaging 19 (3).

Romo, R., Hernandez, A., Zainos, A., and Salinas, E. (1998). *Somatosensory discrimination based on cortical microstimulation*. Nature 392 (6674).

Rose, M. (1928). *Die Inselrinde des Menschen und der Tiere*. Journal f. Psychologie und Neurologie 37 (4).

Roy, C. S., and Sherrington, C. S. (1890). *On the Regulation of the Blood-supply of the Brain*. J Physiol 11 (1-2).

Rudin, D. O., and Eisenman, G. (1954). *The action potential of spinal axons in vitro*. J Gen Physiol 37 (4).

Rushton, N. D., and Brindley, S. G. 1978. Properties of Cortical Electrical Phosphenes, 574-593.

Rushton, W. A. (1927). *The effect upon the threshold for nervous excitation of the length of nerve exposed, and the angle between current and nerve*. J Physiol 63 (4).

Sadaghiani, S., and D'Esposito, M. (2015). *Functional Characterization of the Cingulo-Opercular Network in the Maintenance of Tonic Alertness*. Cereb Cortex 25 (9).

Saleem, K. S., and Logothetis, N. K. (2006). *A Combined MRI and Histology Atlas of the Rhesus Monkey Brain in Stereotaxic Coordinates*: Elsevier Science.

Saleem, K. S., Miller, B., and Price, J. L. (2014). *Subdivisions and connectional networks of the lateral prefrontal cortex in the macaque monkey*. J Comp Neurol 522 (7).

Salomon, R., Ronchi, R., Donz, J., Bello-Ruiz, J., Herbelin, B., Martet, R., Faivre, N., Schaller, K., and Blanke, O. (2016). *The Insula Mediates Access to Awareness of Visual Stimuli Presented Synchronously to the Heartbeat*. J Neurosci 36 (18).

Salzman, C. D., Britten, K. H., and Newsome, W. T. (1990). *Cortical microstimulation influences perceptual judgements of motion direction*. Nature 346 (6280).

Sanides, F. (1968). *The architecture of the cortical taste nerve areas in squirrel monkey (Saimiri sciureus) and their relationships to insular, sensorimotor and prefrontal regions*. Brain Res 8 (1).

Santos, M., Uppal, N., Butti, C., Wicinski, B., Schmeidler, J., Giannakopoulos, P., Heinsen, H., Schmitz, C., and Hof, P. R. (2011). *Von Economo neurons in autism: a stereologic study of the frontoinsular cortex in children*. Brain Res 1380.

Scolari, M., Seidl-Rathkopf, K. N., and Kastner, S. (2015). *Functions of the human frontoparietal attention network: Evidence from neuroimaging*. Curr Opin Behav Sci 1.

Seeley, W. W., Carlin, D. A., Allman, J. M., Macedo, M. N., Bush, C., Miller, B. L., and Dearmond, S. J. (2006). *Early frontotemporal dementia targets neurons unique to apes and humans*. Ann Neurol 60 (6).

Seeley, W. W., Menon, V., Schatzberg, A. F., Keller, J., Glover, G. H., Kenna, H., Reiss, A. L., and Greicius, M. D. (2007). *Dissociable intrinsic connectivity networks for salience processing and executive control*. J Neurosci 27 (9).

Seeley, W. W., Merkle, F. T., Gaus, S. E., Craig, A. D., Allman, J. M., and Hof, P. R. (2012). *Distinctive Neurons of the Anterior Cingulate and Frontoinsular Cortex: A Historical Perspective*. Cerebral Cortex 22 (2).

Seth, A. K., Suzuki, K., and Critchley, H. D. (2011). *An interoceptive predictive coding model of conscious presence*. Front Psychol 2.

Shizgal, P., Conover, K., and Schindler, D. (1991). *Medial forebrain bundle units in the rat: dependence of refractory period estimates on pulse duration*. Behav Brain Res 42 (2).

Shulman, G. L., Fiez, J. A., Corbetta, M., Buckner, R. L., Miezin, F. M., Raichle, M. E., and Petersen, S. E. (1997). *Common Blood Flow Changes across Visual Tasks: II. Decreases in Cerebral Cortex*. J Cogn Neurosci 9 (5).

Sokoloff, L. (1977). *Relation between physiological function and energy metabolism in the central nervous system*. J Neurochem 29 (1).

Sokoloff, L., Reivich, M., Kennedy, C., Des Rosiers, M. H., Patlak, C. S., Pettigrew, K. D., Sakurada, O., and Shinohara, M. (1977). *The [14C]deoxyglucose method for the measurement of local cerebral glucose utilization: theory, procedure, and normal values in the conscious and anesthetized albino rat*. J Neurochem 28 (5).

Sridharan, D., Levitin, D. J., and Menon, V. (2008). *A critical role for the right fronto-insular cortex in switching between central-executive and default-mode networks*. Proc Natl Acad Sci U S A 105 (34).

Stark, P., Fazio, G., and Boyd, E. S. (1962). *Monopolar and bipolar stimulation of the brain*. Am J Physiol 203.

Stein, D. J., Arya, M., Pietrini, P., Rapoport, J. L., and Swedo, S. E. (2006). *Neurocircuitry of disgust and anxiety in obsessive-compulsive disorder: a positron emission tomography study*. Metab Brain Dis 21 (2-3).

Sterzer, P., and Kleinschmidt, A. (2010). *Anterior insula activations in perceptual paradigms: often observed but barely understood*. Brain Struct Funct 214 (5-6).

Streeter, G. L. 1912. The Development of the Nervous System. In *Manual of Human Embryology II*, edited by F. Keibel and F. P. Mall. Philadelphia: J. B. Lippincott Company.

Sultan, F., Augath, M., and Logothetis, N. (2007). *BOLD sensitivity to cortical activation induced by microstimulation: comparison to visual stimulation*. Magn Reson Imaging 25 (6).

Swezey, K. M. (1958). *Nikola Tesla*. Science 127 (3307).

Swick, D., Ashley, V., and Turken, U. (2011). *Are the neural correlates of stopping and not going identical? Quantitative meta-analysis of two response inhibition tasks*. Neuroimage 56 (3).

Tehovnik, E. J. (1996). *Electrical stimulation of neural tissue to evoke behavioral responses*. Journal of Neuroscience Methods 65 (1).

Tehovnik, E. J., Tolias, A. S., Sultan, F., Slocum, W. M., and Logothetis, N. K. (2006). *Direct and indirect activation of cortical neurons by electrical microstimulation*. J Neurophysiol 96 (2).

Ter-Pogossian, M. M., Eichling, J. O., Davis, D. O., and Welch, M. J. (1970). *The measure in vivo of regional cerebral oxygen utilization by means of oxyhemoglobin labeled with radioactive oxygen-15*. J Clin Invest 49 (2).

Ter-Pogossian, M. M., Eichling, J. O., Davis, D. O., Welch, M. J., and Metzger, J. M. (1969). *The determination of regional cerebral blood flow by means of water labeled with radioactive oxygen 15*. Radiology 93 (1).

Terasawa, Y., Shibata, M., Moriguchi, Y., and Umeda, S. (2013). *Anterior insular cortex mediates bodily sensibility and social anxiety*. Soc Cogn Affect Neurosci 8 (3).

Tharwat, A. (2018). *Independent component analysis: An introduction*. Applied Computing and Informatics.

Thulborn, K. R., Waterton, J. C., Matthews, P. M., and Radda, G. K. (1982). *Oxygenation dependence of the transverse relaxation time of water protons in whole blood at high field*. Biochim Biophys Acta 714 (2).

Tolias, A. S., Sultan, F., Augath, M., Oeltermann, A., Tehovnik, E. J., Schiller, P. H., and Logothetis, N. K. (2005). *Mapping cortical activity elicited with electrical microstimulation using FMRI in the macaque*. Neuron 48 (6).

Touroutoglou, A., Bliss-Moreau, E., Zhang, J., Mantini, D., Vanduffel, W., Dickerson, B. C., and Barrett, L. F. (2016). *A ventral salience network in the macaque brain*. Neuroimage 132.

Touroutoglou, A., Hollenbeck, M., Dickerson, B. C., and Feldman Barrett, L. (2012). *Dissociable large-scale networks anchored in the right anterior insula subserve affective experience and attention*. Neuroimage 60 (4).

Ture, U., Yasargil, D. C., Al-Mefty, O., and Yasargil, M. G. (1999). *Topographic anatomy of the insular region*. J Neurosurg 90 (4).

Uddin, L. Q., and Menon, V. (2009). *The anterior insula in autism: under-connected and under-examined*. Neurosci Biobehav Rev 33 (8).

Uddin, L. Q., Nomi, J. S., Hébert-Seropian, B., Ghaziri, J., and Boucher, O. (2017). *Structure and Function of the Human Insula*. Journal of clinical neurophysiology : official publication of the American Electroencephalographic Society 34 (4).

Uddin, L. Q., Supekar, K., Lynch, C. J., Khouzam, A., Phillips, J., Feinstein, C., Ryali, S., and Menon, V. (2013). *Salience network-based classification and prediction of symptom severity in children with autism*. JAMA Psychiatry 70 (8).

Vaden, K. I., Jr., Kuchinsky, S. E., Cute, S. L., Ahlstrom, J. B., Dubno, J. R., and Eckert, M. A. (2013). *The cingulo-opercular network provides word-recognition benefit*. J Neurosci 33 (48).

Valenstein, E. S., and Beer, B. (1961). *Unipolar and bipolar electrodes in self-stimulation experiments*. Am J Physiol 201.

Valentin, A., Anderson, M., Alarcon, G., Seoane, J. J., Selway, R., Binnie, C. D., and Polkey, C. E. (2002). *Responses to single pulse electrical stimulation identify epileptogenesis in the human brain in vivo*. Brain 125 (Pt 8).

van den Heuvel, M. P., and Sporns, O. (2011). *Rich-club organization of the human connectome*. J Neurosci 31 (44).

van den Heuvel, M. P., and Sporns, O. (2013). *Network hubs in the human brain*. Trends Cogn Sci 17 (12).

Vesalius, A. (1543). *De corporis humani fabrica libri septem*. Army medical library, Washington D.C.

Vicq-d'Azur, F. (1786). *Traité d'anatomie et de physiologie*. 2 vols. Vol. 1. Paris: Didot lAîné.

Vincent, J. L., Patel, G. H., Fox, M. D., Snyder, A. Z., Baker, J. T., Van Essen, D. C., Zempel, J. M., Snyder, L. H., Corbetta, M., and Raichle, M. E. (2007). *Intrinsic functional architecture in the anaesthetized monkey brain*. Nature 447 (7140).

Vincent, M., Guiraud, D., Duffau, H., Mandonnet, E., and Bonnetblanc, F. (2017). *Electrophysiological brain mapping: Basics of recording evoked potentials induced by electrical stimulation and its physiological spreading in the human brain*. Clin Neurophysiol 128 (10).

von Bonin, G., and Bailey, P. (1947). *The Neocortex of Macaca Mulatta*: University of Illinois Press.

Wai, M. S., Shi, C., Kwong, W. H., Zhang, L., Lam, W. P., and Yew, D. T. (2008). *Development of the human insular cortex: differentiation, proliferation, cell death, and appearance of 5HT-2A receptors*. Histochem Cell Biol 130 (6).

Warnaby, C. E., Seretny, M., Ni Mhuircheartaigh, R., Rogers, R., Jbabdi, S., Sleigh, J., and Tracey, I. (2016). *Anesthesia-induced Suppression of Human Dorsal Anterior Insula Responsivity at Loss of Volitional Behavioral Response*. Anesthesiology 124 (4).

Watson, K. K., Jones, T. K., and Allman, J. M. (2006). *Dendritic architecture of the von Economo neurons*. Neuroscience 141 (3).

Weishaupt, D., Koechli, V. D., and Marincel, B. (2014). *Wie funktioniert MRI? Eine Einführung in Physik und Funktionsweise der Magnetresonanzbildgebung*: Springer.

Wen, X., Liu, Y., Yao, L., and Ding, M. (2013). *Top-down regulation of default mode activity in spatial visual attention*. J Neurosci 33 (15).

Wernicke, C. (1874). *Der aphasische Symptomencomplex: Eine psychologische Studie auf anatomischer Basis*. Breslau: Cohn.

West, D. C., and Wolstencroft, J. H. (1983). *Strength-duration characteristics of myelinated and non-myelinated bulbospinal axons in the cat spinal cord*. J Physiol 337.

Widom, B. (2002). *Statistical Mechanics: A Concise Introduction for Chemists*: Cambridge University Press.

Wylie, K. P., and Tregellas, J. R. (2010). *The role of the insula in schizophrenia*. Schizophr Res 123 (2-3).

Yeterian, E. H., and Pandya, D. N. (1989). *Thalamic connections of the cortex of the superior temporal sulcus in the rhesus monkey*. J Comp Neurol 282 (1).

Yin, Z., Chang, M., Wei, S., Jiang, X., Zhou, Y., Cui, L., Lv, J., Wang, F., and Tang, Y. (2018). *Decreased Functional Connectivity in Insular Subregions in Depressive Episodes of Bipolar Disorder and Major Depressive Disorder*. Front Neurosci 12.

Zilles, K., and Palomero-Gallagher, N. (2017). *Multiple Transmitter Receptors in Regions and Layers of the Human Cerebral Cortex*. Front Neuroanat 11.

7

STATEMENT OF CONTRIBUTIONS

Jennifer Smuda (JS) helped with the design of the study and was planning and conducting the experiments, together with CAK and HCE. JS subsequently analysed the data and wrote the paper (please find detailed contributions below).

Dr. Henry C. Evrard (HCE), the project's supervisor, designed the study, helped with the experiments, and provided help and ideas throughout the project.

Dr. Carsten A. Klein (CAK) helped with the planning and the conduction of the experiments.

Dr. Yusuke Murayama (YM) provided help and advice during the experiments and the analysis phase.

Axel Oeltermann (AO) provided technical support during the experiments.

Prof. Dr. Nikos Logothetis (NKL) provided all material and staff resources for the monkey experiments.

Detailed contributions of Jennifer Smuda (JS)

Surgeries: The surgeries were planned and prepared by JS and CAK. This included setting up the surgery room and the instruments, gathering all needed materials, organizing schedules, and assembling a team. The preoperational procedures were conducted by the TAs with the help of JS. During the surgeries, JS either assisted the main surgeon (HCE, YM, or NKL) or handed instruments as a scrub nurse. After a successful surgery, JS helped with the postoperative care of the monkeys as well as the monitoring of the animals.

Maintenance of the monkeys: The husbandry of the monkeys was under the care of the vets and the animal care staff. JS was involved in the treatment of sick monkeys and oversaw feeding and treatment schedules. Every three days, or according to need, JS conducted chamber cleanings to maintain sterile, tissue free chambers.

Monkey experiments: The conducted terminal monkey experiments comprised two data collections experiments, as well as tracer injections:

- **Data collection during functional magnetic resonance imaging in combination with electrophysiological recordings or electrical microstimulations:** JS and CAK planned the experiments, including the assembly and the scheduling of a technical staff team and the collection and testing of the needed equipment (e.g. recording and stimulation electrodes, preamplifiers, or stimulation sources).

  On the day of the experiment, the monkeys were put under anaesthesia with help from the technical staff and the complex equipment for the measurements was subsequently set up by JS and CAK. The data collection, which lasted several days, was conducted by JS and CAK.
- **Tracer injections:** The tracer injections were performed at the end of the terminal experiments by JS or HCE. The injected tracers were thoroughly tested by JS prior to injection. This was done in two different ways:

  - *Tracer testing in rats:* A setup for the conduction of rat experiments was assembled by JS. Besides a robot stereotaxic surgery station and different mechanisms for tracer injections, it

contains equipment for optogenetic experiments, as well as extracellular electrophysiological recordings. To enable the insertion of electrodes into both hemispheres simultaneously, a dual-electrode holder was designed by JS and the fine mechanical workshop. Additionally, JS and the fine mechanical workshop conceptualized a new Faraday cage, which is shielding the setup from external magnetic fields. The setup is further equipped with a stimulation source and appliances allowing electrical micro-stimulation in the brain, as well as on peripheral nerves. Besides the peripheral nerve stimulation equipment, electrophysiological recording artifices are also established. Devices to measure the heart rate, the oxygen saturation, the carbon dioxide concentration, the pulse, the breathing rate, and the breathing depth were also added to the setup, to meticulously monitor the animal's physiological signals. Since no commercially available invasive blood pressure device fulfilled the experimental requirements, a new device was designed by AO and JS, which was, like several other components of the setup, also used in the monkey experiments.

Lastly, a device combining recording electrodes, optrodes, and stimulation electrodes in one small diameter casing, was conceptualized.

After successful assembly of the setup, different tracers were tested in rats, and the results analysed.

- *Tracer testing in cell culture:* The second approach was testing the tracer-efficiency in cell culture. For this, JS established cell lines and cell culture protocols and analysed the results.

Brain recovery: The brain recovery in rats was performed by JS, in monkeys by HCE or CAK with the assistance of JS.

Histology: The histological processing of rat and monkey brains was performed by JS and included cryoprotecting the tissue, slicing the brains in 50 μm thin, coronal slices, and performing Nissl or immuno-histochemical stainings.

Analysis: The analysis of the rat experiments as well as the microstimulation experiments in monkeys was done by JS. YM provided invaluable help with the Matlab toolbox and general programming questions. The preliminary neural-event-triggered functional magnetic resonance imaging data analysis was performed by CAK and JS.

Paper: The manuscript was written by JS and revised by HCE. All figures were prepared by JS in MatLab (MathWorks, Natick, MA, USA), Adobe Illustrator, or Adobe Photoshop (Adobe Systems, Dublin, Ireland).

APPENDED MANUSCRIPT

Direct electrical stimulation of the ventral anterior insular cortex in the macaque monkey

Jennifer Smuda [1,2,3], Carsten Klein [2], Yusuke Murayama [2], Axel Oeltermann [2],

Nikos Logothetis [2,4], and Henry Evrard* [1,2]

[1]Werner Reichardt Center for Integrative Neuroscience, Tuebingen, Germany; [2]Max Planck Institute for Biological Cybernetics, Tuebingen, Germany; [3]International Max Planck Research School, Tuebingen, Germany; [4]Imaging Science and Biomedical Engineering, University of Manchester, Manchester, UK

*Corresponding author: henry.evrard@tuebingen.mpg.de

Abstract

Functional imaging studies have implicated the anterior insular cortex (AIC), a key node of the salience network, in several distinct interoceptive, emotional, and cognitive processes, while local electrical microstimulation (EMS) has revealed its influence in autonomic regulation. As a major polymodal integration hub, the AIC has a crucial role in detecting salient events and in asymmetrically orchestrating sympathetic (right AIC) and parasympathetic (left AIC) efferent controls. To examine whether the AIC's involvement in brain-wide functional networks is similarly asymmetrically organized, we conducted EMS in the left and right ventral AIC in three anaesthetised macaque monkeys, while simultaneously acquiring functional magnetic imaging data. General linear model analyses, as well as seed-based correlation analyses, revealed that the AIC

is functionally connected with monosynaptic and polysynaptic cortical and subcortical brain regions. Further, the EMS of the left and right insula led to an asymmetric regulation of the networks: while left and right-sided stimulation shut down the contralateral salience and default mode network, right-sided stimulation further upregulated the ipsilateral salience network and bilaterally shut down the central executive network.

These results strengthen the insula's role as a rich club hub in the salience network and unravel remarkable asymmetric regulations of the main brain-wide functional networks, which could be relevant for the homeostatic assessment of affect and adaptation of motivated behaviours.

Introduction

The anterior insular cortex (AIC) is one of the most consistently activated cortical regions across functional imaging studies in humans (Craig, 2009) and has been proposed to act as a key poly-modal integration hub (Menon and Uddin, 2010). Within the insula, primary, 'objective' interoceptive information advances from the posterior portion of the IC to the mid-IC, where it is integrated with homeostatic motor functions and sensory environmental conditions, before reaching the anterior IC. There, hedonic, motivational, social, and cognitive conditions are integrated, leading to a subjective awareness of oneself in space and time (Craig, 2009). The to-be-integrated-information reaches the IC from a wide net of cortical and subcortical connections (Mesulam and Mufson, 1982b, 1982c; Mufson and Mesulam, 1982). This broad connectivity as well as its central position in the salience network (SN), a complex of brain regions performing bottom-up detection of salient events and top-down adjustments of signals to manage autonomic reactivity (Eckert et al., 2009; Menon and Uddin, 2010; Chen et al., 2016), allow it to assess the relevance of information and to determine attentional resource allocation to salient stimuli (Michel, 2017). As a major hub in

the SN, it furthermore has the capacity to switch between default mode network (DMN) and central executive network (CEN) (Goulden et al., 2014; Chen et al., 2016).

The ventral portion of the anterior insula (vAIC) hosts two specialized projection neurons; the fork neuron and the von Economo neurons (VEN). The latter are remarkable projection neurons inhabiting layer 5b of the lateral anterior insula (Ial, VEN area) (Evrard et al., 2014; Horn et al., in preparation). They possess an elongated, spindle-shaped perikaryon and a unique thick apical and equally thick basal dendrite (Economo, 1926; Seeley et al., 2012) and have been shown to be selectively affected in neurodegenerative diseases (Kim et al., 2012; Butti et al., 2013). Though their specific function remains a mystery until today, they have been hypothesised to play an important role in awareness (Allman et al., 2010), autonomic regulation (Butti et al., 2013), and interoception (Santos et al., 2011).

Stimulating the anterior IC using electrical microstimulation (EMS), a tool that has been extensively used in the past to study brain function and connectivity (Ferrier, 1875; Penfield and Boldrey, 1937; Asanuma and Sakata, 1967; Ekstrom et al., 2008; Logothetis et al., 2010; Matsui et al., 2011; Matsui et al., 2012; Moeller et al., 2017), revealed an asymmetric response of autonomic functions, with left-sided stimulation leading to bradycardia and right-sided stimulation leading to tachycardia (Oppenheimer et al., 1992; Caruana et al., 2011). To investigate if global brain activity appears asymmetric as well, we used EMS alternately in the left and right VEN area in three anesthetized macaque monkeys during functional magnetic resonance imaging (fMRI). Furthermore, we employed a seed-based correlation analysis (SBCA) on this dataset, as well as on a dataset collected during resting state, monitoring the intrinsic spontaneous activity (ISA) in the IC, to investigate the networks arising in both conditions.

Methods

Subjects

Three healthy rhesus macaque monkeys (*Macaca mulatta*) were used in this study (5-10 kg; 7–13 years old; one female). The monkeys were housed in social groups of two to three animals, were fed three times a day, and received water *ad libitum*, except 6 to 12 hours prior to anaesthesia, which required a *nil per os* period. All experimental procedures were conducted with great care to ensure animal wellbeing; they followed the European directive 2010/63/EU and were approved by the local authorities (*Regierungspräsidium*).

Chamber implantation

Custom-made, monkey-specific polyether ether ketone (TecaPEEK Optima, Ensinger, Germany) chambers were surgically implanted under aseptic operative conditions and general anaesthesia, which was maintained by the inhalation anaesthetic isoflurane (1.2 – 1.4 flowrate, CP-Pharma Handelsgesellschaft mbH, Burgdorf, Germany) or Remifentanil (0.2 µg/kg/min, intravenous, GlaxoSmithKline GmbH & Co. KG, Muenchen, Germany). The chambers were fixed to the skull using custom-made ceramic screws (zirconium oxide Y_2O_3-TPZ 5×1; Pfannenstiel, Bad Toelz, Germany). The position for the chambers above the vAIC was on average centred 26.9 mm and +/- 14.6 mm from Frankfurt zero on the X and the Y axis, respectively. Subsequently, a craniotomy was performed in the centre of the chamber though which electrodes were inserted into the brain during experiments.

The day before the surgery, corticosteroids were administered to the animal to prevent inflammations. Post surgically the animals were monitored closely for 36 hours before reverting to their home cages. A pre-emptively antibiotic treatment with Amoxicillin and Clavulanic acid was administered for six days

and a recovery period of at least two weeks was granted before experiments were conducted.

To keep the chambers sterile, a chamber cleaning was performed every three days, or according to need, while the animal was under a short term anaesthesia using glycopyrrolate (Robinul 0.01 mg/kg, intramuscular, Riemser Pharma GmbH, Greifswald, Germany) and ketamine (Ketamin 15 mg/kg intramuscular, WTD eG, Garbsen, Germany).

Experimental anaesthesia

After pre-medication with Robinul and sedation with Ketamin, the monkeys were transported from their home cages to the experimental setup where a 20 gauge intravenous catheter was inserted into their saphenous veins. The monkeys were preoxygenated (EtCo2<30 mmHg) and the main anaesthesia was introduced by applying Fentanyl (0.003 mg/kg, intravenous, Janssen-Cilag GmbH, Neuss, Germany) for analgesia, Trapanal (5 mg/kg, intravenous, Inresa Arzneimittel GmbH, Freiburg, Germany) for anaesthesia, and Lysthenon (0.015 mg/kg, intravenous, Takeda GmbH, Konstanz, Germany) for muscle relaxation. After effect onset of the medication, the monkeys were intubated (3.0 – 3.5 endotracheal tube) and physiological monitoring equipment was connected. During the experiment the anaesthesia was maintained by the non-depolarizing neuromuscular-blocking agent mivacurium chloride (Mivacron 5 mg/kg/h, intravenous, GlaxoSmithKline GmbH & Co. KG, Muenchen, Germany) and the opioid analgesic drug remifentanil (Ultiva 5 mg/kg/min, intravenous, GlaxoSmithKline GmbH & Co. KG, Muenchen, Germany). The depth of the anaesthesia and vital physiological parameters such as heart rate, ECG, temperature (38.5 – 39.5 °C), O_2 saturation (>95 %), end-tidal CO_2 (30 – 33 mmHg), and blood pressure were monitored and maintained appropriately. Additionally, a Laser-Doppler blood flow monitor (moorVMS-LDF, Moor

Instruments, Devon, United Kingdom) was attached to the left and right forearm. To maintain homeostasis, the monkeys received lactated Ringers solution with 20 % glucose (Glucosteril 10 mg/kg/h, intravenous, Fresenius Kabi Deutschland GmbH, Bad Homburg, Germany). The intravascular volume was maintained by administering colloids if needed.

At the end of the experiment the monkeys were euthanized with a lethal dose of pentobarbital (60 mg/kg, intravenous, CP-Pharma Handelsgesellschaft mbH, Burgdorf, Germany) and then immediately transcardially perfused. For this, the abdomen was opened, the diaphragm trepanated, the chest cavity exposed, and a large-bore needle inserted into the aorta, delivering first a sodium chloride solution (0.09 %), followed by 4 % PFA solution (pH 7.4) and 4 % PFA, 5 % sucrose solution (pH 7.4). The brains were recovered and stored in 0.01 M PBS with 30 % sucrose and 0.1 % sodium azide for later histological processing.

fMRI data acquisition and stimulation

After preparation (see experimental anaesthesia) the monkeys were placed in a custom-made MR-compatible chair and a customized 85 mm radiofrequency coil was fixed around their head. The monkeys were then transferred to a vertical 7 T scanner, which had a 60 cm diameter bore (BioSpec 70/60v, Bruker Corporation, Billerica, MA, USA) and an 80 mTm^{-1} actively shielded gradient coil (Bruker, BGA38) with an inner diameter of 38 cm. High-resolution anatomical scans of the head were obtained with a T1 weighted 3D MDEFT imaging sequence, using a repetition time of 15 s, a bandwidth of 50 kHz, a flip angle of 20°, a field of view of 96 x 96 x 64 mm, and a matrix of 192 × 192 × 128 mm.

Subsequently, custom-made single channel glass isolated iridium electrodes (<50 kΩ, 100 μm diameter) were inserted into the monkeys' left and right VEN area using micro drives attached to the cranial chambers. The correct position of the electrodes was confirmed by anatomical scans. The electrodes, the micro

drives, the recording and stimulation equipment, as well as the toolbox for analysis were developed at the Max-Planck Institute for Biological Cybernetics.

Upon correct positioning of the electrodes, the right and the left VEN area was stimulated alternately during separate functional imaging scans. During a 10 minute imaging run, 10 stimulations were performed, each stimulation lasting 16 s followed by a pause of 44 s. During the 16 s there was a 200 ms on-period, in which 200 μs biphasic charge-balanced pulses with an intensity of 400 – 1200 μA were delivered, followed by a 400 ms off-period (Logothetis et al., 2010). Given the similarity of the used stimulation electrodes in terms of resistance and size, as well as the used stimulation parameters, an equal stimulation on both hemispheres can be assumed.

At the same time echo-planar imaging (EPI), with 2 s volume times, a four-shot gradient-echo, a repetition time of 1000 ms, an echo time of 19 ms, a bandwidth of 150 kHz, a flip angle of 30°, a field of view of 96 x 96 mm, a matrix of 96 x 96 mm and 2 mm slice thickness, was performed (reconstruction 128 x 128 mm). The same EPI parameters were used to collect the ISA, which consisted of, on average, 54 runs per monkey.

fMRI data pre-processing

For reconstruction of the recorded MRI data the software Paravision 5.1 (Bruker, Billerica, MA, USA) was utilized. All following data analysis was performed using MatLab (MathWorks, Natick, MA, USA) with a toolbox that was developed in the lab (Logothetis et al., 2012). In a first step, during the pre-processing of the data, a selection of trials was conducted, where all trials containing motion artefacts, ghost artefacts, or contrast changes were excluded from further analysis (less than 2 %). Additionally, trials in which the electrical microstimulation did not activate the vAIC were excluded (less than 10 %). The data was filtered using a spatial Gaussian convolution filter (with a size of 3 x 3 voxels and a sigma of

0.7 voxels) while voxel size was preserved. For spatial reference, the anatomical scans were accurately aligned to the EPI scans using manual landmark apposition and a linear weighted model algorithm for each slice separately. More than 140 regions of interest (ROIs) in the left and right hemispheres were drawn manually using for reference atlases of the rhesus monkey brain (Paxinos et al., 2009; Saleem and Logothetis, 2012) and our recent parcellation of the insula (Evrard et al., 2014).

fMRI data analysis

For the activity maps, a general linear model (GLM) was used, which consisted of a boxcar function, with the stimulation as active periods, convolved with the haemodynamic response function. For the SBCA maps, an average time course was calculated from all the voxels within the seed region (left or right vAIC). This averaged time course was then used to compute correlation coefficients with every voxel of the brain. Both, the activity maps and functional connectivity maps were corrected for multiple comparisons using the false discovery rate (Benjamini–Hochberg procedure), and the threshold was set at 0.0001. Additionally, a spatial clustering algorithm, to eliminate spurious activation, and a mask, based on temporal signal to noise ratios, was applied.

Histological processing and microscope analysis

The cryoprotected brains were frozen at -30 °C onto a sliding microtome (HM 450, Thermo Fisher Scientific, Waltham, Massachusetts, USA) and fixed using Tissue-Tek® O.C.T.™ Compound (Sakura Finetek, Staufen im Breisgau, Germany). They were cut in 50 µm thick coronal slices and subsequently mounted onto gelatin-coated custom-made glass slides (Paul Marienfeld GmbH & Co. KG, Lauda-Königshofen, Germany). After drying, a Nissl stain was performed using a cresyl violet solution (0.16 % in 3.75 % ethanol). For the

analysis the slides were first digitalized using the automatic slide scanner Axio Scan.Z1 (Carl Zeiss Microscopy GmbH, Jena, Germany), equipped with a 10x/0.45 plan-apochromatic objective (Carl Zeiss Microscopy GmbH, Jena, Germany) and a Hitachi HV-F202 digital camera (Hitachi, Tokyoa, Japan), and then analysed using the accompanying ZEN software (Carl Zeiss Microscopy GmbH) and Adobe Photoshop (Adobe Inc., San Jose, California, U.S.). Electrode tracks, presented as darker stained, elongated marks in the tissue, enabled the precise localization of the electrode position during the experiment.

Results

Data sets and microstimulation sites

A total of 120 fMRI scans (10 minutes each) were collected in three anaesthetized monkeys (M1, M2, and M3) during EMS in either the left or right VEN area. Out of these 120 scans, 6 scans were removed due to artefacts (5 from M1 and 1 from M2) and 11 scans were removed due to a lack of blood oxygenation level dependent (BOLD) signal response in the stimulated ROI (2 from M1, 7 from M2, and 3 from M3). Finally, in order to analyse the same number of scans from left and right EMS in each case separately, 11 scans were randomly removed using a pseudorandom number generator. This resulted in analysing the effect of the left and right EMS in 2x18 scans in M1, 2x13 scans in M2, and 2x15 scans in M3. In addition, 2x49 scans without EMS were acquired in M1 and M2 for comparing functional networks between stimulated and resting state cases.

Figure 1A, B, and B' illustrate the positioning of the microstimulating electrodes in one representative case (M1). Both the anatomical MRI scans made during the experiments (fig. 1A), and the post-mortem histological examination (fig. 1B and B') confirmed that the tip of the stimulating electrodes was localized correctly within the VEN area in vAIC. (For M2 and M3, see supplementary fig. S1.) Macroscopically, the VEN area occurred in the subtle but consistent cortical

convexity characterizing the rostral end of the insular cortex, just anterior to the limen insula (fig. 1A). Microscopically, in addition to the presence of VEN and FN, the VEN area was architectonically characterized by the presence of a thin but markedly distinct layer 2 and a broad, large-celled layer 5 with a rather subtle but visible separation from layer 3. These characteristics differed from the features of the adjacent posterior medial (Iapm) and posterior lateral (Iapl) agranular areas of the insula in which there was no VEN and FN, no distinct layer 2, and a rather sharp delimitation between layers 3 and 5 (fig. 1B-B') (Carmichael and Price, 1994; Evrard et al., 2014; Horn et al., in preparation). The position of the electrodes within vAIC was rather similar in the left and right sides in a single monkey, with, in most cases, less than 1.5 mm of difference in anteroposterior (AP), mediolateral (ML) or dorsoventral (DV) placement between the left and the right (fig. S1E). Larger difference occurred only in M3, in which the electrode on the right was placed 2.42 mm more lateral and 2 mm more dorsal than the left electrode. As shown below, despite this difference, the spatial activation patterns produced by the left and right EMS were rather similar within each case taken separately, including M3.

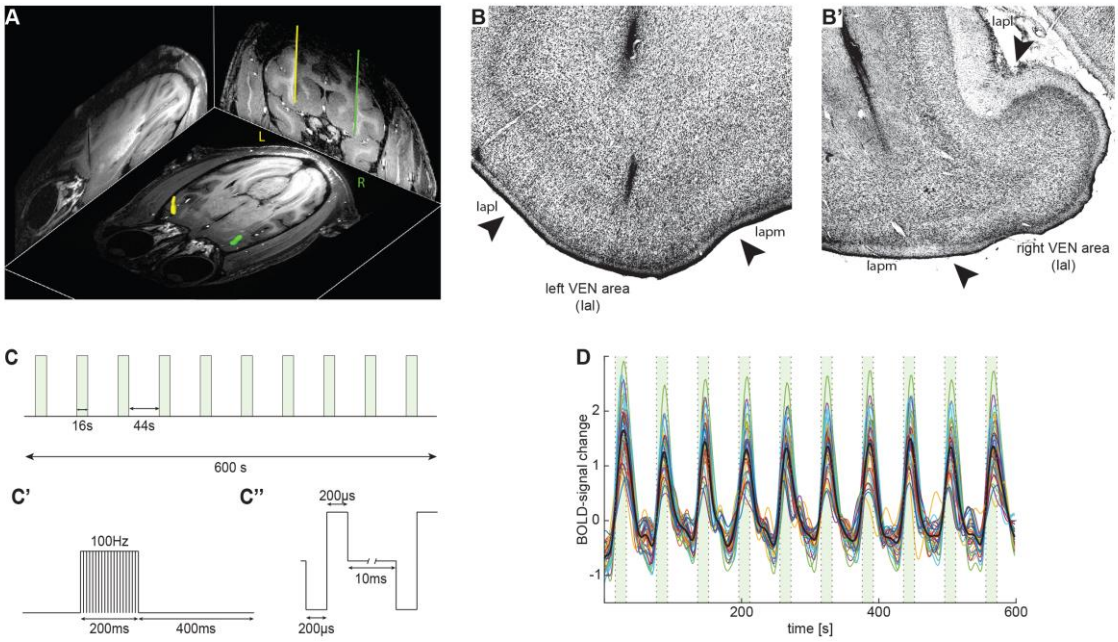

figure 1: EMS in the VEN area of the anesthetized macaque monkey. **A** orthogonal views show the position of the left (yellow) and right (green) electrode in the left and right VEN area. **B** histological Nissl stained coronal section, with 50µm thickness, indicate the electrode position (black tract) in the VEN area on the left (B) and right (B′) side. Black arrowheads indicate the borders of the architectonic areas. **C** schematic representation of the stimulation paradigm. Ten 100 Hz stimulations were delivered over 10 minutes with an amplitude of 400 – 1200 µA. **C′** each stimulation lasted 16 s, with 200 ms on and 400 ms off periods. **C″** each pulse consisted of a 200µs negative pulse, followed by a 200 µs positive pulse and a 10 ms pause. **D** representative BOLD–signal changes in response to EMS over ten minutes with ten stimulations. Green lines indicate the onset and length of the stimulation, colourful traces indicate the BOLD-signal changes for all significant voxels in the ventral AIC (>95%), black trace indicates the average of these significant voxels. Iapl: posterior-lateral agranular insula; Ial: lateral agranular insula; Iapm: posterior-medial agranular insula.

Brain-wide BOLD signal variations induced by unilateral EMS

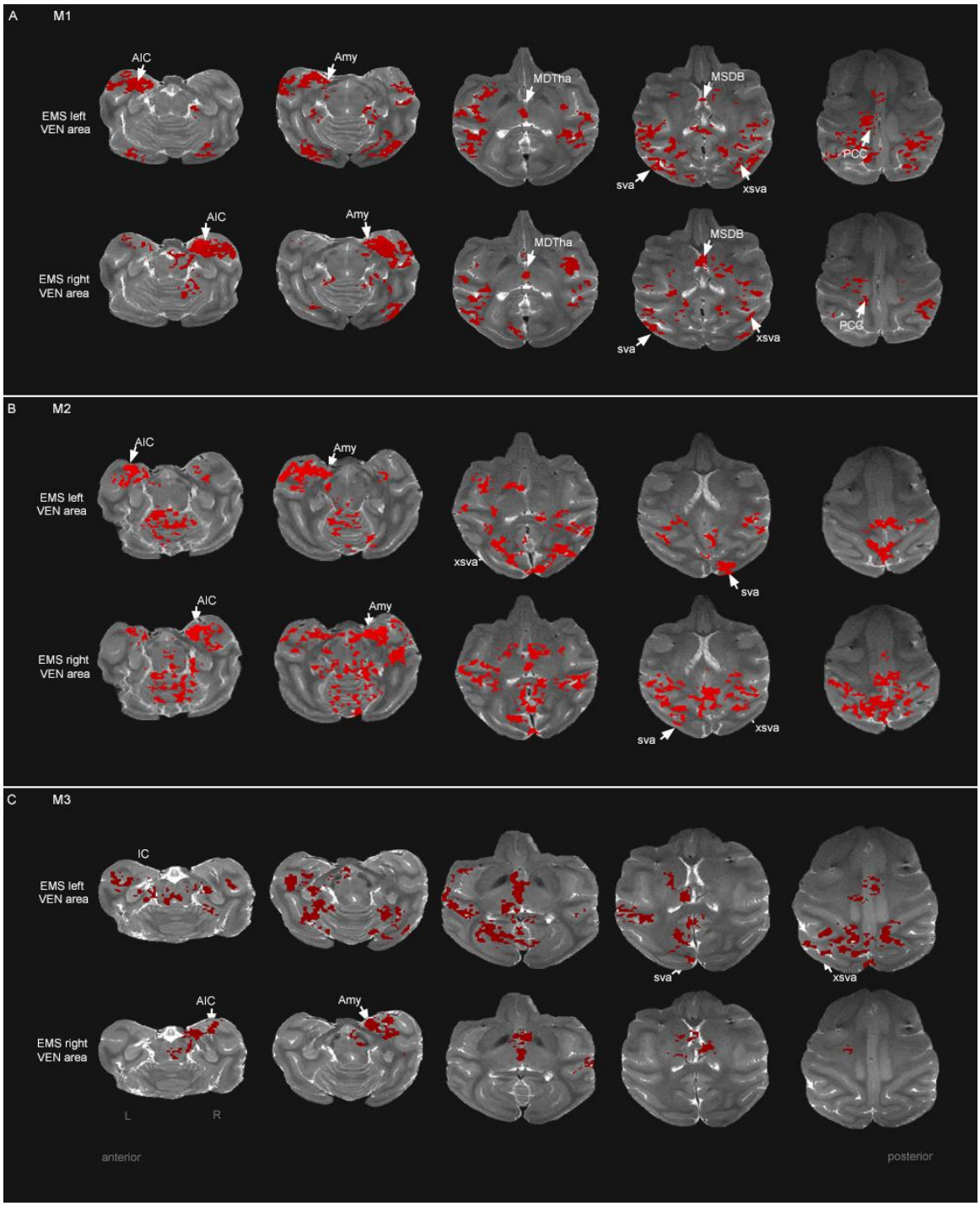

figure 2: Activity maps displaying positive BOLD-signal changes during EMS. **A–C** five representative horizontal brain slices display positive BOLD-signal changes during EMS in the left (upper row) and right (lower row) VEN area for M1 (**A**), M2 (**B**), and M3 (**C**). vAIC: ventral anterior insular cortex; amy: amygdala; MdTha: midline thalamus; MSDB: Medial Septum-Diagonal Band of Broca; PCC: posterior cingulate; sva: striate visual areas; xsva: extrastriate visual areas. Corrected for false discovery rate, p-value: 0.0001.

In all three monkeys, regardless of the stimulated hemisphere, the EMS paradigm (fig. 1C-C') systematically produced a remarkable and consistent increased in BOLD signal directly around the tip of the electrode, in the vAIC ROI (fig. 1D), indicating that the EMS was each time efficient enough to induce a reproducible neurovascular effect indicative of heightened local neuronal firing (Logothetis et al., 2010). Figure 2 shows pairs of maps of the average positive BOLD signal response produced in five horizontal slices of the brain in M1 (fig. 2A), M2 (fig. 2B) and M3 (fig. 2C) with EMS of either the left (top row in each panel) or right (bottom rows) VEN area. The positive BOLD response systematically comprised the ipsilateral vAIC, which contained the stimulation site. There was, however, no or little activation in the contralateral vAIC. A predominantly ipsilateral activation occurred in several distinct subcortical limbic regions including the amygdala (Amy), the claustrum, and the ventral striatum (VS) in the direct vicinity of vAIC, and the midline periventricular thalamic region (MLT), the medial septum region (MS), and the substantia nigra (SNi) further away from the stimulation site. Other subcortical regions, often associated to limbic, autonomic, or emotional arousal, were variably activated across cases but with great similarity across sides, with, for example, the activation of the periaqueductal grey with left and right EMS in M1, or the parabrachial nucleus in M2. In addition to these subcortical regions, two 'categories' of cortical regions were activated. First, limbic cortical regions, such as the anterior cingulate cortex (ACC), posterior cingulate cortex (PCC), or small and variable areal formation in the orbital prefrontal cortex or the insula, were consistently activated, although the exact localization of the activation varied across cases (but not across sides). Second and most conspicuously, a wealth of non-limbic cortical regions that were not known to be monosynaptically connected with the vAIC, were also markedly activated. The exact localization of the activation varied across cases but always included visual areas ranging from V1 to V2-V3, to various temporal visual content processing areas (e.g. MST and Tea). In some cases, activation also

occurred in the intraparietal cortex, the auditory region of the planum temporal, the post-insular vestibular cortex, the secondary somatosensory cortex, and finally, in some rare cases and slices, the primary somatosensory cortex. Throughout these activations, there was no noticeable or consistent asymmetry in either the localization or intensity of the activation. Within a single case, small differences in global brain activation were observed between the left and right sided stimulation in the VEN area, for example in the activation patterns of the visual areas (fig. 2). However, the overall increase in the BOLD-signal occurred overall in similar regions, mainly in the ipsilateral hemisphere, across all cases and sides.

Figure 3 shows representative BOLD signal time courses for several of the above-mentioned brain regions in the three different cases (fig. 3A M1, fig. 3B M2, fig. 3C M3). They indicate that the observed BOLD-signal changes occur in response to the EMS, whose duration is indicated by the light grey bars for stimulation on the left (upper rows) and the right side (lower rows). The positive BOLD-signal changes for regions located in close anatomical proximity to the VEN area (e.g. the amygdala) were stronger than for regions further afield (e.g., posterior cingulate cortex), both, after left and right-sided EMS.

The negative BOLD signal changes for all three experiments are depicted in supplementary figure S2. The EMS produced almost no negative responses except the left EMS in M1 and, more particularly, right EMS in M3. Notably, in M3, the negative BOLD signal response (fig. S2C, bottom row) exceeded the positive signal change (fig. 2C, bottom row). The variations in BOLD signal occurrence and distribution were without any particular effect due to the side of the stimulation per se.

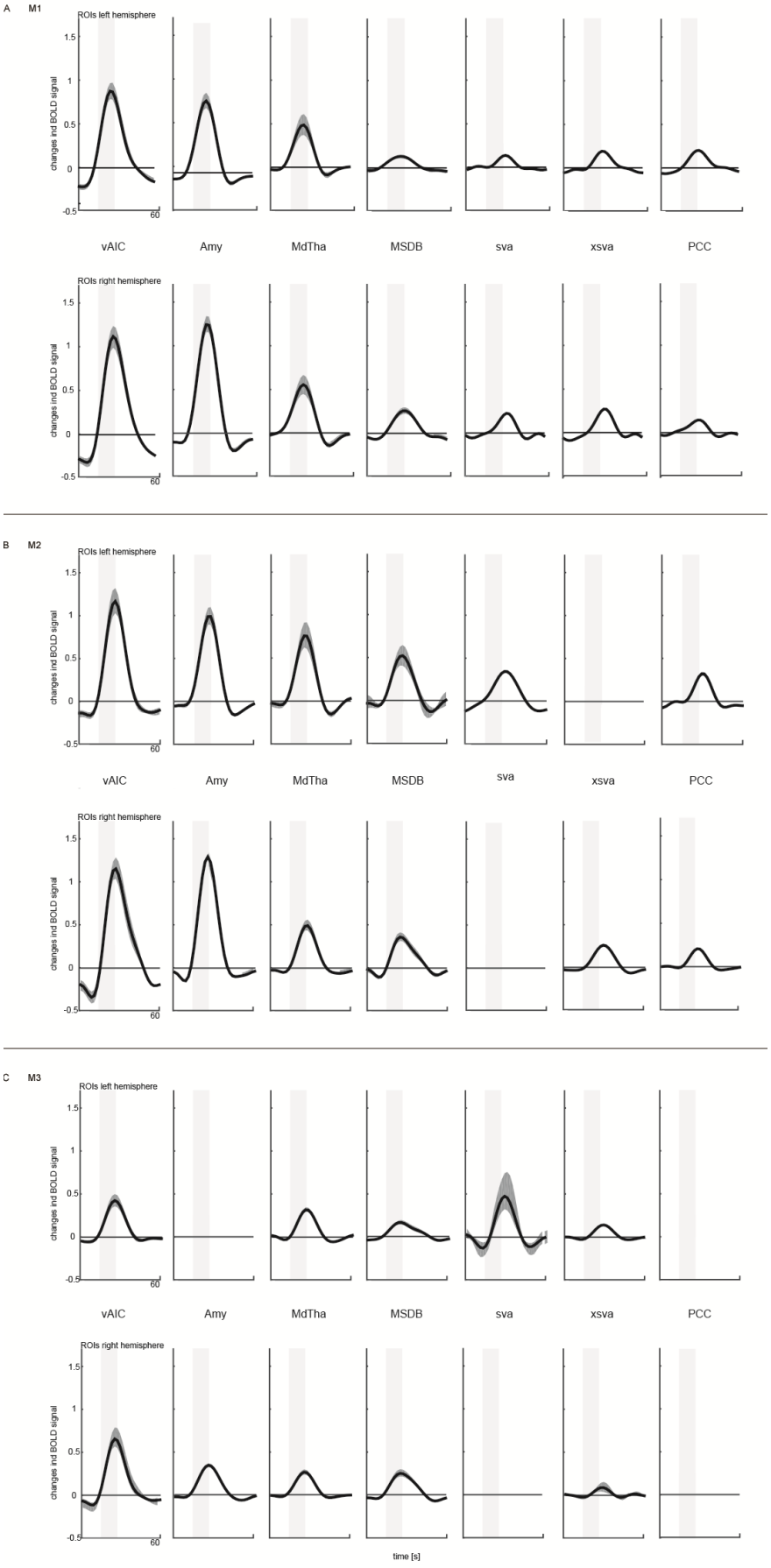

figure 3: exemplary time courses of selected brain regions display the positive BOLD–signal change following EMS on the left (upper row) and right (lower row) side M1 (**A**), M2 (**B**), and M3 (**C**). Light grey bars indicate the onset and duration of the EMS; the black lines depict the average of all significant voxels in the given brain area; dark grey shaded areas indicate the 95 % confidence interval (bootstrap, 1000 repetitions). Empty plots indicate that no voxels were significantly active following the EMS.

Seed-based correlation analysis of functional connectivity in resting vs. stimulated state

To investigate the functional network resulting from EMS, a SBCA was performed on the EMS dataset. For comparison, the same analysis was performed on the ISA dataset, recorded during resting state, to uncover the functional resting state network seeded in the anterior insula. Figure 4A shows an example of correlation maps produced from the left (yellow) or right (green) AIC in M1 during either EMS (top row) or rest (bottom row). In the EMS condition, the seed was placed in the left AIC for the left EMS and right AIC for the right EMS, in the ISA condition, the seed was placed on both sides. Overlapping areas between 'left' and 'right' correlations are indicated with a blend of yellow and green into light green.

The functional network during resting state (fig. 4A') was found to involve both insulae and included several different, bilateral subcortical and cortical brain areas like the amygdala, extrastriate visual areas (xsva), and parts of the temporal and parietal lobe. In contrast, the network resulting from left and right stimulation in the VEN area (fig. 4A) was less extensive and mainly ipsilateral to the stimulation. Unlike in the resting state, there was no correlation with the contralateral AIC. Correlation in cortical areas, like the extrastriate visual areas and the parietal cortex were concentrated on the ipsilateral side, whereas midline regions, like the midline thalamus (MDTha), showed correlations in both hemispheres. Similar correlation patterns were seen in M2 and M3 (see supplementary figure 3).

A subsequent analysis of the percentage of significantly correlated voxels per brain area (Figure 4B-E), averaged over three experiments, confirmed, in contrast to the resting state, that the EMS in the left and right VEN area led to predominantly ipsilateral correlations (B, C) with a 'shutdown' of correlations with the contralateral hemisphere (+49.9 % (ipsilateral) and -74.1 % (contralateral) for left-sided stimulation compared to ISA; +120 % (ipsilateral) and -33.7 %

(contralateral) for right-sided stimulation compared to ISA). Merely some midline regions, like the MDTh, the MS, or the bed nucleus of the stria terminalis (BNST), showed correlations on both sides (13.3 %, 14.2 %, and 5.7 %, respectively, on the right side after left side stimulation; 34.3 %, 14.6 %, and 28.3 % respectively on the left side after right side stimulation). However, these regions also displayed higher correlations in response to the EMS on the ipsilateral side compared to the resting state (36.7 %, 22.9 %, and 24.7 % on the left side after left side stimulation; 50.5 %, 51.3 %, and 38.0% on the right side after right side stimulation). Brain areas like the hippocampus and the periaqueductal grey displayed less correlation during EMS than during ISA (1.0 %, and 3.0 % respectively on the left side after left side stimulation; 2.2 %, and 2.9 % on the right side after right side stimulation). Notably, the correlation during right-sided stimulation was 61.0 % higher than stimulation on the left side.

At rest, the insula displayed correlations with brain areas in both hemispheres alike (D, E). While there were almost no differences in correlation strength between the hemispheres, the correlation strength between areas close to the AIC (e.g. insula, amygdala, or claustrum) as well as subcortical areas (e.g. midline thalamus or MS) was stronger, compared to cortical areas (e.g. visual, sensory, or parietal areas).

figure 4: SBCA maps during EMS and ISA. **A** five representative horizontal brain slices display the results of the SBCA. **A** selected slices of the SBCA map of EMS on the right side with the seed in the right vAIC (green) overlaid with selected slices of a representative SBCA map of the EMS on the left side (yellow) with the seed in the left vAIC. **A'** SBCA map of the ISA dataset with the seed in the right (green) and left (yellow) vAIC. Overlapping regions are marked in light green. Corrected for false discovery rate, p-value: 0.0001. **B-E** bar graphs depicting the percentage of significant positively correlated voxels per brain area for left (**A**) and right (**B**) EMS and for ISA with seeds in the left (**C**) and right (**D**) VEN area during the seed-based correlation analysis,

averaged over three experiments. The seeds were placed in the left ventral AIC (yellow) or in the right ventral AIC (green). Lightly shaded bars indicate the 95 % confidence interval. MdTha: midline thalamus; Hippocamp: hippocampus; BNST: bed nucleus of the stria terminalis; MSDB: Medial Septum-Diagonal Band of Broca; Subst. Nigra: substantia nigra; VTA: ventral tegmental area; Hypothal: hypothalamus; PAG: periaqueductal gray; Temp STS: superior temporal sulcus; visual: includes all striate and extrastriate visual areas.

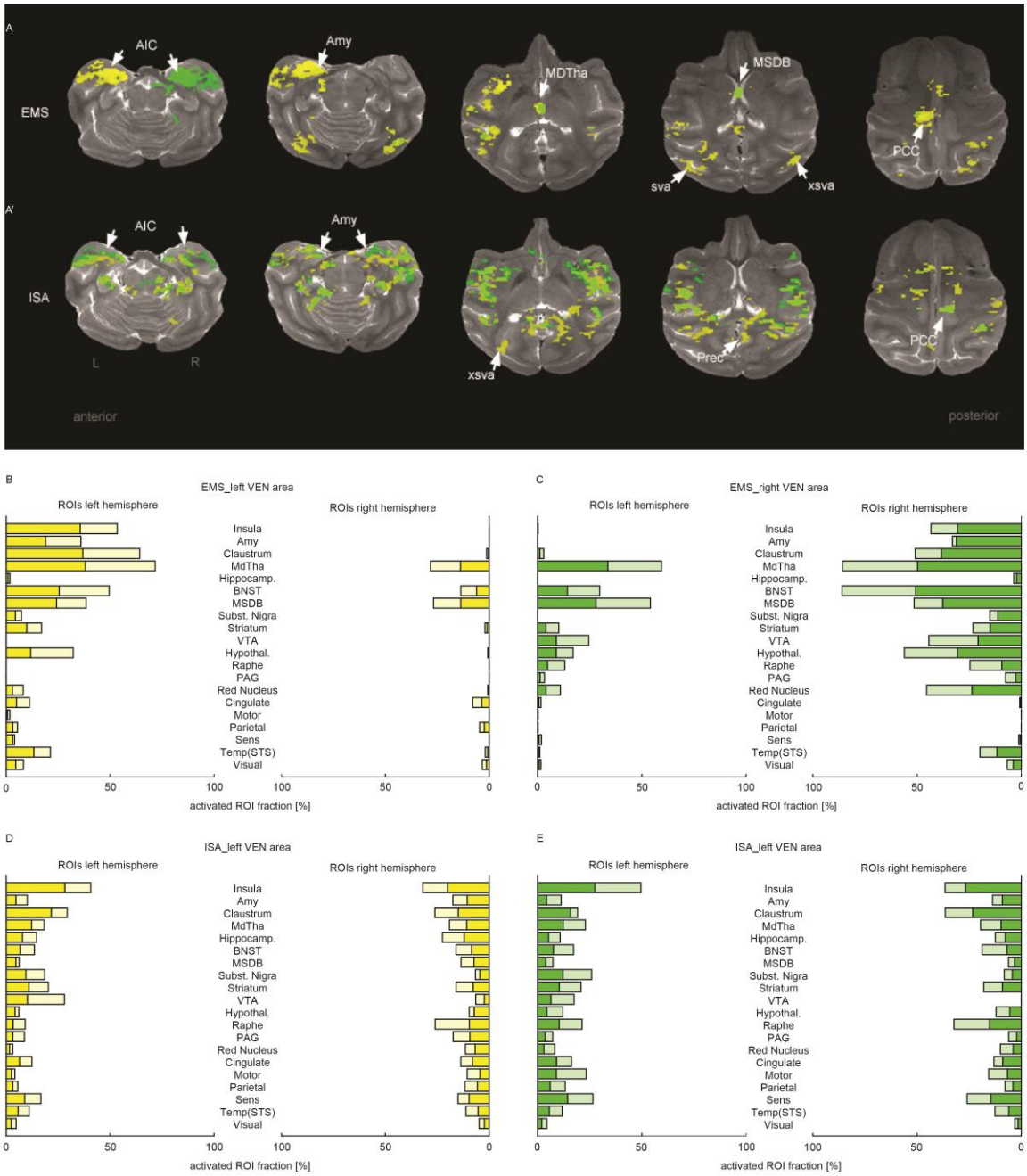

Asymmetric effect of the EMS on functional network correlations

To further analyse the effects of EMS in the left and right VEN area of the anesthetized monkey on specific networks, heat maps were created for the SN, the DMN, and the CEN, based on the percentages of correlated voxels per brain area, obtained from the SBCA analysis, averaged over three experiments (fig. 5). In the present analysis, brain areas that were included in the SN were the anterior cingulate cortex, the amygdala, the ventral striatum, the substantia nigra, and the ventral tegmental area (Seeley et al., 2007). For the DMN, the posterior cingulate cortex, the prefrontal cortex, the hippocampal formation, and the superior temporal sulcus were included (Buckner et al., 2008). The CEN included the intraparietal sulcus and the posterior parietal cortex (Seeley et al., 2007).

At rest, the AIC showed a rather similar functional connectivity with the left and right portions of the SN (~7%), DMN (~7%), and CEN (~5%). However, during the EMS in the left or right VEN area, the functional correlation between the ipsilateral (stimulated) AIC and the contralateral portion of the SN and the DMN was nearly completely shut down, with a 75.6 to 97.7 % reduction in the number of correlated voxels. The percentage of correlated voxels on the ipsilateral side in the left SN and the DMN during the stimulation remained unchanged compared to rest. In contrast, the number of correlated voxels in the right SN, after right-sided stimulation, more than doubled from 6.23 % to 17.12 %. Such a strong effect was not observed during left-sided EMS. Finally, unlike for the SN and DMN, the left EMS barely changed the correlation between AIC with both the ipsilateral and contralateral CEN, whereas, in stark contrast, the right EMS virtually suppresses the correlation with the CEN by 97.6 % – 99.9 % bilaterally.

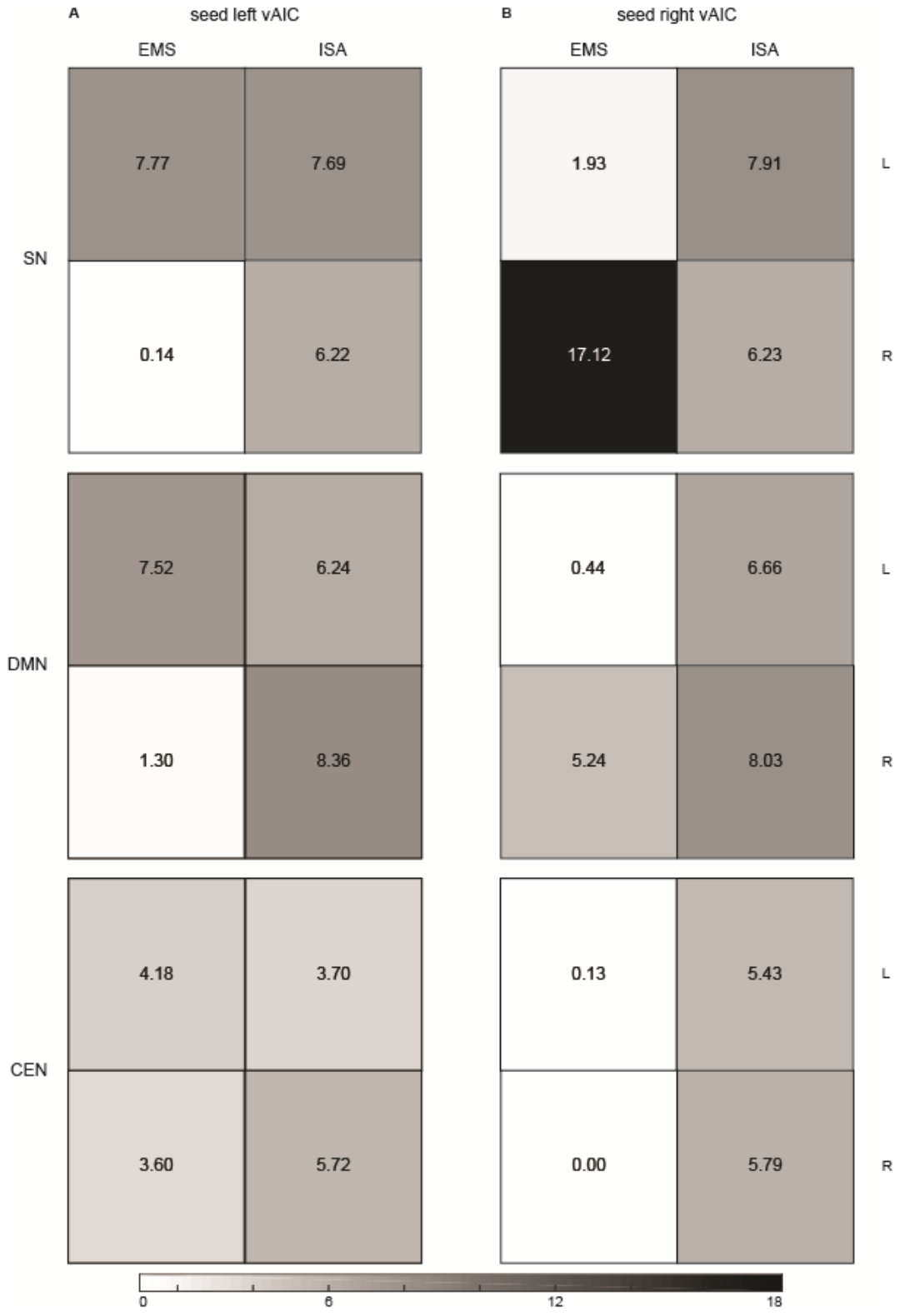

figure 5: Network analysis based on the SBCA for the EMS and ISA condition. The heat maps represent the percentage of correlated voxels per network, averaged over three experiments. The calculations were based on the SBCA data for the left (L) and right (R) hemisphere for the salience network (SN), the default mode network (DMN), and the central executive network (CEN) with the seed in the left (**A**) and right (**B**) vAIC.

Discussion

In the present study, we electrically microstimulated the left and right VEN area in three anesthetized macaque monkeys and analysed the resulting global brain activity. The EMS unsurprisingly activated several distinct close and distant subcortical and cortical-limbic regions (e.g. the amygdala, the midline thalamus, the cingulate cortex), mainly ipsilaterally. In addition, the EMS produced a conspicuous activation in broadly distributed cortical regions including mainly occipital and temporal visual areas and, to a lesser extent, auditory, vestibular, and somatosensory areas. There was, however, no major difference between the overall respective patterns of activation produced by the left and right EMS. In addition, to considering brain regions as individual entities, the present study also examined the effect of the EMS on the functional correlation between the stimulated AIC and three distinct functional networks (SN, DMN, and CEN). Importantly, while the AIC was functionally connected bilaterally with each network at rest, the unilateral EMS produced massive alterations of the contralateral and, even ipsilateral, connectivity, with a distinct difference between the left and right EMS. Indeed, the right EMS disproportionally recruited the ipsilateral SN and completely suppressed the connectivity with the CEN on both sides, whereas the left EMS did not increase the connectivity with the ipsilateral SN and did not affect the connectivity with the CEN. Taken together, these data indicate that the functional engagement of the AIC, mimicked here with EMS, polarizes the interaction of the insula with distinct networks, with an asymmetry that could be behaviourally relevant. In addition, the activation of numerous visual cortical regions that were otherwise not directly connected with the insula indicate a preponderant role of the AIC in integrating interoception with polymodal, in particular visual, activities that could be altogether relevant for the homeostatic assessment of affect and adaptation of motivated behaviours.

Mono- and poly-synaptic activations

The insula possesses vast connections (Mesulam and Mufson, 1982c, 1982b; Mufson and Mesulam, 1982) to, amongst others, the amygdala (Mufson et al., 1981; Amaral and Price, 1984; Hoistad and Barbas, 2008), the claustrum (Augustine, 1985), the ventral striatum (Arikuni and Kubota, 1986), the midline thalamus (Wylie and Tregellas, 2010; Vertes et al., 2015), the substantia nigra (Zhang et al., 2017), and the superior temporal sulcus (Wylie and Tregellas, 2010), making it the ideal centre to integrate interoceptive, exteroceptive, cognitive, motivational, and social signals (Nguyen et al., 2016; Evrard, 2019). These areas were seen to be activated by stimulation of the vAIC, indicating once more anatomical and functional connections. Additionally, other parts of the insula were activated by EMS. This supports the idea of strong intra-insula connections (Augustine, 1996) for the integration of 'objective' signals, from cortical and limbic regions, from the posterior insula to the anterior insula and with that a translation to a subjective representation in the anterior insula (Craig, 2009; Evrard, 2019).

Most of the activations seen subsequently to the EMS can be attributed to direct anatomical connections or known functional connections. A current spill over to brain areas in close proximity to the stimulation side is, in the current context, rather unlikely. As Ranck reviewed in his 1975 publication (Ranck, 1975), a 200 μs pulse with a stimulation strength of 400 — 1200 μA, as used in the present study, will lead to an activation of stimulable neuronal elements within a 2 mm radius of the electrode tip (see also Tolias et al. (2005)), a distance well within the borders of the anterior insula (Horn et al., in preparation). However, not only layer Vb, in which the VENs are present (Economo, 1926; Butti et al., 2013), but all layers will most likely have been stimulated with the given parameters. This, as well as the synchronicity with which the neurons were stimulated, might have

contributed to the strong activation observed. Due to spatiotemporal differences during a natural stimulation, not all cells are activated at once. With EMS, however, all stimulable neuronal elements in close vicinity to the electrode tip are stimulated simultaneously (Tolias et al., 2005; Sultan et al., 2007), leading to the activation of more pathways, including reciprocal ones, explaining the strong BOLD-signal changes observed in this study.

However, functional connections do not only arise from direct anatomical connections but can also occur between areas that are indirectly connected (Vincent et al., 2007; Honey et al., 2009). Visual areas, for example, have been shown to work in accordance with the insula, with the latter mediating access to awareness of visual stimuli (Salomon et al., 2016), without sharing direct connections but indirect connections via the intraparietal sulcus (Uddin et al., 2010) and other subcortical pathways. The activations of the visual areas in the present study most likely arose via cortical-subcortical-cortical pathways, which are preferred over cortical-cortical pathways during EMS (Logothetis et al., 2010). This requires the signal to spread polysynaptically, perhaps via the amygdala (Amaral et al., 2003), which has been shown to occur during electrical microstimulation. In 2011, Matsui and his team confirmed polysynaptic signal propagation by electrically microstimulating neuronal elements in the somatosensory cortex of monkeys (Matsui et al., 2011), corroborating prior results found by Logothetis in 2010 after delivering electrical microstimulations to the visual system in monkeys (Logothetis et al., 2010) and by Asanuma, whose team stimulated neuronal elements in the motor cortex of cats (Asanuma and Rosén, 1973).

Interestingly, some areas, which are known to share direct anatomical connections with the insula, did not display a consistent increased in activity following EMS, e.g. the parabrachial nucleus (PBN). The PBN is thought to be part of the network maintaining consciousness, which also includes includes a crucial functional connectivity with the anterior insular cortex (Fischer et al.,

2016). One possible explanation for the absence of a consistent BOLD signal change in this small brainstem nucleus could be the opioid anaesthesia employed in these experiments or to a more general dependence of these networks on brain states and behavioural engagement. However, prior experiments have shown that the anaesthesia used in the current experiment does not have a major influence on the BOLD signal, at least not during EMS in the visual system (Logothetis et al., 2010). To fully understand the extent of the anaesthesia on the BOLD signal, it would be necessary to conduct similar experiments in awake monkeys.

Absence of direct asymmetric effect

Interestingly, the brain activity in the respective hemisphere after left and right VEN area activation did not differ significantly. This is an interesting finding because some asymmetry between the left and the right side had been hypothesized prior to the experiments. This hypothesis was motivated by studies, which found changes in bodily physiology after EMS in the insula. Kaada and his colleagues found that stimulation of the insular cortex can lead to bradycardia (Kaada et al., 1949). These results were taken even further by Oppenheimer and his colleagues, who showed that stimulation of the left insula in humans leads to bradycardia, whereas stimulation of the right insula leads to tachycardia (Oppenheimer et al., 1992), a result which was also found by Caruana et al. for the left insula (bradycardia) in the alert macaque monkey (Caruana et al., 2011). Furthermore, lesion studies revealed that lesions in the right insula can lead to electrocardiographic abnormalities (Abboud et al., 2006), arterial fibrillation, atrioventricular blockage, premature contractions, and T-wave inversions (Christensen et al., 2005). These and other studies suggest that the insula plays a crucial role in the regulation of the cardiovascular functions (Eckardt et al., 1999; Nagai et al., 2010) and this regulation to be asymmetric. This

central asymmetry has been proposed to reflect the asymmetric anatomical innervation of the organs of the body by the left and right efferent nerves of the sympathetic (right-dominant) and parasympathetic (left-dominant) nerves (Craig, 2005). In an elegant model of emotional forebrain asymmetry, Craig suggested that parasympathetic and sympathetic afferents ascend in parallel via the lamina I/the nucleus tractus solitarii to the thalamus and into the posterior insular cortex and then to the mid-insula. However, before reaching the anterior insula, Craig proposed that the afferents cross over, so that the left AIC mainly represents parasympathetic activity, whereas the right AIC mainly represents sympathetic activity. Based on these asymmetries, we expected to find global brain asymmetry following EMS of the left or right vAIC. While, these asymmetries in global brain asymmetry were not found in the present study, an asymmetry in network regulation was revealed (see below). Additionally, we did not see any changes in bodily physiology, which was monitored closely and analysed offline (data not shown). Therefore, with this study, we cannot conclude if there is a global brain asymmetry during asymmetric insula activity. All recent microstimulation studies were made in awake human and macaque monkey subjects (Oppenheimer et al., 1992; Caruana et al., 2011). The absence of asymmetrical effect of our microstimulations on the overall brain activation pattern and on bodily physiology could be due to the anaesthesia and/or to the fact that the animals (and their insula) were not engaged in any salient stimuli processing that could conspicuously engage AIC with perhaps asymmetric contributions.

Asymmetric network regulation

In the second part of the study, a SBCA was conducted where the seeds were placed in the left and right vAIC during the EMS and during ISA. The analysis revealed an interhemispheric symmetry in the functional network at rest. It

included both insulae, as well as many cortical and subcortical areas. In contrast, the functional network during the EMS was ipsilateral. Similar lateralization has been found in different EMS studies in the visual system (Tolias et al., 2005), the face patch system (Moeller et al., 2017), the frontal eye field (Ekstrom et al., 2008), and the superior colliculus (Field et al., 2008) of monkeys. While natural stimuli and intrinsic activity usually activate both hemispheres, unless stimuli are purposefully only presented to one hemisphere, the resulting global brain activity shows symmetrical behaviour, amongst others, due to callossal (arising from the corpus callosum) and commissural (arising from the anterior and posterior commissure) connections (Johnston et al., 2008). However, in this, and the other aforementioned studies, the stimulation was presented unilaterally, resulting in brain activity that was majorly on the ipsilateral side.

The AIC has been described as a central component of the SN (Menon and Uddin, 2010; Menon, 2015) as well as a rich club hub (van den Heuvel and Sporns, 2013), i.e. a "highly connected node that shows a strong tendency to connect with other highly connected nodes" (Grayson et al., 2014)), with the capacity to drive switching between the DMN and the CEN (Goulden et al., 2014; Chen et al., 2016). The data in the current study suggest that, besides driving the switching between the DMN and the CEN network, the insula is also capable of up- and down-regulating the networks. The complete, bilateral shutdown of the CEN after right-sided vAIC stimulation could occur due to an insula-initiated focus shift. The insula integrates multimodal signals (see below) and assesses the relevance of salient stimuli to determine priorities in the processing of information and the allocation of energetic resources (Michel, 2017). If the insula's assessment demands a shift of attention, the CEN might be switched off, to re-allocated resources to a different network. However, this shutting down only occurred after right-sided stimulation. Right-sided stimulation furthermore increases the ipsilateral correlations with the SN, while left-sided stimulation did not. Both these effects, subsequent to right-sided stimulation, might reflect

greater importance accredited to the sympathetic nervous system (represented predominantly on the right side) compared to the parasympathetic system in terms of resource allocation, stimuli evaluation, and top-down regulation of autonomic processes, to ensure fast and reliable adaptations to salient stimuli.

Basis for a self-referential integration of polymodal activities

The rather conspicuous activation of non-limbic cortical areas during EMS and the corresponding correlations in the ISA could be explained considering the functions of the insula. As an information hub (Sterzer and Kleinschmidt, 2010), the insula integrates external, internal, social, emotional, and motivational signals (Nguyen et al., 2016), arriving from a wide net of anatomically connected cortical and subcortical brain regions (Mesulam and Mufson, 1982c, 1982b; Mufson and Mesulam, 1982). This multimodal integration and sensory processing (Umarova et al., 2010; Gogolla et al., 2014) includes, for example, auditory, visual, or tactile stimuli (Downar et al., 2000; Butti and Hof, 2010; Sterzer and Kleinschmidt, 2010) as well as visceral, proprioceptive**,** and vestibular stimuli (Seth, 2013). This integration of polymodal stimuli could enable the insula to generate a neurobiological activity underlying sense of self-reference and subjective self-awareness in humans (Tallon-Baudry et al., 2018; Evrard, 2019). It was found, that the loss of this subjective self-awareness in humans is tightly correlated with the activation of the AIC. With its suppression, the frontoparietal networks gets shut down which leads to a state of unconsciousness (Warnaby et al., 2016).

These processes and functions of the insula would require ongoing input and communication with cortical and subcortical areas to obtain multimodal information for integration and therefore would explain the uniformly distributed correlations seen in the ISA analysis.

Further functional interpretations

In the SBCA, some correlations between the insula and subcortical brain regions, besides the brain regions that lie in close proximity to the stimulation side, like the amygdala and the claustrum, were found to be more correlated during the EMS than during the ISA. One of these areas was the medial septum (MS). The MS is a cholinergic nucleus (Liu et al., 2018) with strong projections from the insula and with projections to the hippocampus (Nyakas et al., 1987). Prior studies in rats (McLennan and Miller, 1974), rabbits (Bruecke et al., 1959), and monkeys (Green and Arduini, 1954) showed that these connections control inhibitory neurons in the hippocampus (Chamberland and Topolnik, 2012) and drive the theta frequency. Even though direct connections between the anterior insula and the hippocampus have been shown (Ghaziri et al., 2018), as well as indirect pathways, which do not go via the MS (Mesulam and Mufson, 1982a), there was no correlation between the hippocampus and the insula in the present study. One reason could be that the insula-MS pathways is functionally more potent than the insula-hippocampal pathway. Therefore, the MS could drive the hippocampal activation, which would then result in a theta frequency of 4 – 8 Hz (Logothetis, 2008), which is not correlated with the 100 Hz stimulation that was delivered during the EMS. The activation of the hippocampus from the insula via the MS could have effects on attention and memory (McGarrity et al., 2017).

Two other areas that showed stronger correlations during the EMS than during the ISA were the bed nucleus of the stria terminalis (BNST) and the midline thalamus. The insula and BNST have been shown to be involved in the monitoring of threat levels in the environment (Somerville et al., 2010). The relatively small correlation during the ISA could be due to the anesthetized state of the monkey, which does not allow an assessment of environmental threads. However, an electrical stimulus in the vAIC seems to activate the pathway. Interestingly, the right-sided stimulation yielded higher activation of the BNST,

falling in line with the proposed forebrain emotional asymmetry model (Craig, 2005) discussed earlier. The midline thalamus is known to share many connections with limbic areas, like the insula, the hippocampus, the claustrum, the striatum, or the amygdala, to name a few (Vertes and Hoover, 2008). It is hypothesized that the midline thalamus is involved in emotional and cognitive aspects of goal-directed behaviour (Vertes, 2006) and in cooperation with the insula implied in limbic association functions (Vertes et al., 2015). Furthermore, it drives hippocampal functions (Jung et al., 2019) and gates the hippocampal mediation of the ventral tegmental area (Zimmerman and Grace, 2016). The stronger correlation of the above-mentioned brain areas during the EMS, compared to the ISA, indicate that the synchronous stimulation of vAIC cells activates specific pathways, which are only weakly active during resting state.

Conclusion

Taken together, the data in the present study strengthens the role of the insula as a major hub in the salience network, capable of not only switching system activity between networks, like the DMN and the CEN, but also regulating the networks to react adequately to salient stimuli. Further, this regulation was found to be asymmetric, which could have implications on emotional, cognitive, and behavioural processes. While the global brain activity did not display asymmetries, it did reveal functional connections between the insula and monosynaptically and polysynaptically connected cortical and subcortical brain areas, underlining the insula's function to integrate multimodal signals in a process that could contribute to engendering self-awareness in humans, to regulate autonomic processes, and to detect and evaluate salient events. Electrical microstimulation studies in alert monkeys are now needed to further investigate the insulas network behaviour and influence on autonomic processes during natural rest and during affective and/or cognitive tasks.

Abbreviations

ACC	anterior cingulate cortex
AIC	anterior insular cortex
amy	amygdala
ap	in anteroposterior
BOLD	blood oxygenation level dependent
CEN	central executive network
DMN	default mode network
dv	dorsoventral
EMS	electrical microstimulation
EPI	echo-planar imaging
fMRI	functional magnetic resonance imaging
GLM	general linear model
Ial	lateral anterior insula (= VEN area)
Iapl	posterior lateral agranular areas of the insula
Iapm	posterior medial posterior lateral agranular areas of the insula
IC	insular cortex
ISA	intrinsic spontaneous activity
MDTh	midline thalamus
ml	mediolateral
MLT	midline periventricular thalamic region
MS	medial septum
PCC	posterior cingulate
ROI	regions of interest
SBCA	seed based correlation analysis
SN	salience network
SNi	substantia nigra
sva	striate visual areas
vAIC	ventral anterior insula
VEN	von Economo neurons
VS	ventral striatum
xsva	extrastriate visual areas

References

Abboud, H., Berroir, S., Labreuche, J., Orjuela, K., Amarenco, P., and Investigators, G. (2006). *Insular involvement in brain infarction increases risk for cardiac arrhythmia and death*. Ann Neurol 59 (4).

Allman, J. M., Tetreault, N. A., Hakeem, A. Y., Manaye, K. F., Semendeferi, K., Erwin, J. M., Park, S., Goubert, V., and Hof, P. R. (2010). *The von Economo neurons in the frontoinsular and anterior cingulate cortex*. Ann N Y Acad Sci 1225.

Amaral, D. G., Behniea, H., and Kelly, J. L. (2003). *Topographic organization of projections from the amygdala to the visual cortex in the macaque monkey*. Neuroscience 118 (4).

Amaral, D. G., and Price, J. L. (1984). *Amygdalo-cortical projections in the monkey (Macaca fascicularis)*. J Comp Neurol 230 (4).

Arikuni, T., and Kubota, K. (1986). *The organization of prefrontocaudate projections and their laminar origin in the macaque monkey: a retrograde study using HRP-gel*. J Comp Neurol 244 (4).

Asanuma, H., and Rosén, I. (1973). *Spread of mono- and polysynaptic connections within cat's motor cortex*. Experimental Brain Research 16 (5).

Asanuma, H., and Sakata, H. (1967). *Functional Organization of a Cortical Efferent System Examined with Focal Depth Stimulation in Cats*. Journal of Neurophysiology 30 (1).

Augustine, J. R. (1985). *The insular lobe in primates including humans*. Neurol Res 7 (1).

Augustine, J. R. (1996). *Circuitry and functional aspects of the insular lobe in primates including humans.* Brain Research Reviews 22.

Bruecke, F., Petsche, H., Pillat, B., and Deisenhammer, E. (1959). *[The influencing of the "hippocampus arousal reaction" in the rabbit by electrical stimulation in the septum]*. Pflugers Arch Gesamte Physiol Menschen Tiere 269.

Buckner, R. L., Andrews-Hanna, J. R., and Schacter, D. L. (2008). *The brain's default network: anatomy, function, and relevance to disease*. Ann N Y Acad Sci 1124.

Butti, C., and Hof, P. R. (2010). *The insular cortex: a comparative perspective*. Brain Struct Funct 214 (5-6).

Butti, C., Santos, M., Uppal, N., and Hof, P. R. (2013). *Von Economo neurons: clinical and evolutionary perspectives*. Cortex 49 (1).

Carmichael, S. T., and Price, J. L. (1994). *Architectonic subdivision of the orbital and medial prefrontal cortex in the macaque monkey*. J Comp Neurol 346 (3).

Caruana, F., Jezzini, A., Sbriscia-Fioretti, B., Rizzolatti, G., and Gallese, V. (2011). *Emotional and social behaviors elicited by electrical stimulation of the insula in the macaque monkey*. Curr Biol 21 (3).

Chamberland, S., and Topolnik, L. (2012). *Inhibitory control of hippocampal inhibitory neurons*. Front Neurosci 6.

Chen, T., Cai, W., Ryali, S., Supekar, K., and Menon, V. (2016). *Distinct Global Brain Dynamics and Spatiotemporal Organization of the Salience Network*. PLoS Biol 14 (6).

Christensen, H., Boysen, G., Christensen, A. F., and Johannesen, H. H. (2005). *Insular lesions, ECG abnormalities, and outcome in acute stroke*. J Neurol Neurosurg Psychiatry 76 (2).

Craig, A. D. (2005). *Forebrain emotional asymmetry: a neuroanatomical basis?* Trends Cogn Sci 9 (12).

Craig, A. D. (2009). *How do you feel-now*. Nature Neuroscience 10.

Downar, J., Crawley, A. P., Mikulis, D. J., and Davis, K. D. (2000). *A multimodal cortical network for the detection of changes in the sensory environment*. Nat Neurosci 3 (3).

Eckardt, M., Gerlach, L., and Welter, F. L. (1999). *Prolongation of the frequency-corrected QT dispersion following cerebral strokes with involvement of the insula of Reil*. Eur Neurol 42 (4).

Eckert, M. A., Menon, V., Walczak, A., Ahlstrom, J., Denslow, S., Horwitz, A., and Dubno, J. R. (2009). *At the heart of the ventral attention system: the right anterior insula*. Hum Brain Mapp 30 (8).

Economo, C. v. (1926). *Eine neue Art Spezialzellen des Lobus Cinguli und Lobus Insulae*. Zeitschrift für die gesamte Neurologie und Psychiatrie 100 (1).

Ekstrom, L. B., Roelfsema, P. R., Arsenault, J. T., Bonmassar, G., and Vanduffel, W. (2008). *Bottom-up dependent gating of frontal signals in early visual cortex*. Science 321 (5887).

Evrard, H. C. (2019). *The organization of the primate insular cortex*. Frontiers in Neuroanatomy.

Evrard, H. C., Logothetis, N. K., and Craig, A. D. (2014). *Modular architectonic organization of the insula in the macaque monkey*. J Comp Neurol 522 (1).

Ferrier, D. (1875). *Experiments on the brain of monkeys.—No. I*. Proceedings of the Royal Society of London 23 (156-163).

Field, C. B., Johnston, K., Gati, J. S., Menon, R. S., and Everling, S. (2008). *Connectivity of the primate superior colliculus mapped by concurrent microstimulation and event-related FMRI*. PLoS One 3 (12).

Fischer, D. B., Boes, A. D., Demertzi, A., Evrard, H. C., Laureys, S., Edlow, B. L., Liu, H., Saper, C. B., Pascual-Leone, A., Fox, M. D., and Geerling, J. C. (2016). *A human brain network derived from coma-causing brainstem lesions*. Neurology 87 (23).

Ghaziri, J., Tucholka, A., Girard, G., Boucher, O., Houde, J. C., Descoteaux, M., Obaid, S., Gilbert, G., Rouleau, I., and Nguyen, D. K. (2018). *Subcortical structural connectivity of insular subregions*. Sci Rep 8 (1).

Gogolla, N., Takesian, A. E., Feng, G., Fagiolini, M., and Hensch, T. K. (2014). *Sensory integration in mouse insular cortex reflects GABA circuit maturation*. Neuron 83 (4).

Goulden, N., Khusnulina, A., Davis, N. J., Bracewell, R. M., Bokde, A. L., McNulty, J. P., and Mullins, P. G. (2014). *The salience network is responsible for switching between the default mode network and the central executive network: replication from DCM*. Neuroimage 99.

Grayson, D. S., Ray, S., Carpenter, S., Iyer, S., Dias, T. G., Stevens, C., Nigg, J. T., and Fair, D. A. (2014). *Structural and functional rich club organization of the brain in children and adults*. PLoS One 9 (2).

Green, J. D., and Arduini, A. A. (1954). *Hippocampal electrical activity in arousal*. J Neurophysiol 17 (6).

Hoistad, M., and Barbas, H. (2008). *Sequence of information processing for emotions through pathways linking temporal and insular cortices with the amygdala*. Neuroimage 40 (3).

Honey, C. J., Sporns, O., Cammoun, L., Gigandet, X., Thiran, J. P., Meuli, R., and Hagmann, P. (2009). *Predicting human resting-state functional connectivity from structural connectivity*. Proc Natl Acad Sci U S A 106 (6).

Horn, F. M., Logothetis, N., and Evrard, H. C. (in preparation). *Novel elemental localization in the primate cerebral cortex*.

Johnston, J. M., Vaishnavi, S. N., Smyth, M. D., Zhang, D., He, B. J., Zempel, J. M., Shimony, J. S., Snyder, A. Z., and Raichle, M. E. (2008). *Loss of resting interhemispheric functional connectivity after complete section of the corpus callosum*. J Neurosci 28 (25).

Jung, D., Huh, Y., and Cho, J. (2019). *The ventral midline thalamus mediates hippocampal spatial information processes upon spatial cue changes*. J Neurosci.

Kaada, B. R., K.H., P., and J.A., E. (1949). *Respiratory and vascular responses in monkeys from temporal pole, insula, orbital surface and cingulate gyrus*. Journal of Physiology.

Kim, E. J., Sidhu, M., Gaus, S. E., Huang, E. J., Hof, P. R., Miller, B. L., DeArmond, S. J., and Seeley, W. W. (2012). *Selective frontoinsular von Economo neuron and fork cell loss in early behavioral variant frontotemporal dementia*. Cereb Cortex 22 (2).

Liu, A. K. L., Lim, E. J., Ahmed, I., Chang, R. C., Pearce, R. K. B., and Gentleman, S. M. (2018). *Review: Revisiting the human cholinergic nucleus of the diagonal band of Broca*. Neuropathol Appl Neurobiol 44 (7).

Logothetis, N. K. (2008). *What we can do and what we cannot do with fMRI*. Nature 453 (7197).

Logothetis, N. K., Augath, M., Murayama, Y., Rauch, A., Sultan, F., Goense, J., Oeltermann, A., and Merkle, H. (2010). *The effects of electrical microstimulation on cortical signal propagation*. Nat Neurosci 13 (10).

Logothetis, N. K., Eschenko, O., Murayama, Y., Augath, M., Steudel, T., Evrard, H. C., Besserve, M., and Oeltermann, A. (2012). *Hippocampal-cortical interaction during periods of subcortical silence*. Nature 491 (7425).

Matsui, T., Koyano, K. W., Tamura, K., Osada, T., Adachi, Y., Miyamoto, K., Chikazoe, J., Kamigaki, T., and Miyashita, Y. (2012). *FMRI activity in the macaque cerebellum evoked by intracortical microstimulation of the primary somatosensory cortex: evidence for polysynaptic propagation*. PLoS One 7 (10).

Matsui, T., Tamura, K., Koyano, K. W., Takeuchi, D., Adachi, Y., Osada, T., and Miyashita, Y. (2011). *Direct comparison of spontaneous functional connectivity and effective connectivity measured by intracortical microstimulation: an fMRI study in macaque monkeys*. Cereb Cortex 21 (10).

McGarrity, S., Mason, R., Fone, K. C., Pezze, M., and Bast, T. (2017). *Hippocampal Neural Disinhibition Causes Attentional and Memory Deficits*. Cereb Cortex 27 (9).

McLennan, H., and Miller, J. J. (1974). *The hippocampal control of neuronal discharges in the septum of the rat*. J Physiol 237 (3).

Menon, V. (2015). *Salience Network*.

Menon, V., and Uddin, L. Q. (2010). *Saliency, switching, attention and control: a network model of insula function*. Brain Struct Funct 214 (5-6).

Mesulam, M. M., and Mufson, E. J. (1982a). *Insula of the Old World Monkey III: Efferent Cortical Output and Comments on Function*. The Journal of Comparative Neurology 212 (1).

Mesulam, M. M., and Mufson, E. J. (1982b). *Insula of the old world monkey. I. Architectonics in the insulo-orbito-temporal component of the paralimbic brain*. J Comp Neurol 212 (1).

Mesulam, M. M., and Mufson, E. J. (1982c). *Insula of the old world monkey. III: Efferent cortical output and comments on function*. J Comp Neurol 212 (1).

Michel, M. (2017). *A role for the anterior insular cortex in the global neuronal workspace model of consciousness*. Conscious Cogn 49.

Moeller, S., Crapse, T., Chang, L., and Tsao, D. Y. (2017). *The effect of face patch microstimulation on perception of faces and objects*. Nat Neurosci 20 (5).

Mufson, E. J., and Mesulam, M. M. (1982). *Insula of the old world monkey. II: Afferent cortical input and comments on the claustrum*. J Comp Neurol 212 (1).

Mufson, E. J., Mesulam, M. M., and Pandya, D. N. (1981). *Insular interconnections with the amygdala in the rhesus monkey*. Neuroscience 6 (7).

Nagai, M., Hoshide, S., and Kario, K. (2010). *The insular cortex and cardiovascular system: a new insight into the brain-heart axis*. J Am Soc Hypertens 4 (4).

Nguyen, V. T., Breakspear, M., Hu, X., and Guo, C. C. (2016). *The integration of the internal and external milieu in the insula during dynamic emotional experiences*. Neuroimage 124 (Pt A).

Nyakas, C., Luiten, P. G., Spencer, D. G., and Traber, J. (1987). *Detailed projection patterns of septal and diagonal band efferents to the hippocampus in the rat with emphasis on innervation of CA1 and dentate gyrus*. Brain Res Bull 18 (4).

Oppenheimer, S. M., Gelb, A., Girvin, J. P., and Hachinski, V. C. (1992). *Cardiovascular effects of human insular cortex stimulation*. Neurology 42 (9).

Paxinos, G., Huang, X. F., and Toga, A. W. (2009). *The Rhesus Monkey Brain in Stereotaxic Coordinates*. San Diego: Academic Press.

Penfield, W., and Boldrey, E. (1937). *Somatic motor and sensory representation in the cerebral cortex of man as studied by electrical stimulation*. Brain 60 (4).

Ranck, J. B., Jr. (1975). *Which elements are excited in electrical stimulation of mammalian central nervous system: a review*. Brain Res 98 (3).

Saleem, K., and Logothetis, N. K. L. (2012). *A Combined MRI and Histology Atlas of the Rhesus Monkey Brain in Stereotaxic Coordinates*: Academic Press.

Salomon, R., Ronchi, R., Donz, J., Bello-Ruiz, J., Herbelin, B., Martet, R., Faivre, N., Schaller, K., and Blanke, O. (2016). *The Insula Mediates Access to Awareness of Visual Stimuli Presented Synchronously to the Heartbeat*. J Neurosci 36 (18).

Santos, M., Uppal, N., Butti, C., Wicinski, B., Schmeidler, J., Giannakopoulos, P., Heinsen, H., Schmitz, C., and Hof, P. R. (2011). *Von Economo neurons in autism: a stereologic study of the frontoinsular cortex in children*. Brain Res 1380.

Seeley, W. W., Menon, V., Schatzberg, A. F., Keller, J., Glover, G. H., Kenna, H., Reiss, A. L., and Greicius, M. D. (2007). *Dissociable intrinsic connectivity networks for salience processing and executive control*. J Neurosci 27 (9).

Seeley, W. W., Merkle, F. T., Gaus, S. E., Craig, A. D., Allman, J. M., and Hof, P. R. (2012). *Distinctive Neurons of the Anterior Cingulate and Frontoinsular Cortex: A Historical Perspective*. Cerebral Cortex 22 (2).

Seth, A. K. (2013). *Interoceptive inference, emotion, and the embodied self*. Trends Cogn Sci 17 (11).

Somerville, L. H., Whalen, P. J., and Kelley, W. M. (2010). *Human bed nucleus of the stria terminalis indexes hypervigilant threat monitoring*. Biol Psychiatry 68 (5).

Sterzer, P., and Kleinschmidt, A. (2010). *Anterior insula activations in perceptual paradigms: often observed but barely understood*. Brain Struct Funct 214 (5-6).

Sultan, F., Augath, M., and Logothetis, N. (2007). *BOLD sensitivity to cortical activation induced by microstimulation: comparison to visual stimulation*. Magn Reson Imaging 25 (6).

Tallon-Baudry, C., Campana, F., Park, H. D., and Babo-Rebelo, M. (2018). *The neural monitoring of visceral inputs, rather than attention, accounts for first-person perspective in conscious vision*. Cortex 102.

Tolias, A. S., Sultan, F., Augath, M., Oeltermann, A., Tehovnik, E. J., Schiller, P. H., and Logothetis, N. K. (2005). *Mapping cortical activity elicited with electrical microstimulation using FMRI in the macaque*. Neuron 48 (6).

Uddin, L. Q., Supekar, K., Amin, H., Rykhlevskaia, E., Nguyen, D. A., Greicius, M. D., and Menon, V. (2010). *Dissociable connectivity within human angular gyrus and intraparietal sulcus: evidence from functional and structural connectivity*. Cereb Cortex 20 (11).

Umarova, R. M., Saur, D., Schnell, S., Kaller, C. P., Vry, M. S., Glauche, V., Rijntjes, M., Hennig, J., Kiselev, V., and Weiller, C. (2010). *Structural connectivity for visuospatial attention: significance of ventral pathways*. Cereb Cortex 20 (1).

van den Heuvel, M. P., and Sporns, O. (2013). *Network hubs in the human brain*. Trends Cogn Sci 17 (12).

Vertes, R. P. (2006). *Interactions among the medial prefrontal cortex, hippocampus and midline thalamus in emotional and cognitive processing in the rat*. Neuroscience 142 (1).

Vertes, R. P., and Hoover, W. B. (2008). *Projections of the paraventricular and paratenial nuclei of the dorsal midline thalamus in the rat*. J Comp Neurol 508 (2).

Vertes, R. P., Linley, S. B., and Hoover, W. B. (2015). *Limbic circuitry of the midline thalamus*. Neurosci Biobehav Rev 54.

Vincent, J. L., Patel, G. H., Fox, M. D., Snyder, A. Z., Baker, J. T., Van Essen, D. C., Zempel, J. M., Snyder, L. H., Corbetta, M., and Raichle, M. E. (2007). *Intrinsic functional architecture in the anaesthetized monkey brain*. Nature 447 (7140).

Warnaby, C. E., Seretny, M., Ni Mhuircheartaigh, R., Rogers, R., Jbabdi, S., Sleigh, J., and Tracey, I. (2016). *Anesthesia-induced Suppression of Human Dorsal Anterior Insula Responsivity at Loss of Volitional Behavioral Response*. Anesthesiology 124 (4).

Wylie, K. P., and Tregellas, J. R. (2010). *The role of the insula in schizophrenia*. Schizophr Res 123 (2-3).

Zhang, Y., Larcher, K. M. H., Misic, B., and Dagher, A. (2017). *Anatomical and functional organization of the human substantia nigra and its connections*. eLife 6.

Zimmerman, E. C., and Grace, A. A. (2016). *The Nucleus Reuniens of the Midline Thalamus Gates Prefrontal-Hippocampal Modulation of Ventral Tegmental Area Dopamine Neuron Activity*. J Neurosci 36 (34).

Supplementary

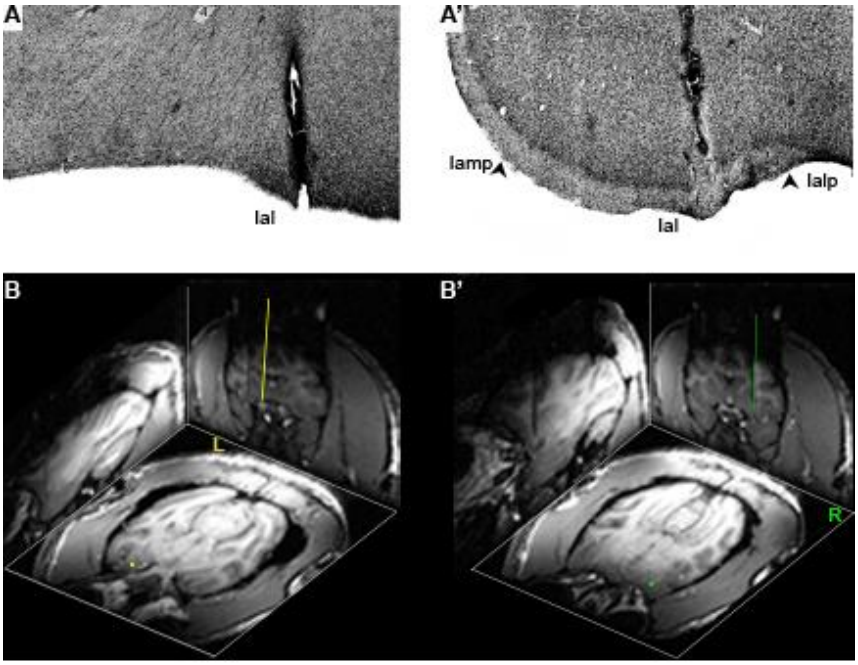

E	Left [mm]	Right [mm]	
AP	13.50	12.20	M1
ML	24.45	23.01	
DV	11.00	9.00	
AP	13.22	11.78	M2
ML	28.71	27.87	
DV	9.00	9.50	
AP	10.00	12.42	M3
ML	27.95	27.66	
DV	10.00	8.00	

supplementary figure 1: B, D orthogonal views show the position of the left (yellow) and right (green) electrode in the left and right VEN area for M2 (**B, B'**) and M3 (**D**). **A, C** histological Nissl stained coronal section, with 50µm thickness, indicate the electrode position (black tract) in the VEN area on the left (**A, C**) and right (**A', C'**) side for M2 (A, A') and M3 (C, C'). Black arrowheads indicate the borders of the architectonic areas. **E** table listing the exact electrode positions in the brain based on Frankfurt zero for all three monkeys.

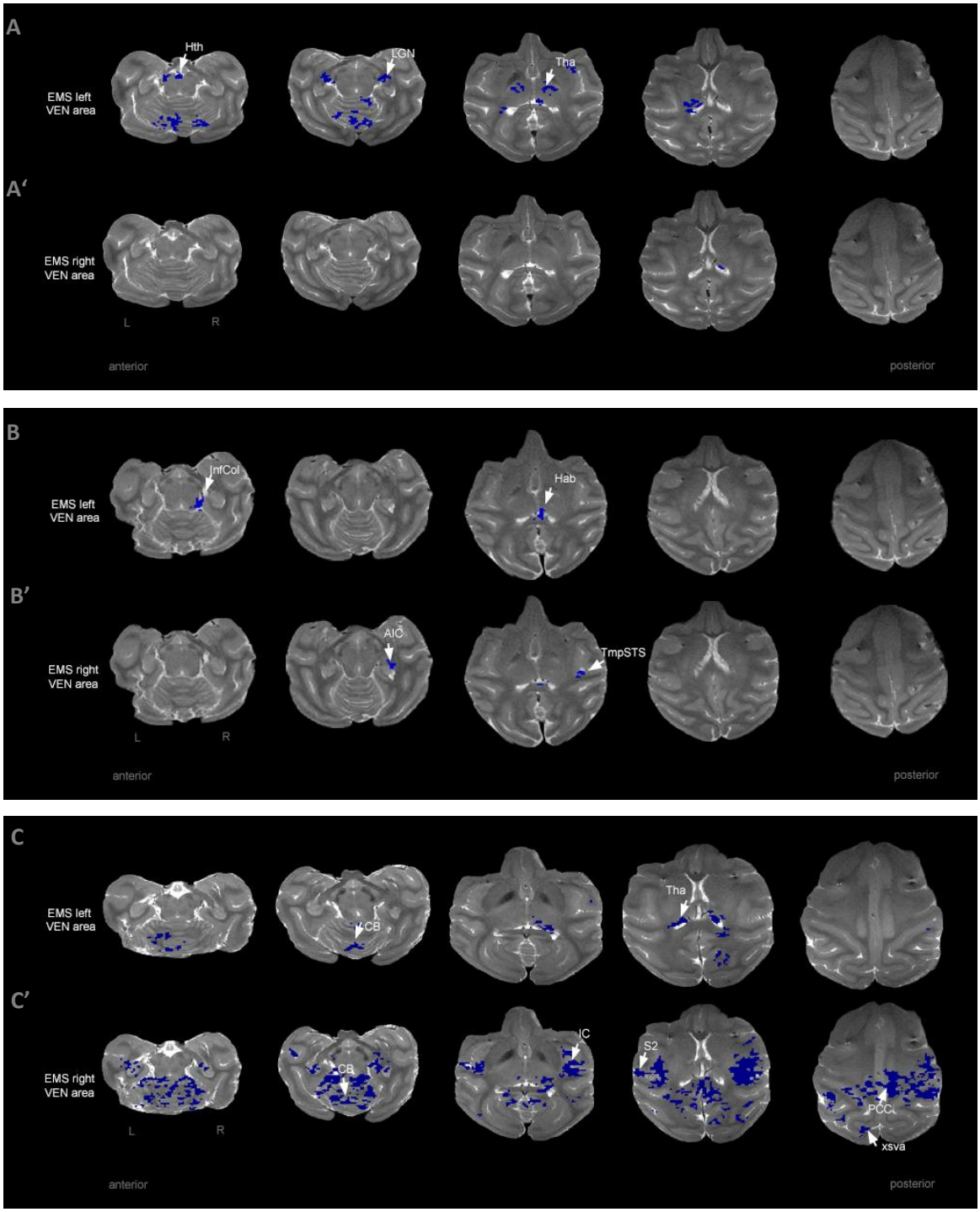

supplementary figure 2: Activity maps depicting negative BOLD-signal changes during left and right-sided EMS. Five representative horizontal brain slices display negative BOLD–signal changes during EMS in the left (**A, B, C**) and right (**A', B', C'**) VEN area in three experiments. Corrected for false discovery rate, p-value: 0.0001. Abbreviations as in figure 2. CB: cerebellum; IC: insular cortex; LGN: lateral geniculate nucleus; S2: secondary somatosensory cortex; Tha: Thalamus;

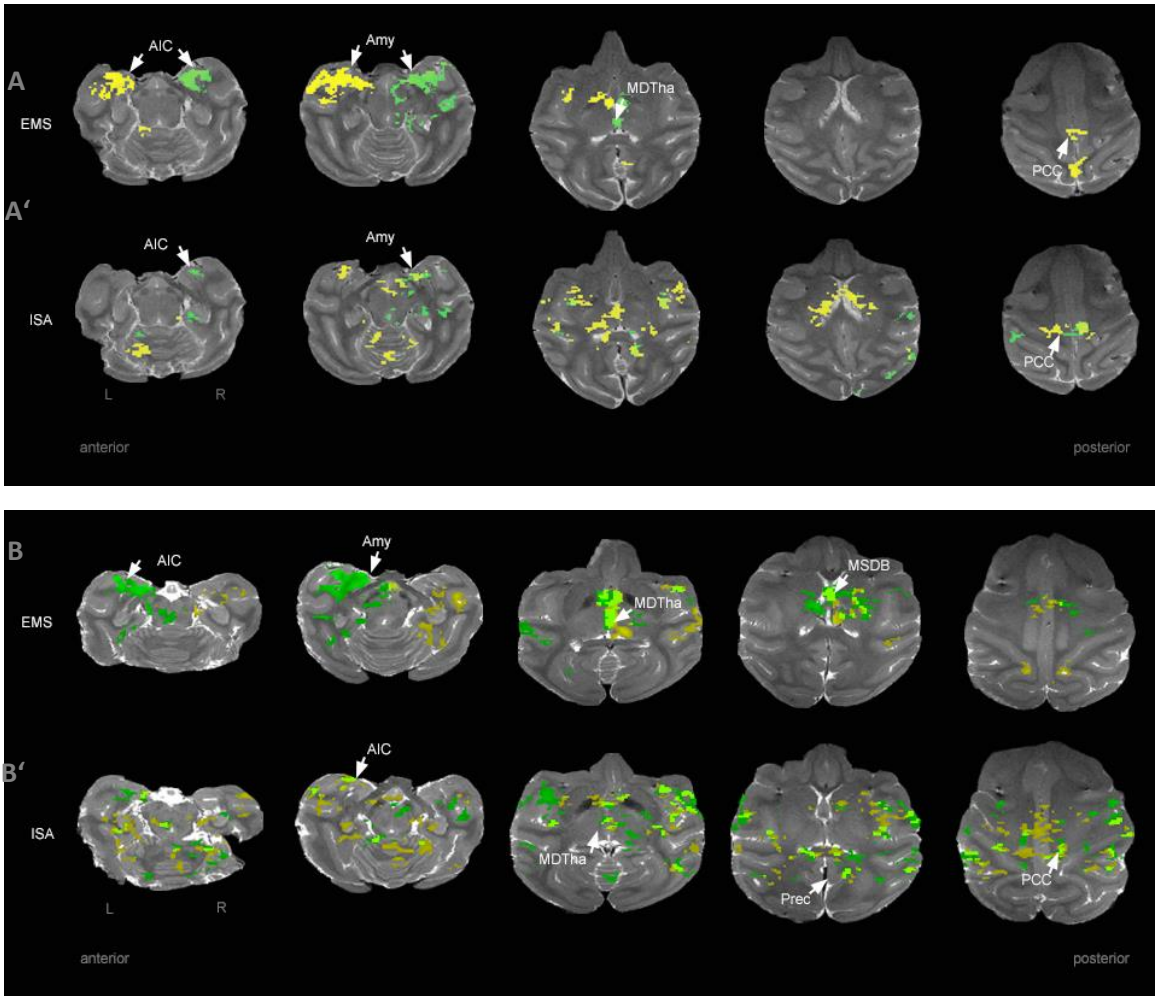

supplementary figure 3: SBCA maps during EMS and ISA. Five representative horizontal brain slices display the results of the SBCA for M2 (A, A') and M3 (B, B'). **A, B** selected slices of the SBCA map of EMS on the right side with the seed in the right vAIC (green) overlaid with selected slices of a representative SBCA map of the EMS on the left side (yellow) with the seed in the left vAIC. **A', B'** SBCA map of the ISA dataset with the seed in the right (green) and left (yellow) vAIC. Overlapping regions are marked in light green. Corrected for false discovery rate, p-value: 0.0001. Abbreviations as in figure 3. Prec: precuneus.

M1	EMS left VEN area		EMS right VEN area	
	activated voxels left hemisphere [%]	activated voxels right hemisphere [%]	activated voxels left hemisphere [%]	activated voxels right hemisphere [%]
amygdala	31.17	0	2.92	32.13
claustrum	63.45	5.09	9.64	62.96
ventral striatum	20.14	3.21	5.85	31.19
midline thalamus	12.22	2.59	7.78	7.76
MSDB*	2.78	5.49	30.56	32.97
nucleus ruber	0	0	0	10.98
substantia nigra	8.55	0	0	12.42
striate visual areas	6.93	3.49	5.44	9.20
extra-striate visual areas **	21.50	20.23	8.81	9.56
temporal sulcus	25.87	9.56	3.27	22.77
prefrontal cortex	0.95	0	0.09	0.82
cingulate cortex	13.18	7.47	2.15	2.84

* medial septal-diagonal band of Broca.

** includes: V2V3, V4, V5.

Table 1: percentage of activated voxels per region of interest after EMS of the left and right VEN area for monkey I.

9

ACKNOWLEDGEMENTS

"You can do it, but you cannot do it alone" a friend of mine told me at the beginning of my scientific journey. Words, which I experienced to be so very true whilst I was working towards the completion of my PhD. It was a long and difficult journey, and I would not have made it to the end if I did not have the love, support, and help of my family, my friends, and my colleagues. Moreover, I am incredibly grateful to everyone who has helped me in the last four years to achieve this milestone.

Firstly, I would like to thank Dr. Henry Evrard for being the supervisor of my PhD project, for providing resources, and for supporting my work.

Further, I would like to express my gratitude to Prof. Dr. Nikos Logothetis for granting me the opportunity to conduct my research in such an excellent environment with extraordinary people, infrastructure, and support.

I am particularly grateful for the selfless help provided by Dr. Yusuke Murayama throughout the experiments and the analysis phase. I greatly benefited from his willingness to generously take the time to answer every toolbox-related question and from his unconditional support, patience, and teachings of programming skills.

My thanks are further extending to Dr. Carsten Klein. His support, his patience, and his professional guidance during the experiments not only greatly influenced my project but also made me a better, more meticulous researcher.

For the excellent and calm help with the electronics during the experiments, I would like to thank Axel Oeltermann.

Joachim Werner I would like to greatly thank for the unconventional IT support that was available 24/7, no questions asked.

For the assistance and the maintenance of the animals during the experiments, I would like to thank the vets, the TAs, and the animal care staff, namely Dr. Silvia Slesiona-Kuenzel, Daniel Havel, Mirko Lindig, Deniz Ipek, Thomas Steudel, and Mariana Pitscheider.

Furthermore, the support from the workshop for the rat and the monkey project was invaluable. Thank you Mirsat Memaj, Johannes Boldt, Oliver Holder, Theodor Steffen, Matthias Arndt, Joshi Walzog, and Eduard Krampe for always providing prompt, personalized help and solutions.

Felicitas Horn I would like to thank for a wonderful friendship, which has developed over the past years and which has gotten me through some of the hardships that came with the job. Our conversations provided a source of fun, joy, and replenishment.

"With love and patience nothing is impossible" said Japanese writer Daisaku Ikeda. Love and patience were only two of the plethora of things my parents generously gifted to me all my life and especially in the last ten years since I set out on my journey to become a scientist. Without their love and support, I would not be the person I am today, and I will be forever grateful.

My sister and best friend Debbie, and her husband Udo, I would like to thank for always being there for me, for encouraging me to follow my path, for listening and understanding every problem, and for having helpful comments and solutions at hand anytime.

My dearest Vishal, I would like to thank for supporting me in every possible way with incredible patience, for believing in me, and for encouraging me to carry on. For always being a source of strength and inspiration and for all the joy and happiness that you are bringing to my life.

Last but not least, I would like to express my utmost gratitude for the monkeys, who gave their lives in the course of the experiments. With their sacrifice, I was

able to contribute a small piece to the endless puzzle of understanding the brain, which, hopefully, one day, will provide the basis for improving the lives of people.

Afoot and light-hearted I take to the open road,

Healthy, free, the world before me,

The long brown path before me leading wherever I choose.

Walt Whitman